2018-01-01

Assessment Of Climate Change Impact On Hydraulic Design Procedures Of Bridges

Anjuman Ara Akhter
University of Texas at El Paso, anjuman.zhumu@gmail.com

ASSESSMENT OF CLIMATE CHANGE IMPACT ON HYDRAULIC DESIGN PROCEDURES OF BRIDGES

ANJUMAN ARA AKHTER

Master's Program in Civil Engineering

APPROVED:

Vivek Tandon, Ph.D., Chair

Raed Al-Douri, Ph.D.

Vinod Kumar, Ph.D.

Charles Ambler, Ph.D.
Dean of the Graduate School

Dedication

I want to dedicate my thesis to my parents, without whose encouragement and prayer, I could not achieve my goal.

ASSESSMENT OF CLIMATE CHANGE IMPACTS ON HYDRAULIC DESIGN PROCEDURES OF BRIDGES

by

ANJUMAN ARA AKHTER, B.Sc

THESIS

Presented to the Faculty of the Graduate School of

The University of Texas at El Paso

in Partial Fulfillment

of the Requirements

for the Degree of

MASTER OF SCIENCE

Department of Civil Engineering

THE UNIVERSITY OF TEXAS AT EL PASO

December 2018

Acknowledgements

First and foremost I like to express my deepest gratitude to my Professor, Committee chair and Mentor, Dr. Vivek Tandon for his constant support, encouragement and patience throughout my M.Sc in the University of Texas, El Paso (UTEP). Without his Constant guidance, this thesis wouldn't happen.

I would also like to express my appreciation to South Plain Transportation Center (SPTC), the funding agency for this study.

My sincere admiration goes to my friend and teammates Dr. Megha Sharma and Armando Esquivel for their valuable insights and helps in the study. I would also like to extend my gratitude to the faculty and staff of the Department of Civil Engineering making my time in UTEP a wonderful experience.

Last but not least, I would like to thank my parents for their love, prayer, patience and beliefs, which make this journey possible.

Abstract

The significant change in climate is evident from the records of increased temperature, changed precipitation pattern, increased frequency of extreme weather events like storms, floods, and so forth. Like other infrastructure highway infrastructures also suffer the consequences of these climate change. Since the hydraulic design of these infrastructures is performed using historical climate data, the designs may not be able to provide services because designs are not considering climate change influence especially in terms of precipitation intensity. This study aims at identifying the most accurate source of climate database that predicts future climate change with less uncertainty and links them into the evaluation of vulnerability and risk of the bridges so that the impact of future climate can be incorporated into the design of new infrastructures. In this study, the NARCCAP database has been used to extract the future climate data for different cities of SPTC representing states. Climate models have predicted as high as 10.2% increase in precipitation for Houston, Texas, which leads to an increase in the magnitude of streamflow in that region. A hydraulic model has been established using HEC-RAS for streamflow modeling. Overtopping depth and scour depth have been estimated as the primary vulnerability stressors of the bridge. This study has estimated the range of the return periods of the floods for which bridge may fail under the predicted future climate scenarios. The annual economic loss has been calculated for the bridges, and possible adaptation strategies have been suggested using HYRISK software.

Table of Contents

List of Tables

List of Figures

Chapter 1: Introduction

1.1Statement of the Problem

Although the impact of climate change on bridge infrastructure needs to be evaluated, the complexity and interdependency of various factors make the aggregation of them to predict the effect of climate change is difficult and challenging. However, assessment of an individual factor such as precipitation is quite possible. Changes in mean precipitation levels have less impact on transportation infrastructure than sea level rise. Though, the runoff resulting from increased precipitation leads to increased peak stream flow, which then impacts the sizing requirement for bridges and other hydraulic structures (Warren et al., 2004).

The prediction of intensity and frequency of precipitation and associated runoff due to climate change can be estimated using existing climate models developed by various agencies (NOAA, USGS, etc.). The available global climate models predict future climate conditions for regions which need to be downscaled and modified before the data can be used for a particular area within the region, thus, further increasing the uncertainty inherent in climate prediction. Additionally, the influence of data from climate model for use in highway infrastructure is a crucial step, which can lead to erroneous conclusions if not inferred correctly.

The modification of existing bridges to survive future climate events can have very large cost implications. Overestimating climate event can result in costly oversizing of infrastructure while underestimating will leave them vulnerable. Therefore, risk and reliability analysis need to be performed to predict the future condition of the structure under climate change.

Based on the discussion, there is a need to evaluate the impact of intensity and frequency of precipitation on existing bridges and propose effective solutions to enhance the service life of highway infrastructure by making them resilient.

1.2 Objectives and Scopes of the Study

The following objectives have been formulated in understanding the climate change impacts on the hydraulic design of bridge infrastructures:

1) To identify the primary climatic stressor for the performance of bridge hydraulics.

2) To recognize and analyze the future change in the climate factor, predicted by climate model simulation.

3) To evaluate the bridge hydraulic design criteria for future climate through risk and vulnerability assessment.

4) To suggest possible adaptation strategies.

Laying focus on the objectives stated above the research has been conducted within the scope of the following tasks:

1) Theoretical Review on the bridge hydraulic design practices followed by different State and Federal agencies.

2) Extracting simulated future climate data from climate models from NARCCAP (North American Regional Climate Change Assessment Program) and modified with an appropriate method.

3) Developing a hydraulic model for the studied bridges using HEC-RAS (Hydraulic Engineering Center-River Analysis System) and communicate the climatic factor to the hydraulic model.

1.3 Contents of the Thesis

In six chapters, this study contains discussion on climate change influence on the hydraulic design of bridge infrastructure by describing various aspects.

- Chapter 1 presents the brief introduction to the nature of the problem and objectives and scopes of the study.
- Chapter 2 provides the literature part of the study which contains review of different climate models, general bridge hydraulics and vulnerability assessment models of bridges

along with the hydraulic design practices by different Department of Transportations (DOTs).

- Chapter 3 contains the extracted climate data from different climate models and analysis of the data.
- Communicating of climate data to the developed hydraulic model have been discussed in chapter 4.
- Chapter 5 describes the vulnerability and risk analysis of the bridge from overtopping and scour and the possible adaptation techniques.
- The thesis ends with chapter 6 that contains the summary, conclusion and recommendations for further research.
- References
- Appendix A contains the bias-corrected climate data for cities of Texas, New Mexico, Louisiana, Oklahoma and Arkansas.

Chapter 2: Literature

2.1 Background

Climate scientists have been conducting studies on the recognition of the pattern of change in different climatic variables and their impacts on the earth systems. In their 5^{th} assessment report, published in 2013, Intergovernmental Panel on Climate Change (IPCC) has been reported an increase of global mean temperature by 0.78^0 C and rising of the sea level by 7.5 inches, over the past century. A report by the U.S. Climate Change Science Program (CCSP) in 2008 provides evidence of changes in weather and climate extremes such as temperature, precipitation which includes droughts, heavy precipitation, tropical storms and cyclones, winter storms etc. According to CCSP 2008 report, in the continental U.S. intense precipitation (the heaviest 1% of the daily precipitation totals) has been increased by about 20% over the past 100 years, while total precipitation increased by only 7%.

A clear indication of climate change leads many agencies to conduct climate change impact studies, such as the Gulf Coast study (Phase I & Phase II).This study includes the impact of climate change on transportation infrastructures. Like other infrastructure systems, transportation infrastructures are also vulnerable to change in different climatic variables like heavy precipitation, rising temperature, increase in sea levels, the frequency of extreme events like hurricanes and storm surges etc. Agencies like the United States Department of Transportation (USDOT) and Federal Highway Administration (FHWA) has done several studies on the impact of the climate change on the transportation infrastructures.

USDOT Gulf Coast Study Phase I (Savonis, Burkett and Potter, 2008), has been done for U.S. central Gulf Coast between Galveston, Texas and Mobile, Alabama. This study showed the vulnerability of the transportation infrastructure to the temperature increase, flooding due to rising sea level and changed precipitation patterns. According to this study, 27% of the major roads, 9% of the rail lines, and 72% of the ports are built on the land which is below 122 cm (4 feet) in elevation and is more vulnerable to frequent or permanent inundation due to change in precipitation pattern. It also reported, more than half of the area's major highways, rail lines, 29

airports and lower elevation ports are in danger of damage due to inundation during hurricane storm surges.

To quantify the vulnerability of the transportation infrastructures to the changing climate, USDOT has developed some tools and approaches in their second phase of the Gulf Coast Study (Hayhoe and Stoner, 2012), which is done in Mobile, Alabama. This study has analyzed the impacts based on future climate data collected from climate models. They have developed a sensitivity matrix to identify potential climate stressors in transportation components. They have also created Vulnerability Assessment Scoring Tool (VAST) which qualitatively evaluate the assets vulnerability.

In 2010 to 2011, different DOTs and Metropolitan Planning Organizations (MPOs) have conducted five climate change resilient pilots, to assess the climate change impacts on different transportation assets. These studies have been conducted based on FHWA's conceptual risk assessment model (FHWA website).

Metropolitan Transportation Commission: San Francisco Bay (FHWA,2012) has developed inundation maps for the coast region using future projection climate data. They reported nearly all the shoreline assets would be inundated with the extreme sea level rise scenario. The future projection shows minor flooding in mid-century, but the end of the century will face major flooding which will require drastic adaptation strategies. A pilot study done by the New Jersey Transportation Planning Authority (FHWA,2012), showed the impact of increased heat on transportation assets and the rise of sea level to infrastructures near the shoreline. It was reported that temperatures higher than 95°F would increase the risk of rail kinks and during extreme heat overhead wires may sag or experience pulley failures.

In 2013-2015, FHWA did 19 pilot studies with the help of different DOTs and MPOs based on the 'Climate Change and Extreme Weather Vulnerability Assessment Framework, 2012', which is illustrated in Figure 2.1, which has been later modified in the 3rd edition of the report (Filosa et al.,2017). In these studies, different agencies worked on climate change impact on different

transportation assets. They have used the FHWA's framework to assess the vulnerability of the assets and come up with adaptation options and resiliency improvement.

Iowa DOT (Anderson et al.,2015) has conducted a climate change impact study on the vulnerability of bridges, specially due to the increase in peak stream flow resulted from increased precipitation, predicted by 19 climate models. They have analyzed 6 bridges in Iowa and suggest possible adaptation strategies. Connecticut DOT (Hogan et al., 2014) have conducted a system-level vulnerability assessment of bridge and culvert for inland flooding resulted from rainfall events. In this study, they evaluated 52 structures for current precipitation data and analyzed their sufficiency in design. 65% of the structure satisfied design criteria. They have shown the connection of precipitation data to a hydraulic model of the channel using USGS regression equations or stream stats. Moreover, the Minnesota DOT (Almodovar-rosario et al., 2014) have studied bridge and culverts resiliency against flash flooding, predicted for future climate scenarios. They have evaluated structures for three risk level, low, medium and high represented by RCP 4.5, 6.0 and 8.5). The study also analyzed the adaptation options through economic analysis using COAST tool.

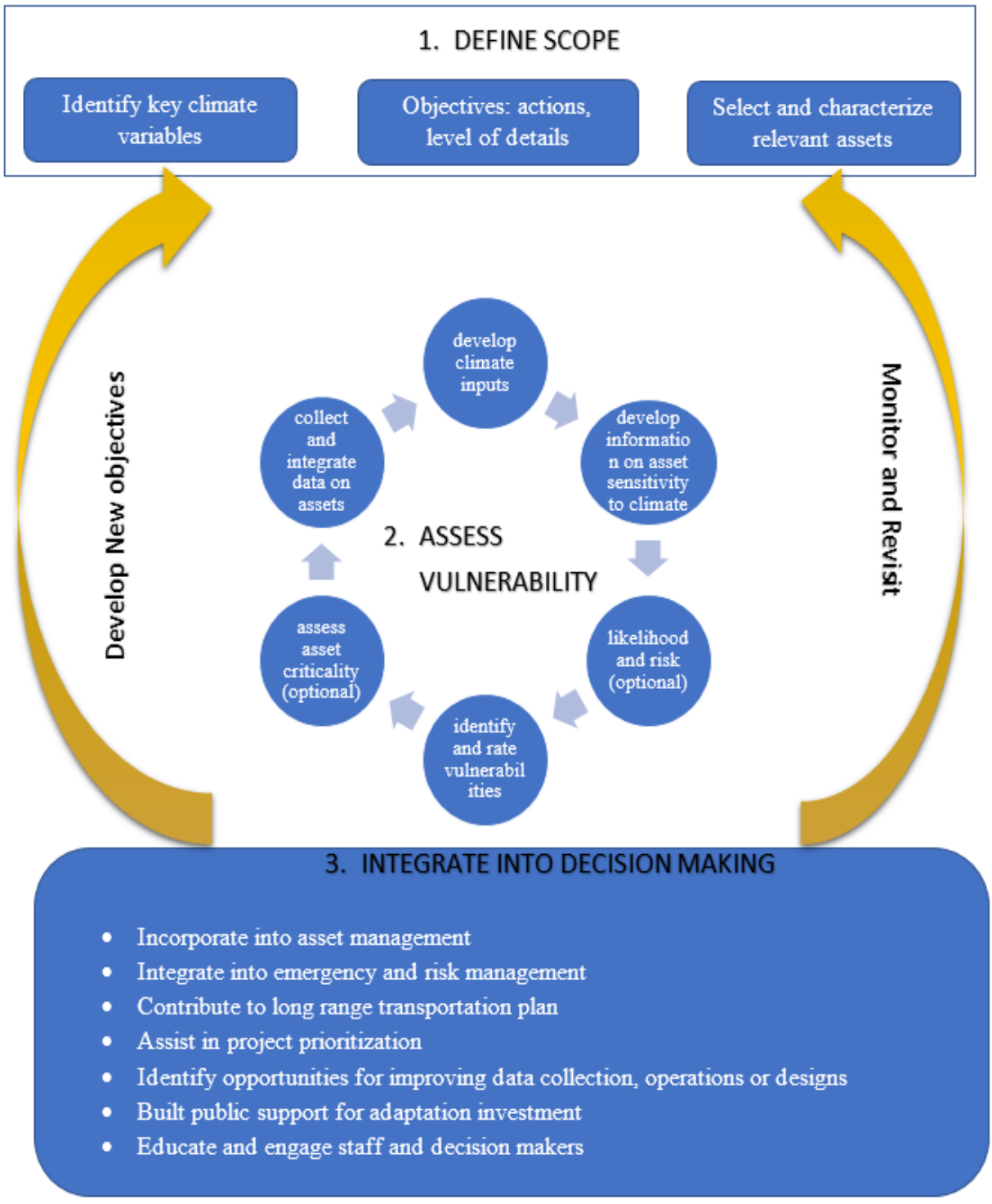

Figure 2-1 Framework for Vulnerability Assessment due to Climate Change and Adaptation (FHWA, 2012)

Research has been less focused on rectifying the disparity between the output of the climate models and the needed input for bridge hydraulic engineers to incorporate climate change in current design practices. Climate models are generally too coarse spatially and temporally for use in hydraulic design, nor are climate models built with the intent to design new bridges. Hydraulic design techniques rely on rigorous statistical analysis of historical observations whereas climate is based on complex sets of interdependent parameters to describe the physical processes between the atmosphere, ocean and land. Hydraulic design techniques of bridges look at stationary sets of past data to project the future, whereas climate models are trained on past observations but then are forced by assumed increases in greenhouse gases to predict the future, often in a non-stationary manner. Therefore, this study focuses on draw inferences from climate data to check on the resiliency of the bridge infrastructures for this future climate and identify the possible adaptation techniques.

2.2 Climate Models

Climate scientists have established General Circulation Models or Global Climate Models (GCMs), based on the assumptions of the changes in greenhouse gas (GHG) concentrations. Although there are several greenhouse gases whose are responsible for climate change, CO_2 is the main anthropogenic GHG, and all other gases are generally reported as the equivalent of CO_2. Based on the assumptions of the future projected changes in GHG concentrations along with other factors, such as technological changes, economic conditions etc., climate modelers have designed different emission scenarios. IPCC has published their first formal set of emission scenarios in the Special Report on Emission Scenarios (SRES) in 2000. Based on socio-economic conditions and technological changes in the 21st century, the SRES scenario set consists of four descriptive storylines.

- A1 scenario: Rapid growth of the economy, peaks of the global population in the mid-century and declining after that, the introduction of new and efficient technologies,

encompasses the storyline behind A1 emission scenario set. This particular scenario further deduces into three more categories based on their technological emphases, such as fossil intensive energy source (A1F1), non-fossil energy source (A1T) or a balance across all sources (A1B).

- A2 scenario: This storyline describes the segmented development, where economic growth will be regionally oriented, technological changes will be fragmented and slower than other storylines. But in this storyline, the global population will increase continuously.
- B1 scenario: Like storyline A1, this also describes a world with peaks of the population in the mid-century and decline thereafter, but rapid changes of the economy towards service and information economy and the introduction of clean resource technologies. This includes global solutions toward social, economic and environmental sustainability, but no climate initiatives.
- B2 scenario: Like B1 this storyline also emphasis on solutions to economic, social and environmental sustainability, but locally. It describes a continuously increasing global population with a rate of less than A2, medium level of economic development and diverse technological change.

According to NOAA (2016), at the end of 2015, the concentration of CO_2 was recorded as 400 ppm. Meanwhile, SRES scenarios predict the increase of CO_2 concentration as high as 750 ppm. And for high-end scenarios like A2, the concentration of CO_2 is not even stabilize at the end of the 21st century and will continue to increase (Kilgore et al., 2016).

In their Fifth Assessment Report (AR5) in 2013, IPCC has published their second set of emission scenarios named the Representative Concentration Pathways (RCPs). The improvement in the RCP scenario sets are, they consist of the potential changes in climate policy and the effects of potential adaptation strategies. Four RCP have been established based on the projected radiative forcing pathway, where radiative forcing is a measure of the change in the energy balance on the earth caused by increases in the concentration of GHGs.

- RCP 2.6 describes a very low greenhouse gas emission. The peak radiative forcing will be at 3 W/m^2 before 2100, which will then decline to 2.6 W/m^2 by 2100.
- RCP 4.5 is a stabilization scenario, where stabilization occurs at 4.5 W/m^2.
- RCP 6.0 is also a stabilization scenario, where stabilization occurs at 6.0 W/m^2 after 2100.
- RCP 8.5 describes an increasing greenhouse gas emission scenario, where radiative forcing rises to 8.5 W/m^2 by 2100.

As GCMs produces a coarse output, to perform local-scale or regional impact studies, GCM outputs cannot be used directly. Hence the downscaling is necessary to produce data in finer spatial resolution. Downscaling methods are mainly categorized either as statistical downscaling or dynamic downscaling. Statistical downscaling uses a statistical relationship between GCMs output and historical measurements of climate variable of interest. Some common statistical downscaling methods are, Bias Corrected Constructed Analogues (BCCA), Asynchronous Regional Regression Model (ARRM), and Bias-Corrected Spatially Downscaled (BCSD). The advantages of using these statistical methods include low computational cost and application to a diverse set of GCMs with ease. The major limitation in using statistical method is that these approaches assume a constant relationship between large-scale GCMs variable and local variable under climate change. Dynamic downscaling uses high resolution, small spatial distribution Regional Climate Models (RCMs), which are produced from the GCMs by applying initial and lateral boundary conditions (LBDs). Possessing finer resolution and critical dynamic processes make the prediction of RCMs more reliable. Advantages of using dynamic downscaling also include, RCMs accounts for the influence of mountains, lakes and coastlines which are absent in case of the parent GCM. Researchers (Gutowski et al., 2010 and Roads et al., 2003) also showed that RCMs could capture extreme climatic events more accurately. Limitations in the account of dynamic downscaling methods are the high computational cost which leads to the limited application in GCMs.

Based on the emission scenarios, GCMs and downscaling methods, there are several sources available to climate projection data for different variables. The preferred sources by FHWA are as follows:

- DCHP (*Downscaled CMIP3 and CMIP5 Climate and Hydrology Predications*), which predicts future climate data for most fine spatial resolution of 1/8 degree or roughly 7.5 × 7.5 miles. CMIP3 consists of downscaled projected climate result from 25 GCMs which use SRES scenarios A2, A1b and B1. CMIP5 comprises downscaled data from 29 GCMS using RCP scenario sets.
- USGS geodata portal has downscaled data from a variety of sources. They use statistical downscale method ARRM.
- NA-CORDEX (*North American Coordinated Regional Climate Downscaling Experiment*) is a web data source that provides dynamically downscaled datasets for various RCMs.
- NARCCAP (*North American Regional Climate Change Assessment Program*) consists dynamically downscaled data of 12 climate models comprising six RCMs and four GCMs, based on SRES A2 scenarios for spatial resolution of 50 x 50 km.

  In this study, we have used the NARCCAP data sources for the climate projection data.

2.3 Bridge Hydraulic Design Practices

2.3.1 General Bridge Hydraulics

Given that hydraulic analysis of bridges depends on a range of factors, like topographic data, river conditions, proper streamflow estimation, accuracy in flow modelling approaches or the floodplain conditions etc., it is a complicated process. Besides, regulatory requirements set by different agencies (i.e. FHWA, USACE, FEMA etc.) must be satisfied to choose a proper hydraulic analysis model for bridges (Zevenbergen, Arneson, Hunt and Miller, 2012).

Generally, hydraulic analysis of bridges is done by computing the energy losses caused by the structure. Creating the proper model of the bridge section is primarily important for this. Modelling of bridge sections depends on:

- Bridge cross-section locations
- Flow types of the bridge sites
- Hydraulic flow computation

Bridge cross-section locations

The performance of hydraulic analysis of the bridge required four cross sections along the river. These cross sections help to capture the characteristics (contraction and expansion) of the flow through bridge opening. Figure 2-2 shows the plan view of the four controlled sections. The first cross-section, the cross-section one should be located sufficiently downstream of the structure. The function of this cross section is to capture the expansion of the flow after passing through the bridge opening. Cross section 2 and three should be located near to the bridge at upstream and downstream respectively. However, they should not be placed at the immediate face of the bridge deck, to let the flow have some expansion and contraction respectively. The cross-section 4 is an upstream cross-section which takes in the distance to capture the contraction characteristic of the flow. In Figure 2-2, the Le and Lc values represent the distance between two downstream cross-section and upstream cross-section respectively. These values are generally determined from the field observation during the high flows. Although, usually Le value is twice to the Lc value.

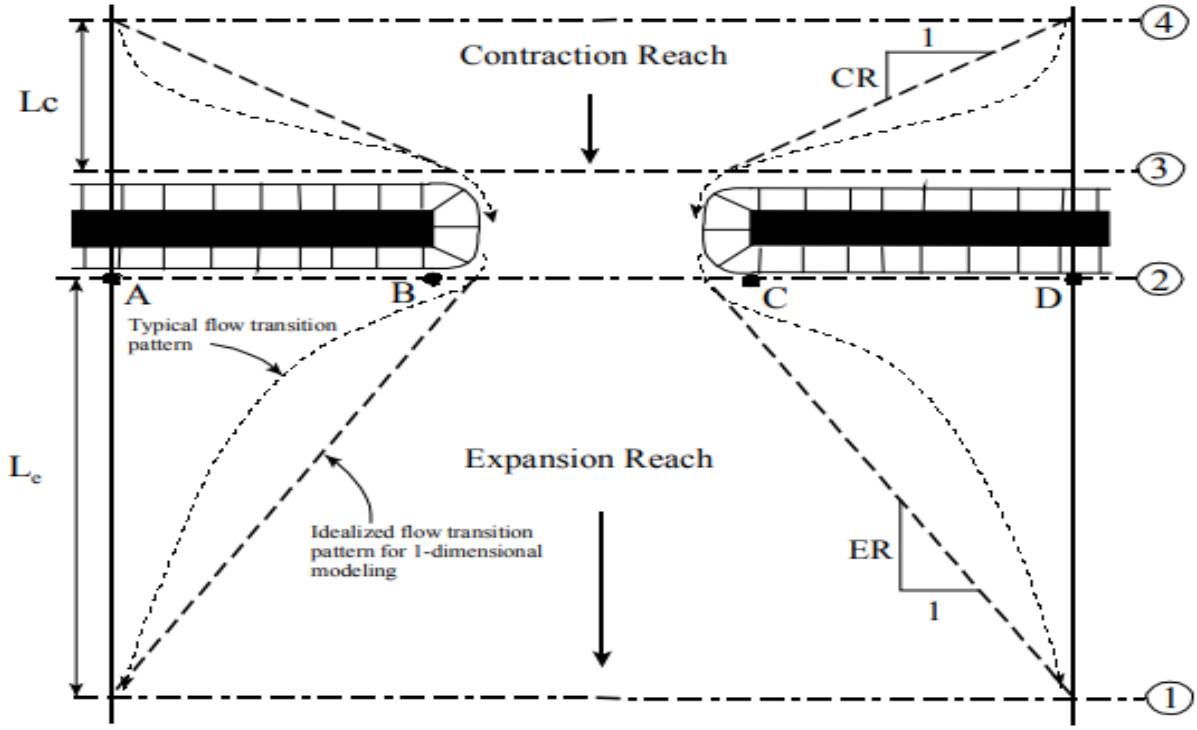

Figure 2-2 Plan View of Cross-sections needed for Bridge Hydraulics (Brunner et al., 2008)

Flow types of the Bridge Sites

Understanding the exact flow types that bridge is going to encounter, is one of the significant factors in hydraulic computations of bridges. Flows corresponding to bridge structure can be either a low flow or high flow.

Low flow exists when the flow can pass through the bridge opening. Figure 2 3 shows an example of Low flow condition in the bridge. Low flows are classified (A to C) based on the depth of the flow with respect to the critical depth of the flow. When the depth of the flow exceeds the critical depth (or normal water surface), subcritical flow condition takes place. Similarly, when the depth of flow is below the critical depth supercritical flow condition takes place. Class A low flow is entirely subcritical flow, meaning the flow depth exceeds the critical depth, where gravitational forces dominate, and the flow behaves subtly. Conversely, Class C flow is completely supercritical flow. Class B can be either subcritical or supercritical.

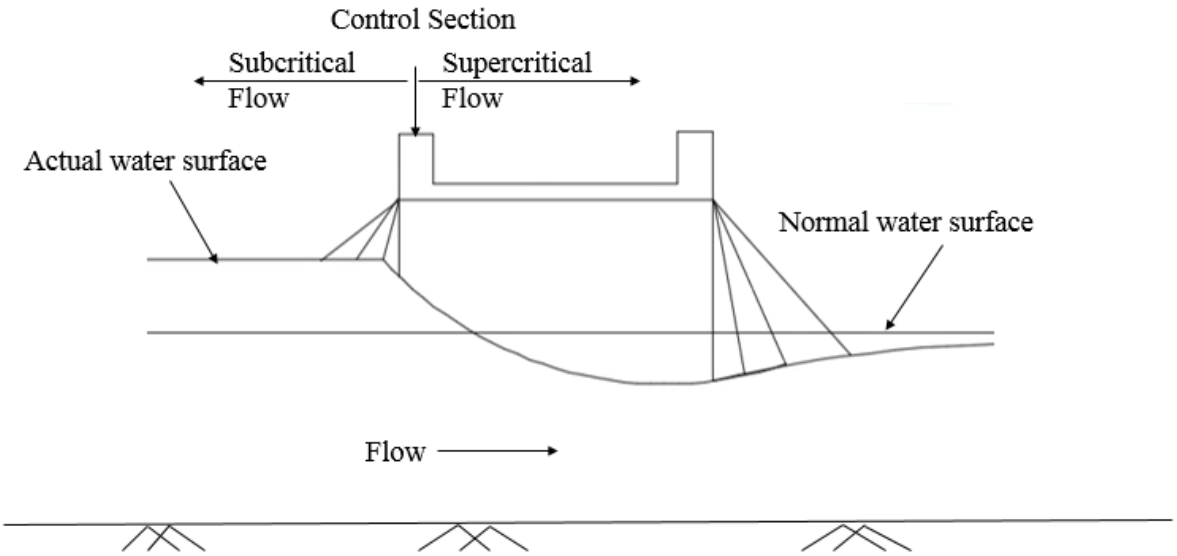

Figure 2-3 An Example of Low Flow in Bridge

High flow occurs when the flow depth exceeds the elevation of the high point of the low chord of the bridge. High flows can be estimated as sluice gate flow, orifice type flow or weir type flow. Figure 2-4 shows the example of the high flows in the bridge.

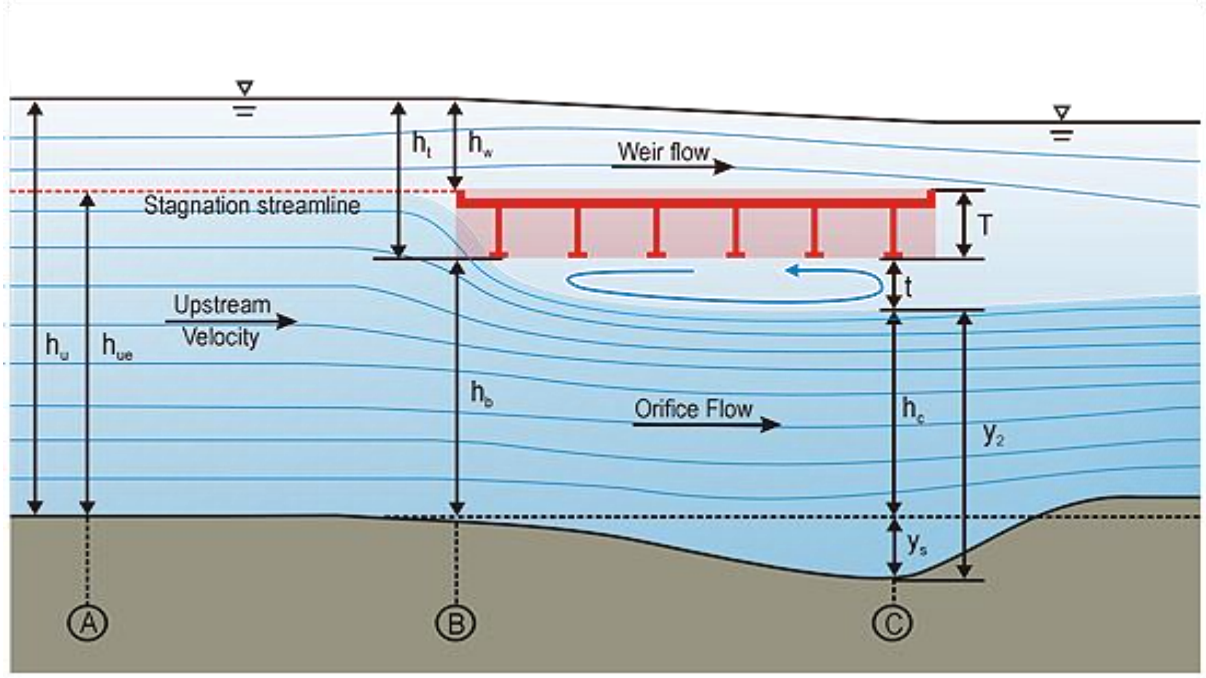

Figure 2-4 An Example of High Flow in Bridge (Shan et al., 2012)

- Sluice gate type flow exists when the water surface is in level with the low chord in upstream and below in the downstream.
- Orifice type flow occurs when low chord at both upstream and downstream is submerged.
- Weir type flow exists when the roadway, even the whole bridge is submerged.

Hydraulic flow computation

The methods available for low flow and high flow conditions are as follows:

For low flow computations:

- **Energy Equation or Standard Step Method**: Based on the energy losses between an upstream and downstream section of the bridge this method computes the water surface profile.
- **Momentum Balance Method:** This method performs the flow computation based on momentum balance between flow areas of two sections (downstream to upstream sections).
- **Yarnell Equation:** This is an empirical method that predicts the change in water surface from downstream to upstream section. This method is not dependent on the bridge opening, size of abutments or width of the bridge. So this method is only reliable where energy losses of the bridge mostly occur in piers.
- **FHWA WSPRO Method:** This method also computes the water surface profile by solving the energy losses between sections from downstream to upstream. The only difference for this method is that it considers the sections sufficiently upstream and sufficiently downstream.

And for high flow computations one of the following methods has to be chosen:

- **Energy Equation or Standard Step Method:** For high flow, this method also performs the same way as for low flow.
- **Pressure Flow Method:** This method performs the flow computation when the flow reaches to the point of the low chord of the bridge or submerged the bridge.

2.3.2 Overtopping and Scour Assessment

Vulnerability has been delineated as the magnitude to which a transportation infrastructure can sustain by tolerating the harms caused by climatic events. It is a function of the sensitivity of the infrastructure to the effects of climate change, adaptive capacity and the degree of exposure. The primary objectives of a climate change vulnerability assessment are to determine how climate change may impact transportation assets and prioritize measures to maximize the impact and minimize costs.

The vulnerability of bridges is mainly assessed based on the overtopping potential or scour criticality potential during an extreme climatic event. During an extreme climate event like flooding bridges along with the roadways get vulnerable to be overtopped, results in closure of the roads.

Some agencies have developed some method to identify and locate vulnerable locations in the transportation system (Filosa and Oster, 2015).

- The Danish Road Directorate follows the Blue Spot method- a four-level analysis to identify roadway locations where the likelihood of floods is high, and consequence of flooding is significant.
- The ROADAPT research project, a joint research effort supported by several European countries, developed a preliminary risk assessment method that can identify vulnerable locations in the transportation network, understand the probabilities and consequences that climate change events could have on these locations, and provide options for adaptation actions.

Given that one of the most concerning cause of bridge failures is from floods scouring bed material from around bridge foundations, estimation of the depth of scour is a complex practice. According to the researcher (Lagasse et al., 2007, Wardhana and Hadipriono, 2003), 50 % to 60% of the bridge failures in the USA are caused by scouring. Scouring can remove the soil from the foundation of the bridge, and in case of heavy loss of soil particle the bridge collapse. In 2003,

during a heavy rain of 11 inches, the Loon Mountain Bridge in Lincoln, New Hampshire collapse due to scouring.

According to Bridge Scour Evaluation Program, run by FHWA in 2011 on a total number of 493,473 bridges including Interstate, National Highway System (NHS) and Non-National Highway System bridges. They have reported total 23,034 bridges are scour critical including all three categories, which results in 4.7% of total bridges. Table 2-1 shows the status of that report.

Table 2-1 Survey Report of Bridge Scour Evaluation by FHWA (Arneson et al., 2012)

Total Number of Bridges Surveyed	Evaluation Criteria	Interstate Bridges	NHS Bridges	Non-NHS Bridges	Total	Percent of Total
493,473	Needing Evaluation	80	136	3,701	3,917	0.80%
	Foundation Unknown	55	703	40,067	40,825	8.30%
	Scour Critical	937	1,936	20,181	23,034	4.70%

The principal scours tool for U.S. bridge designers is Hydraulic Engineering Circular No. 18 (HEC-18) published by the FHAWA (Arneson et al., 2012). The currently available version of the documents is the 5th edition which presents the state of knowledge and practices for the design, evaluation and inspection of bridges for scouring. This document contains updated material from previous editions and combined research by FHWA, state DOTs and universities.

HEC-18 suggests scouring estimation based on soil and rock criteria along with other geotechnical considerations. The total scour compiles the contraction scour, and local scour as pier and abutment scour. Contraction scour occurs due to the reduction of the flow area of the stream at flood stage by a natural contraction of the channel or by a structure (Arneson et al., 2012). The underlying mechanism causing local scour at piers or abutments is the formation of vortices at their base (Arneson et al., 2012). The steps and equations adopted in HEC-18 for these scour estimations have been summarized below:

Contraction Scour:

Based on the mechanism of the transport of the bed material contraction can be estimated as live-bed sour or clear-bed scour. For the live-bed scour estimation the following equation has been used, which is a modified version of Laursen (1963) equation:

$$\frac{y_2}{y_1} = (Q_2/Q_1)^{6/7}(W_1/W_2)^{k1} \quad (2\text{-}1)$$

$$y_s = y_2 - y_0 \quad (2\text{-}2)$$

Where,

y_1 = Water depth in the upstream main channel

y_2 = Water depth in the contracted section

y_0 = Existing depth in the contracted section before scour

Q_1 = Flow in the upstream section

Q_2 = Flow in the contracted channel

W_1 = The Bbottom width of the upstream main channel

W_2 = The Bbottom width of the contracted main channel

$k1$ = Exponent explaining mode of bed material transport

The equation used for clear-bed contraction scour estimation is stated below, which is also derived from the Laursen's (1963) equation.

$$y_2 = \left[K_u Q^2/D_m^{2/3}W^2\right]^{3/7} \quad (2\text{-}3)$$

$$y_s = y_2 - y_0 \quad (2\text{-}4)$$

Where,

y_2 = Water depth in the contracted section

y_0 = Existing depth in the contracted section before scour

K_u = 0.0077

Q = Discharge through the bridge

W = Width of the bridge section

D_m = Diameter of the smallest non-transportable bed material

Pier Scour:

For the estimation of the scour on the pier, HEC-18 has adopted the Colorado State University (CSU) equation, which is stated below:

$$\frac{y_s}{a} = 2.0K_1K_2K_3(y_1/a)^{0.35}Fr_1^{0.43} \quad (2\text{-}5)$$

Where,

y_s = Scour depth

y_1 = Flow depth immediately upstream of the pier

a = Pier width

K_1 = Correction factors for pier nose shape

K_2 = Correction factor for the angle of attack of flow

K_3 = Correction factor for bed condition

Fr_1 = Froude number immediately upstream of the pier

Abutment Scour:

HEC-18 suggests the use of Froehlich's (TRB 1989) live bed scour equation or the HIRE equation in HDS 6 (FHWA 2001a) for abutment scour estimation. The Froehlich's equation which is based on 170-lab experiments for live bed scour is stated as below:

$$\frac{y_s}{y_a} = 2.27K_1K_2(L'/y_a)^{0.43}Fr^{0.61} + 1 \quad (2\text{-}6)$$

Where,

K_1 = Coefficient for abutment shape

K_2 = Coefficient for the angle of the embankment to flow

L' = Length of the flow obstructed by the embankment

y_a = The average depth of flow on the floodplain

Fr = Froude number for the approaching flow on the upstream of the abutment

Based on the field data of scour at the end of spurs in Mississippi River, FHWA derived the following equation, named HIRE equation in 2001:

$$\frac{y_s}{y_1} = 4\, Fr^{0.33} \frac{K_1}{0.55} K_2 \qquad (2\text{-}7)$$

Where,

y_s = Scour depth

y_1 = Depth of flow in the main channel

Fr = Froude number

K_1 = Abutment shape coefficient

K_2 = Coefficient of the skew angle of the abutment to flow

2.3.3 Bridge Hydraulic Design Practices by DOTs

This section discusses the common practices adopted by DOTs of the SPTC representative states: Texas (TxDOT), New Mexico (NMDOT), Louisiana (LDOT), Oklahoma (ODOT) and Arkansas (ArDOT).

DOTs follow the similar principle in hydraulic analysis during the design of bridges. The analysis should be performed based on the effects of a backwater, flow distribution and velocities and potential scour measurements for a particular flood frequency (TxDOT, 2004; ASHTD, 1982; NMDOT, 1998; LDOT, 2011). According to all DOTs risk associated with these parameters should be checked for bridge hydraulic design.

The flood frequency or the Annual exceedance probability (preferred by TxDOT) for hydraulic design of a bridge is 50-years or 2% (AEP), which is practised by most DOTs. Louisiana Department of Transportation (LDOT) preferred 25-years or 50-years based on the local condition. However, design flood frequencies must be justified by risk analysis.

According to AASHTO Load and Resistance Factor Design (AASHTO LRFD) (2005), backwater effect should be estimated for 100-year flood as base flood and for a 500-year flood.

The following Table 2-2 shows the standard design floods for hydraulic, scour and scour countermeasures suggested by FHWA.

Table 2-2 Design Flood Frequencies for Hydraulic Design, Scour Design and Scour Design Countermeasures (Arneson et al., 2012)

Flood Frequency for Hydraulic design	**Flood Frequency for Scour**	**Flood Frequency for Scour Countermeasures**
Q_{10}	Q_{25}	Q_{50}
Q_{25}	Q_{50}	Q_{100}
Q_{50}	Q_{100}	Q_{200}
Q_{100}	Q_{200}	Q_{500}

For scour, potential measurement all DOTs follow the guidelines and regulations of HEC-18 by FHWA. However, ODOT, NMDOT and LDOT follow the AAHSTO LRFD Bridge Design Specifications. The zest of the specifications are as follows:

- Using HEC-RAS for hydraulic analysis and HEC-18 for scour analysis
- Hydrologic analysis should be done for 2,5,10,25,50,100,200,250 and 500-year floods
- Scour should be estimated for 100-year flood and 500-year flood or overtopping flood if the overtopping flood is less than the 500-year flood.
- Scour depth prediction is mainly emphasis on pier and contraction scour
- For abutment scour countermeasures or armouring is preferred

Given Louisiana has great potential for flooding and migrating, predicted scour depth is the same for all the piers and end bents of main bridges as well as relief bridges.
FHWA increases the standard for scouring design flood from 100-yr to 200-yr floods, although the hydraulic design flood frequency is 100-yr.

DOTs followed the guidelines proposed in the HEC-23 manual by FHWA for the prevention and protection measures for bridges against scouring or overtopping. For pier scour, the general considerations are:

- Reduced number of piers in the main channel,
- Using circular piles,

- Using drilled shaft foundations,
- Aligning the bents to the flow direction and increasing bridge length for reduced through bridge velocities.
- HEC-23 suggests concrete riprap, stone protection, gabions and grout-filled or sand/ cement filled bags for armouring of pier or abutments to prevent from scouring.

Along with these measures, LDOT also prefers to maintain the slope of the abutment as 3:1, (horizontal to vertical ratio) and minimum total scour depth at 5 feet (LDOT,2011).

Chapter 3: Climate Data

3.1 Selection of Climate Stressor

The identification of appropriate climatic stressor for the risk and vulnerability assessment of transportation infrastructure is a must to employ an effective adaptation strategy. The Federal Highway Administration's Climate Change and Extreme Weather Vulnerability Assessment Framework (FHWA,2012), have lined up the procedure to identify the essential climate variables, such as temperature, extreme precipitation events, Sea-level and coastal storm surge, permafrost thaw, snowmelt hydrology etc.

Hydraulic design of bridges is generally done for various frequency and intensity of flood events. Precipitation is the primary climatic variable that contributes directly to flood flow. Although, the temperature is often considered as a climatic factor in bridge vulnerability due to its role in flood events. For instance, a warmer atmosphere can hold more water, and this could lead to larger storms with increased intensities and frequencies. Although warmer atmosphere leads to the drier soil which increases the infiltration of water to soil consequently decreases the amount of runoff. For this study, precipitation has been chosen as the primary climatic stressor.

3.2 Climate Data Extraction

Global climate models (GCMs) capture the future trajectories of greenhouse gas emissions and reaction of the global climate system to it. But GCMs provide information for rather high spatial regions. For local climate change impact analysis, data from GCMs must be downscaled to the local scale with finer spatial resolution employing downscaling methods. Among the various sources mentioned in the previous chapter, the North American Regional Climate Change Assessment Program (NAARCAP) data source has been used in this study for future climate change projections of different parameters. The reasons behind using this source are as follows:

- **Availability:** The data are easily downloadable given the fact this comes up with grid maps. So, for known coordinates (Latitudes and Longitudes) of the stations, the data can be retrieved from the portal.
- **Spatial and Temporal Resolution:** The source provides data with 50 X 50 km spatial resolution and 3-hr temporal resolution.
- **Downscaling Method:** NARCCAP uses the dynamic downscaling for the projection of the future climate data.

NARCCAP program covers the climate change simulations for Conterminous United States (CONUS) and most of Canada (Mearns et al., 2007). This program has been established based on A2 emission scenario set from SRES for climate projections of the 21st century. Using the boundary conditions derived from GCMs, Regional Climate Models (RCMs) have been developed to generate climate data at higher resolution. Climate models established with GCMs and RCMs in this program performs simulation at a spatial resolution of 50 X 50 km.

NARCCAP source uses four GCMs and six RCMs. The used RCMs are: 1) Canadian Regional Climate Model (CRCM); 2) Hadley Regional Model 3 (HadRM3); 3) Mesoscale Model 5 (MM5); 4) the National Center for Atmospheric Research, Weather Research and Forecasting (WRF); 5) RegCM3; and 6) Regional Spectral Model (RSM). The GCMs used in NARCCAP programs are: 1) CCSM; 2) HadCM3; 3) CGM3 and 4) the GFDL model. Twelve climate models available in NARCCAP data source using these GCMs and RCMs are listed in Table 3.1.

NAARCAP program is a two-phase program, wherein phase I, six RCMs use boundary conditions from the NCEP-DOE Reanalysis 2 for production of 25 years (1980-2004) simulations. In phase II, NARCCAP uses 4 GCMs and 6 RCMs to run simulations of 30 years (1971-2000) current data and production of 30 years (2041-2070) future data.

NARCCAP data are accessible to download for a location using the geographic coordinate system (Latitude and Longitude). Using available grid cell maps within the NARCCAP program, different climate variables from RCMs can be extracted.

Table 3-1 Climate Models in NARCCAP

RCMs	**GCMs**	**Emission Scenario**
CRCM	CCSM	A2 Storyline
CRCM	CGM3	A2 Storyline
ECP2	GFDL	A2 Storyline
ECP3	HADCM3	A2 Storyline
HRM3	GFDL	A2 Storyline
HRM3	HADCM3	A2 Storyline
MM5I	CCSM	A2 Storyline
MM5I	CGM3	A2 Storyline
RCM3	GFDL	A2 Storyline
RCM3	CGM3	A2 Storyline
WRFG	CCSM	A2 Storyline
WRFG	CGM3	A2 Storyline

3.3 Climate Data Plots

This study analyses the climate change phenomenon for all the SPTC representative states (Texas, New Mexico, Louisiana, Oklahoma and Arkansas). This section presents the future climatic conditions of different cities of different states regarding the change in mean annual precipitation and means annual temperature concerning existing observed climate data. Existing temperature and precipitation data have been collected from AASHTOware pavement ME design software website, which documents the data from North American Regional Reanalysis (NARR) program in NOAA.

Figure 3-1 to 3-5 shows the future mean annual precipitation predicted by climate models with a comparison of existing one, for different cities of Texas, New Mexico, Louisiana, Oklahoma and Arkansas. Most of the climate models predict an increase in precipitation for the cities of Texas and New Mexico, where existing mean annual precipitation ranges between 10 to 45 inches and 10 to 15 inches. But for Louisiana, Oklahoma and Arkansas, most of the models predict a decrease in precipitation, where existing precipitation ranges between 50 to 60 inches, 30 to 40 inches and 40 to 50 inches.

Figure 3-6 to 3-10 shows the future mean annual temperature predicted by climate models with a comparison of the existing one, for different cities of Texas, New Mexico, Louisiana, Oklahoma and Arkansas. Most of the climate models predict an increase in mean annual temperature for cities of Texas, Louisiana, Oklahoma and Arkansas, but decrease for New Mexico.

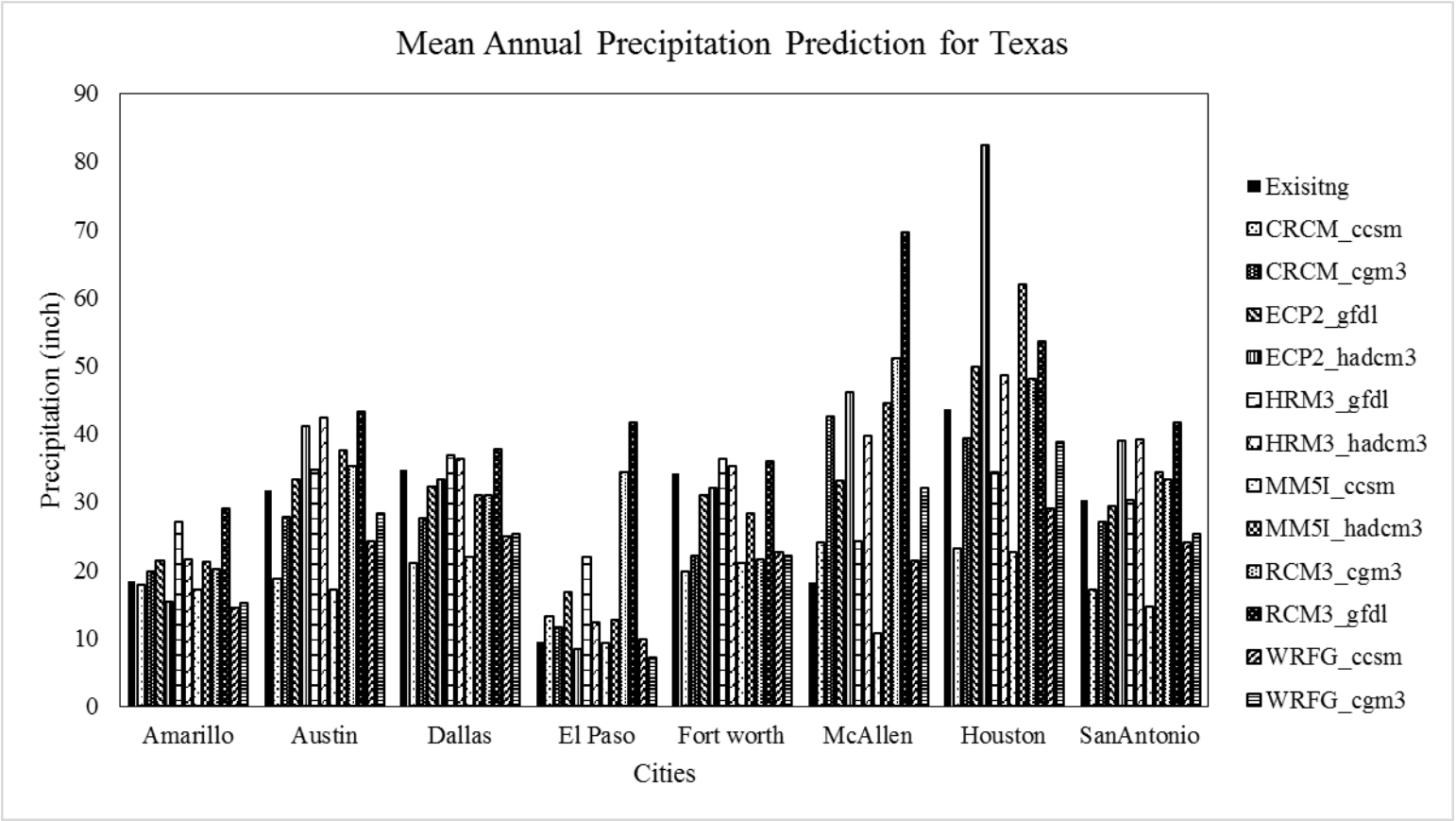

Figure 3-1 Mean Annual Precipitation of Different Cities of Texas for Climate Prediction Models (2041-2070)

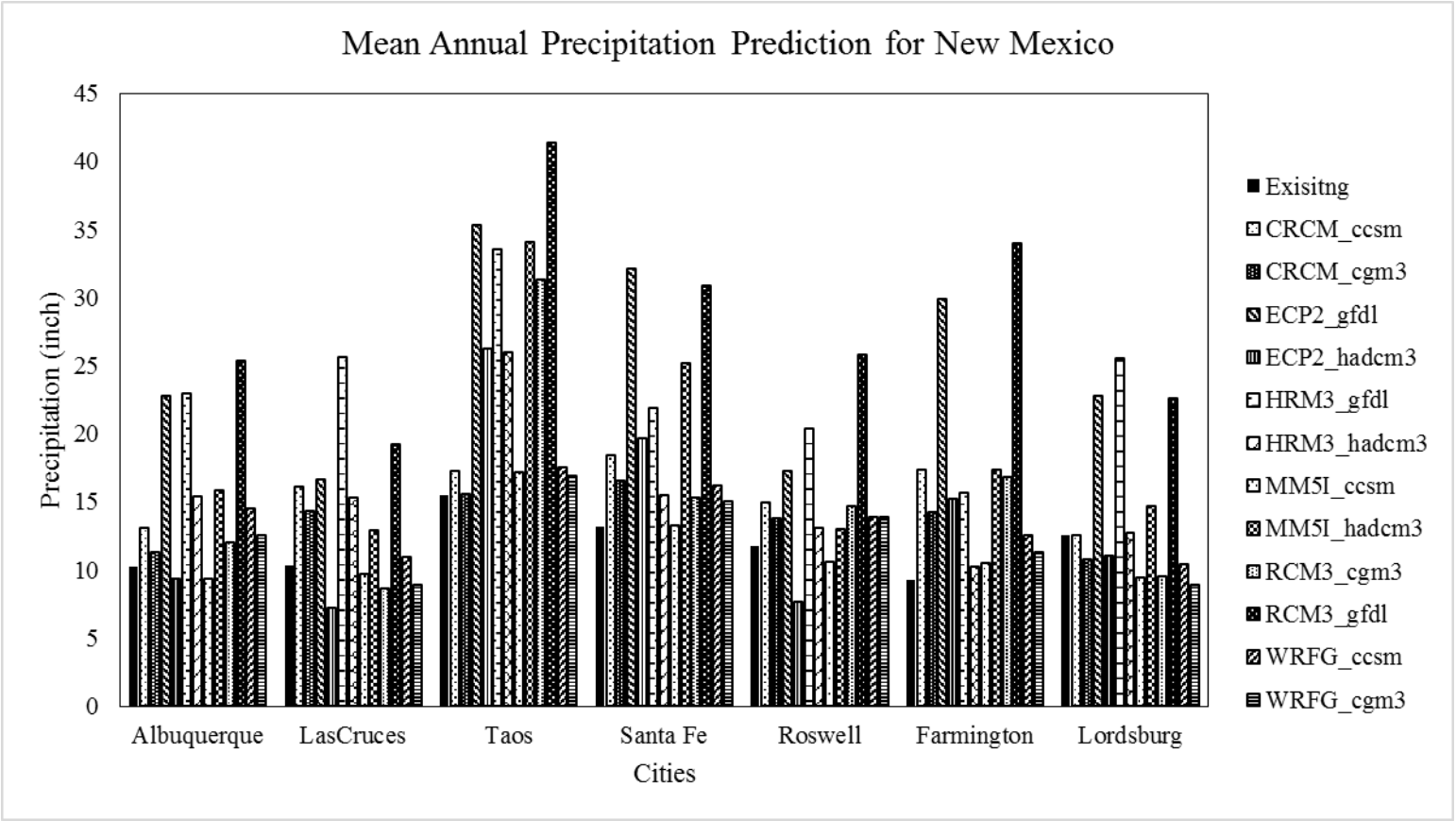

Figure 3-2 Mean Annual Precipitation of Different Cities of New Mexico for Climate Prediction Models (2041-2070)

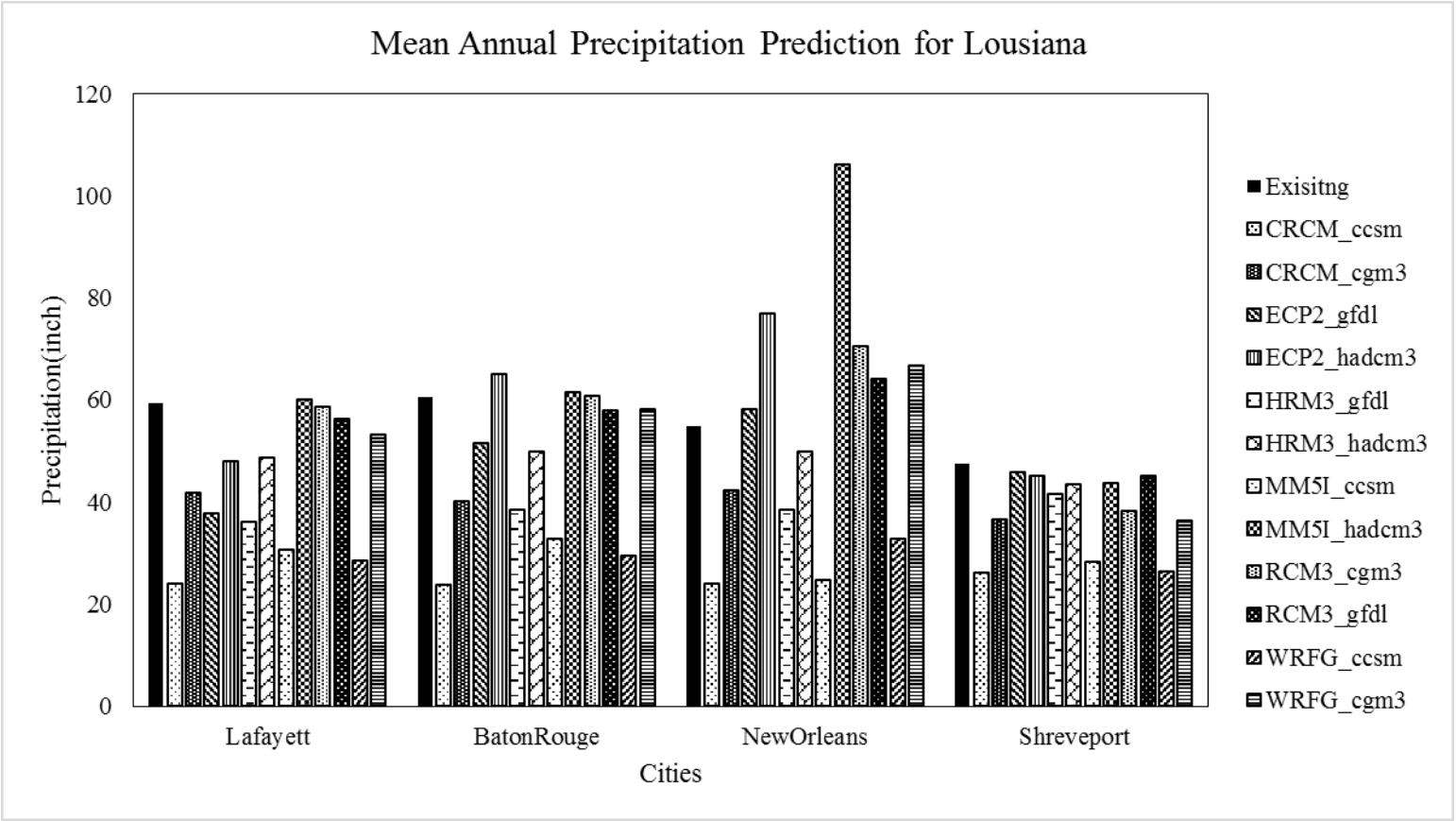

Figure 3-3 Mean Annual Precipitation of Different Cities of Louisiana for Climate Prediction Models (2041-2070)

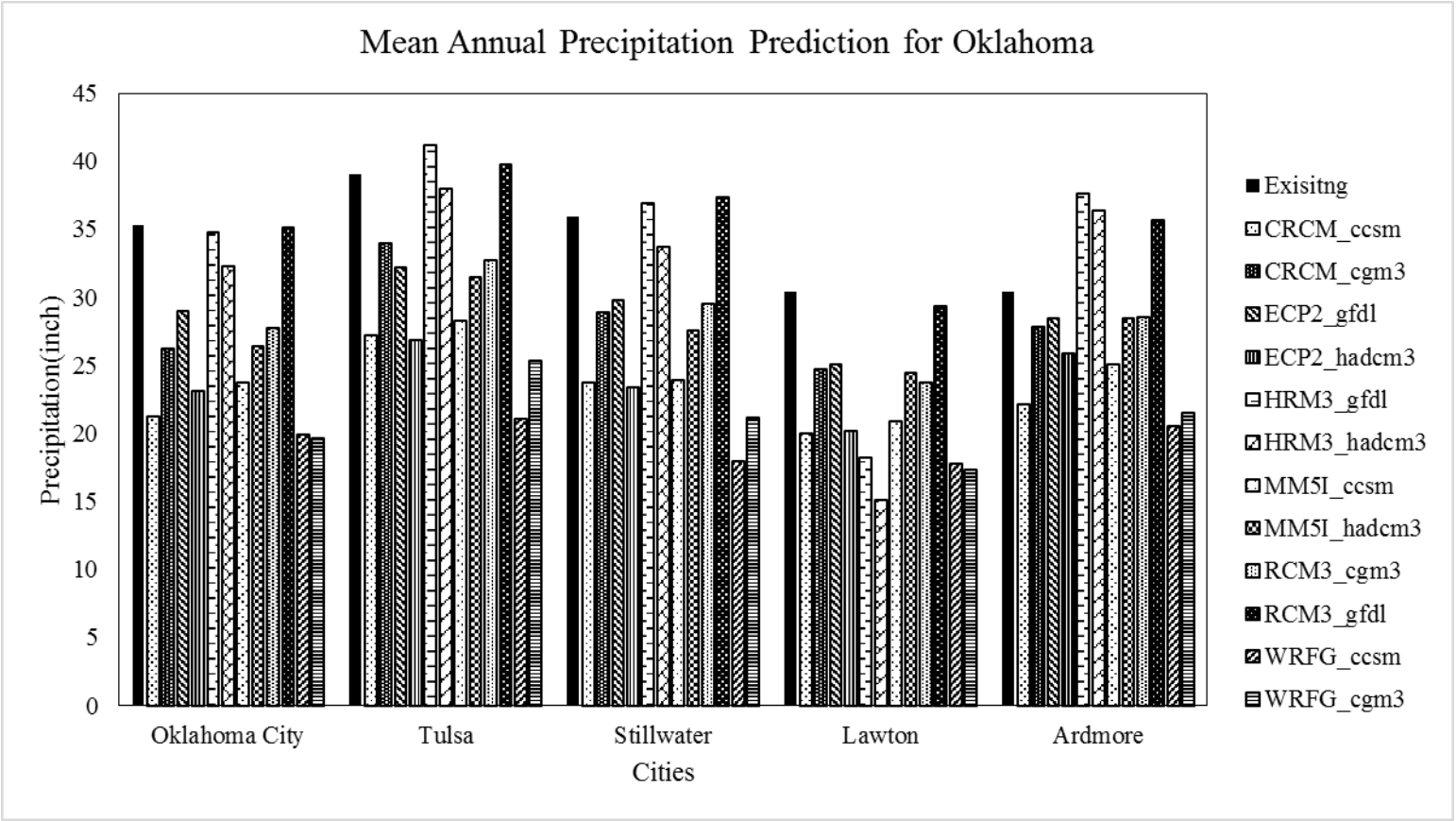

Figure 3-4 Mean Annual Precipitation of Different Cities of Oklahoma for Climate Prediction Models (2041-2070)

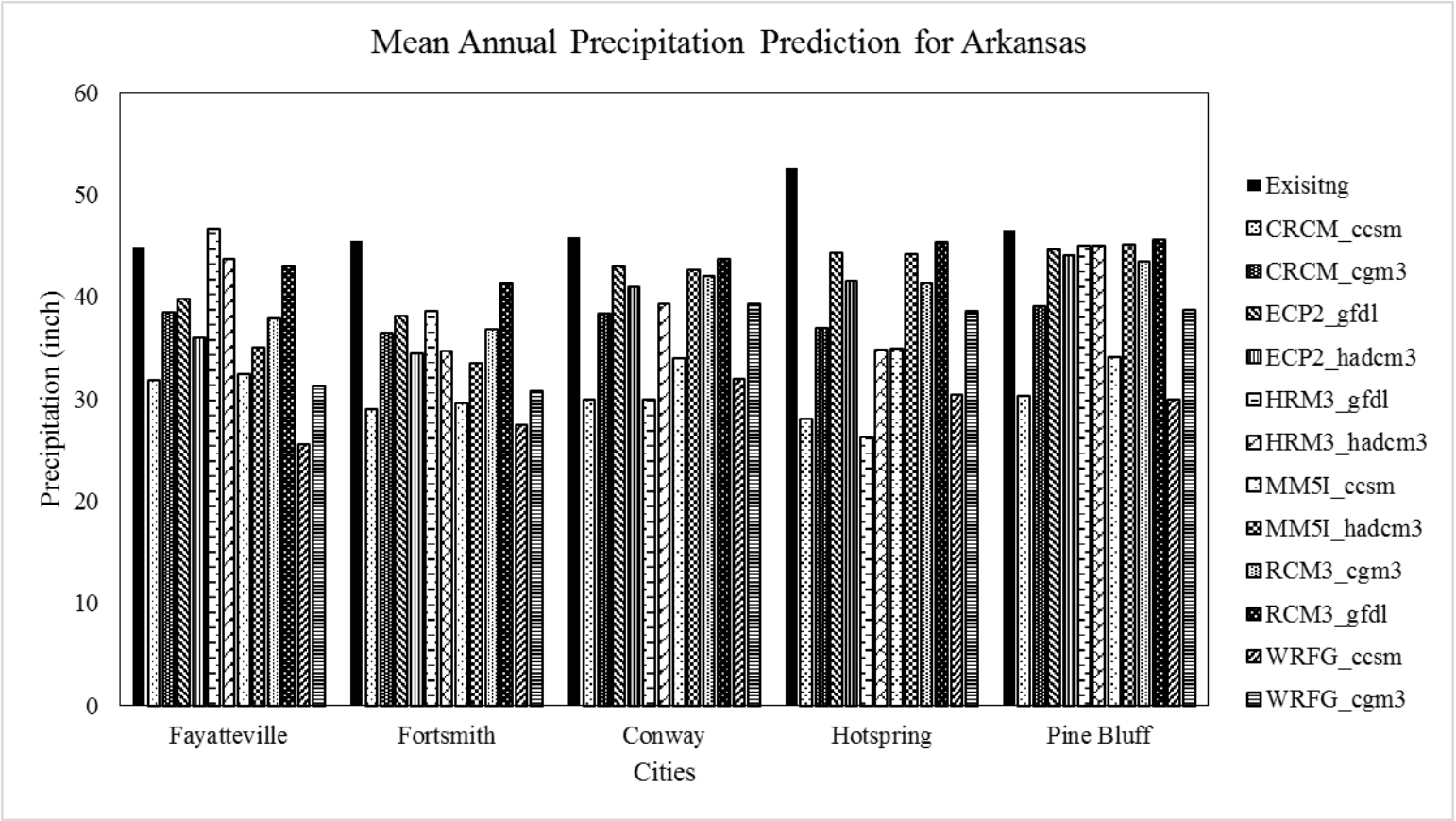

Figure 3-5 Mean Annual Precipitation of Different Cities of Arkansas for Climate Prediction Models (2041-2070)

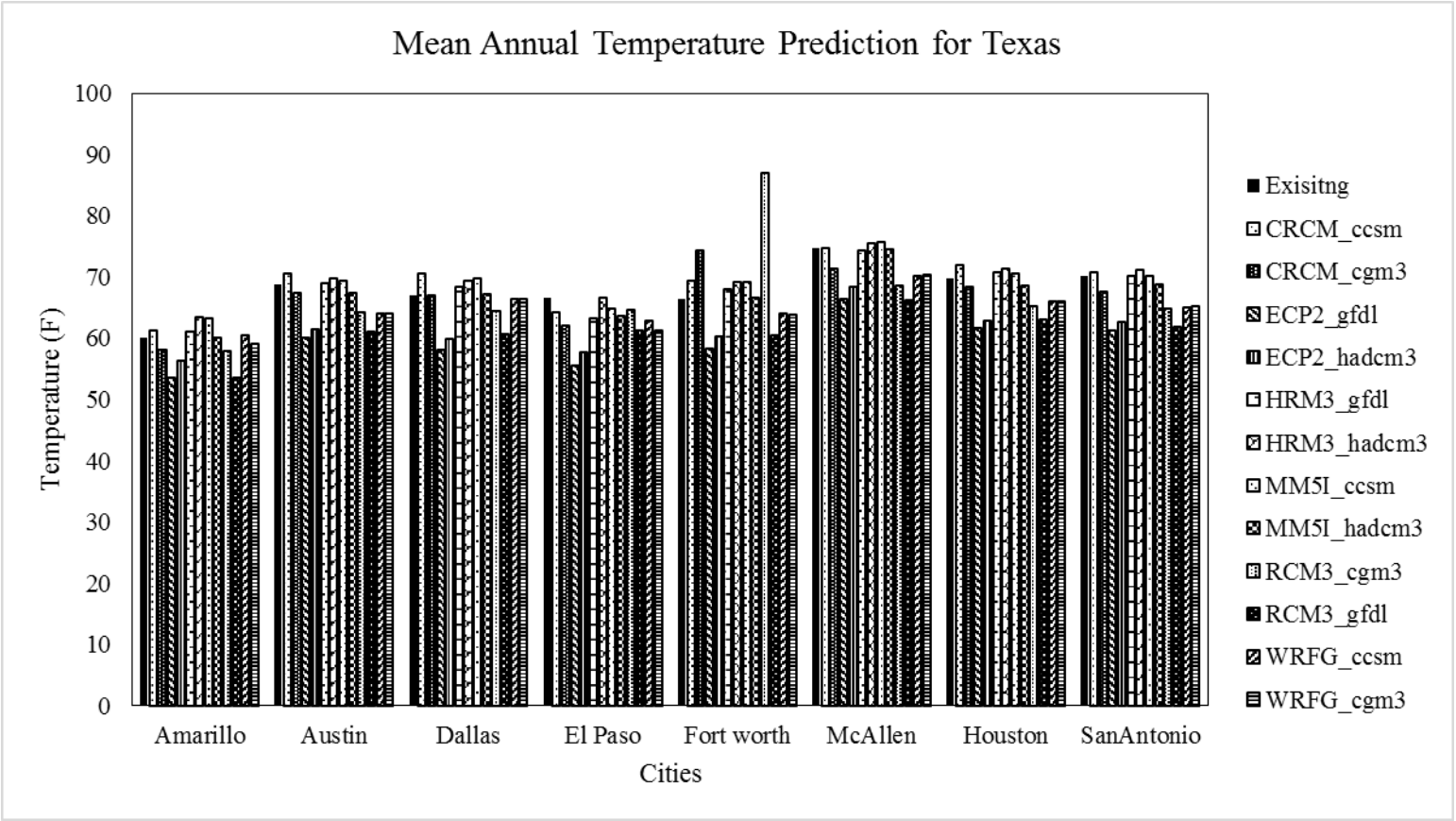

Figure 3-6 Mean Annual Temperature of Different Cities of Texas for Climate Prediction Models (2041-2070)

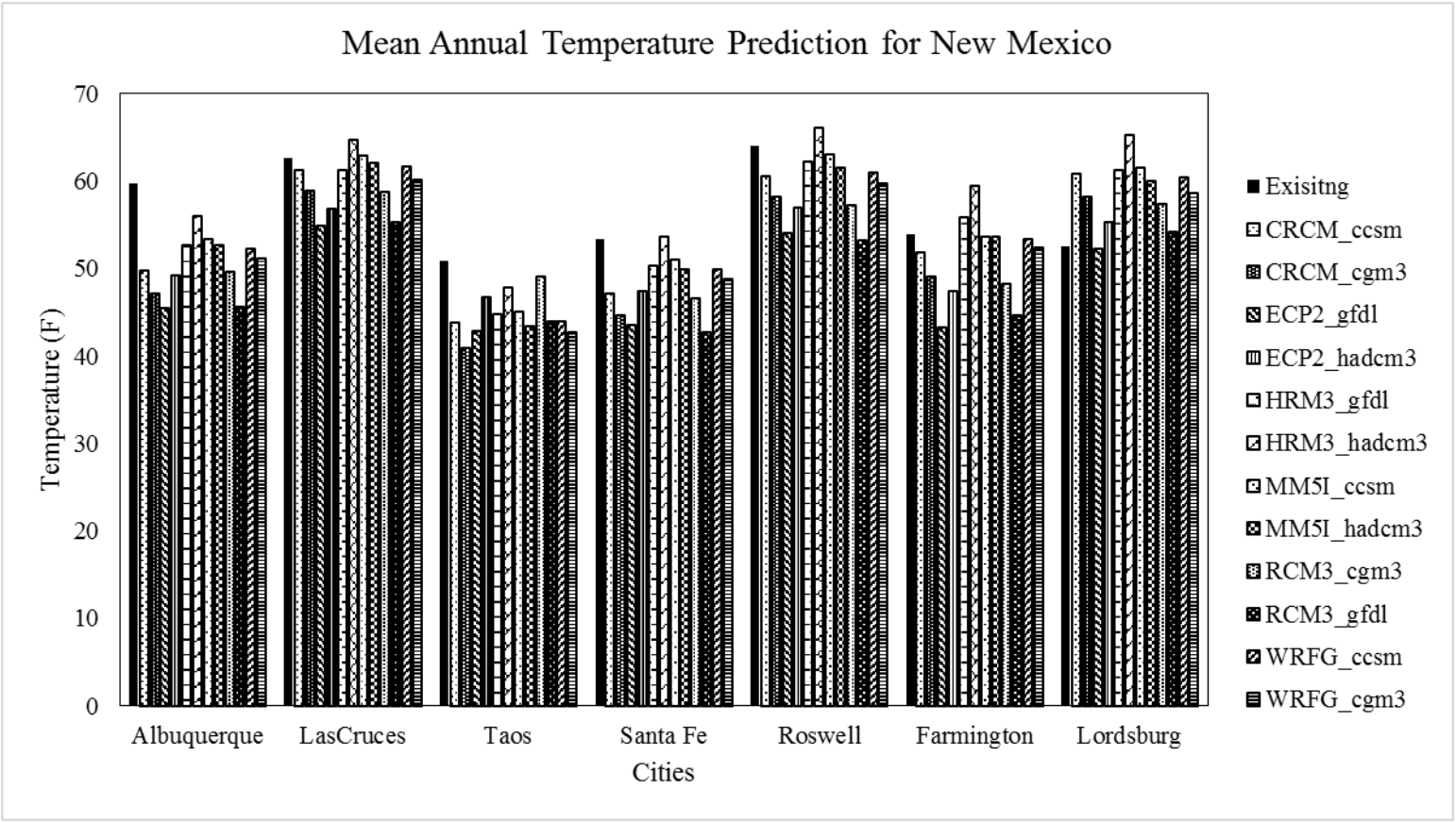

Figure 3-7 Mean Annual Temperature of Different Cities of New Mexico for Climate Prediction Models (2041-2070)

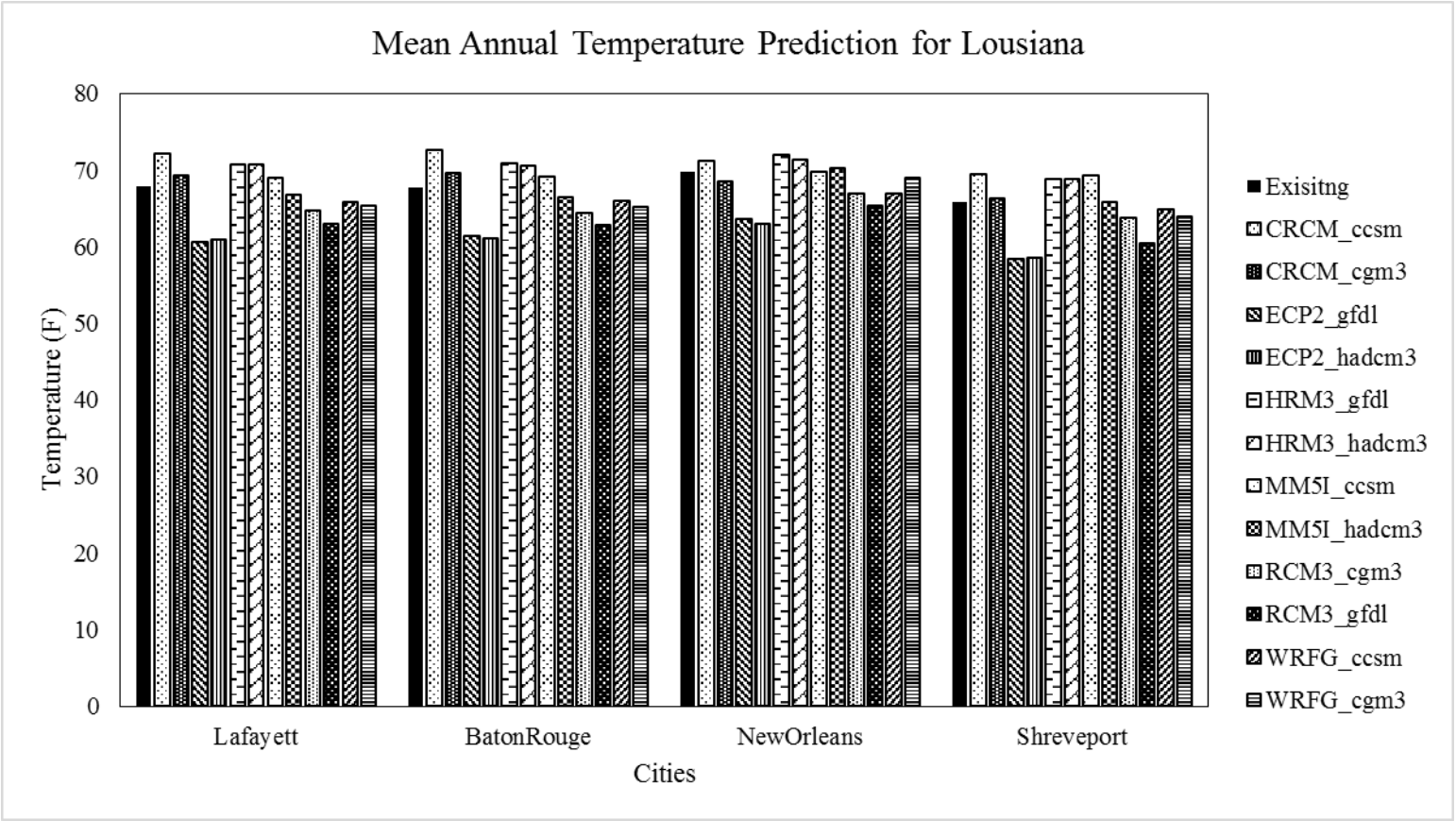

Figure 3-8 Mean Annual Temperature of Different Cities of Louisiana for Climate Prediction Models (2041-2070)

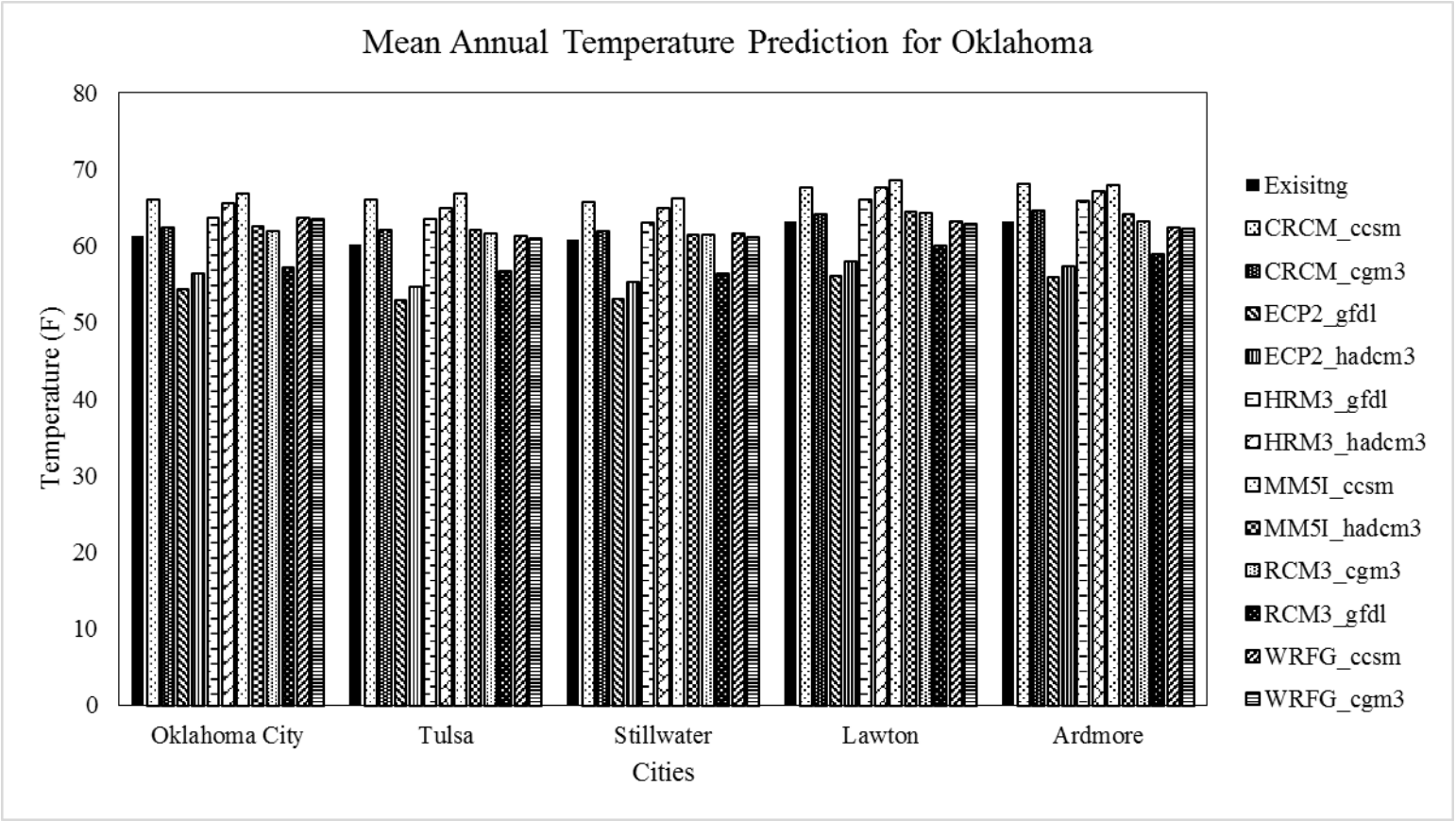

Figure 3-9 Mean Annual Temperature of Different Cities of Oklahoma for Climate Prediction Models (2041-2070)

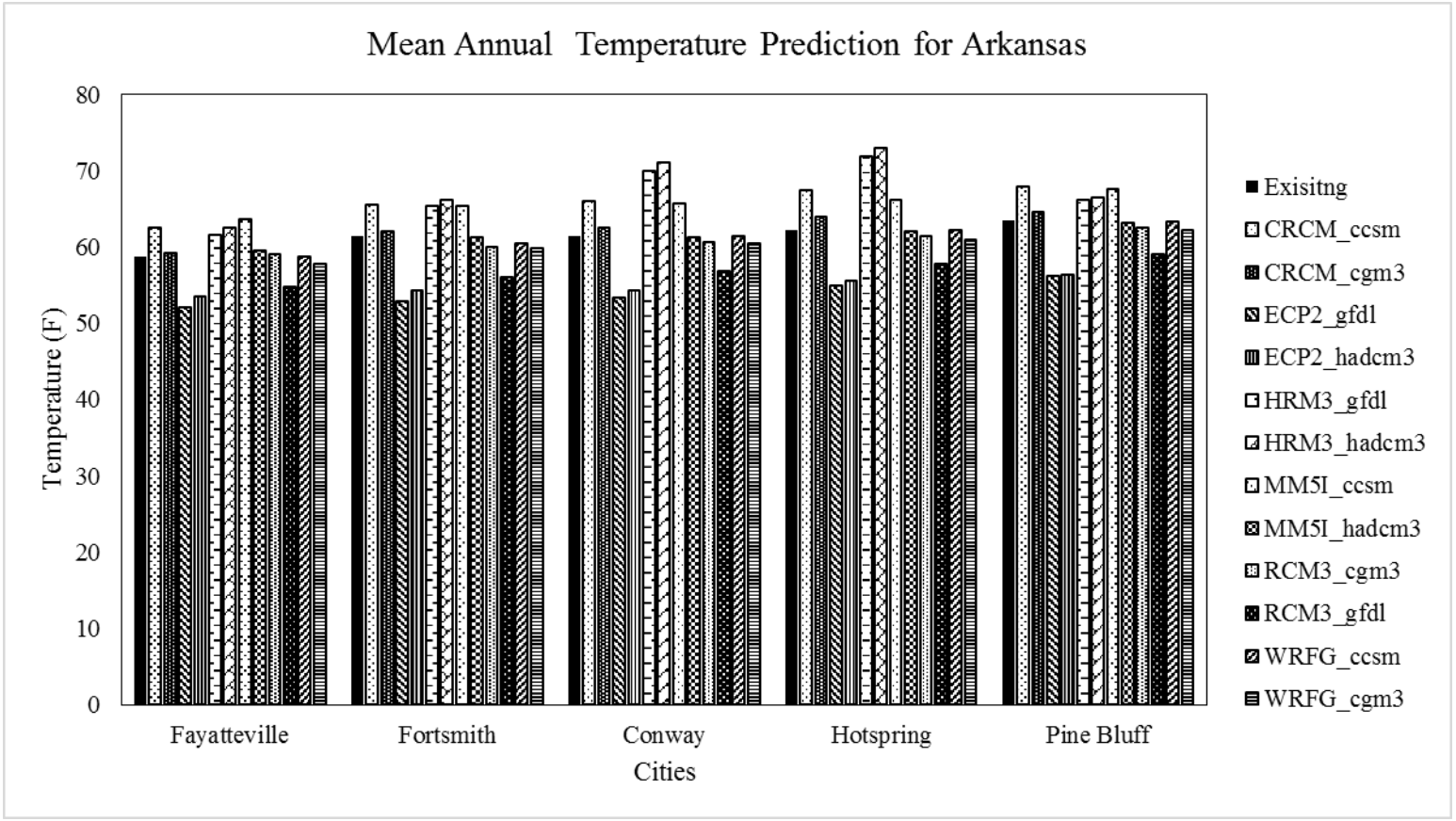

Figure 3-10 Mean Annual Temperature of Different Cities of Arkansas for Climate Prediction Models (2041-2070)

3.4 Bias Correction

Climate models possess inherent uncertainty. So, here, models simulated climate data has been analyzed with respect to observed climate data (Collected from NOAA) to evaluate the accuracy in the prediction of these models. For this analysis mean annual precipitation data for the period of 1979 to 1999 has been used. Figure 3 11 shows that the model simulated data predict much higher precipitation than the observed values. So, models produced climate data needs to be corrected using bias correction methods before using them in any climate change impact study. The bias correction methods provide adjustment factors to minimize the error between the historical observed data and model produced current climate data (Hempel et al. 2013). Moreover, using that adjustment factor future, climate data also have been adjusted.

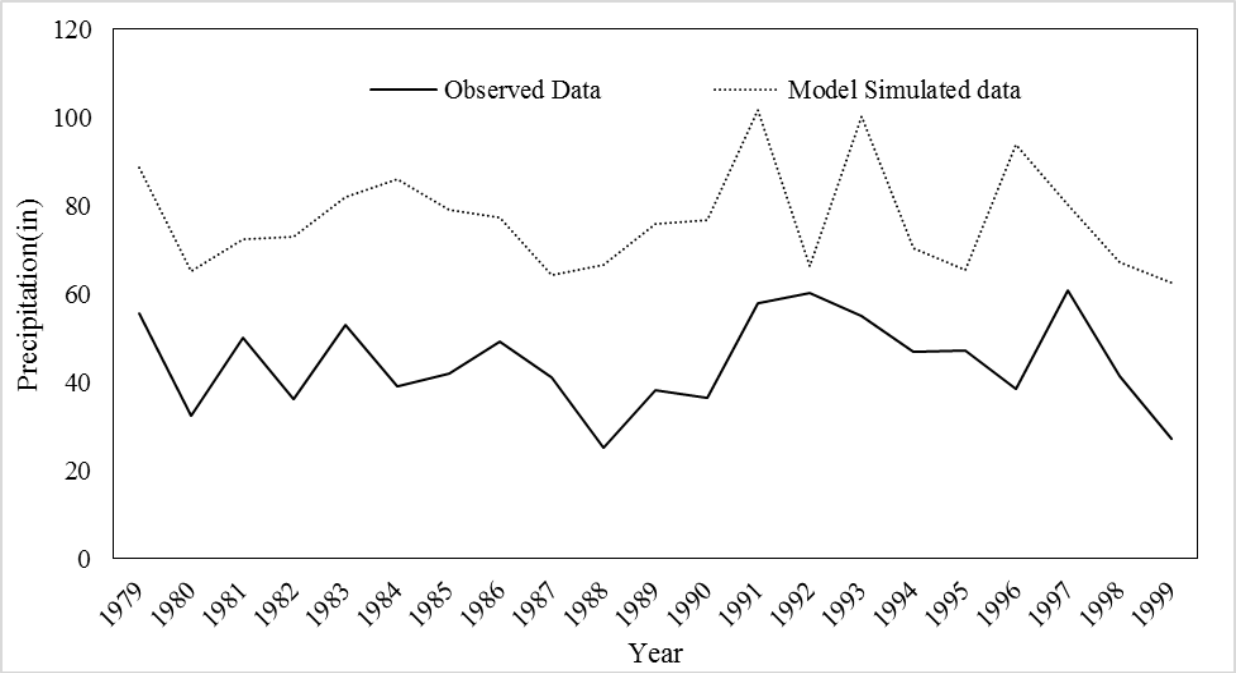

Figure 3-11 Model Simulated and Observed Precipitation Data

While various statistical methods are in practice to adjust the bias of the modelled climate data, in this study the ‘delta-change’ method has been used. This is a simple statistical bias

correction method. Biases are corrected by taking the difference between observed climate data and model produced current climate data.

Temperature Bias Correction is done using the following equations (3-1 and 3-2), where δ is calculated as the difference between othe bserved mean annual temperature ($\overline{T}_{obs}$) and mean model simulated temperature ($\overline{T}_{mod}$). And the bias corrected temperature (T_{bias}) is found just simply adding to the $\overline{T}_{mod}$.

$$\delta = \overline{T}_{obs} - \overline{T}_{mod} \quad (3\text{-}1)$$

$$T_{bias} = T_{mod} + \delta \quad (3\text{-}2)$$

While Precipitation Bias Correction is done using equation 3.3 and 3.4., where δ is calculated by taking the ratio of observed mean annual precipitation ($\overline{P}_{obs}$) to model simulated mean annual precipitation ($\overline{P}_{mod}$). And then the bias corrected mean annual precipitation (P_{bias}) is estimated by multiplying with P_{mod}.

$$\delta = \overline{P}_{obs}/\overline{P}_{mod} \quad (3\text{-}3)$$

$$P_{bias} = P_{mod}\ X\ \delta \quad (3\text{-}4)$$

As the climate models are predicting more changes for precipitation, bias correction has been done for precipitation according to the Delta change method. Table 3-2 shows the bias-corrected precipitation data for Houston, Texas, which has been illustrated in Figure 3-12.

Table 3-2 Bias Corrected Precipitation Data, Houston, Texas

Climate Models	Future Simulation (in)	Current Simulation (in)	Bias-Corrected (in)
CRCM-CCSM	23.2	25.7	39.4
CRCM-CGCM3	39.4	42.1	40.8
ECP2-GFDL	49.9	56.8	38.2
ECP2-HADCM3	82.4	77.1	46.6
HRM3-GFDL	34.3	37.5	39.8
HRM3-HADCM3	48.1	45.2	44.9
MM5I-CCSM	22.6	25.2	37.9
MM5I-HADCM3	61.9	57.1	48.0
RCM3-CGCM3	48.1	47.1	44.5
RCM3-GFDL	53.6	50.1	46.6
WRFG-CCSM	29.0	28.8	43.9
WRFG-CGCM3	38.8	39.6	42.7

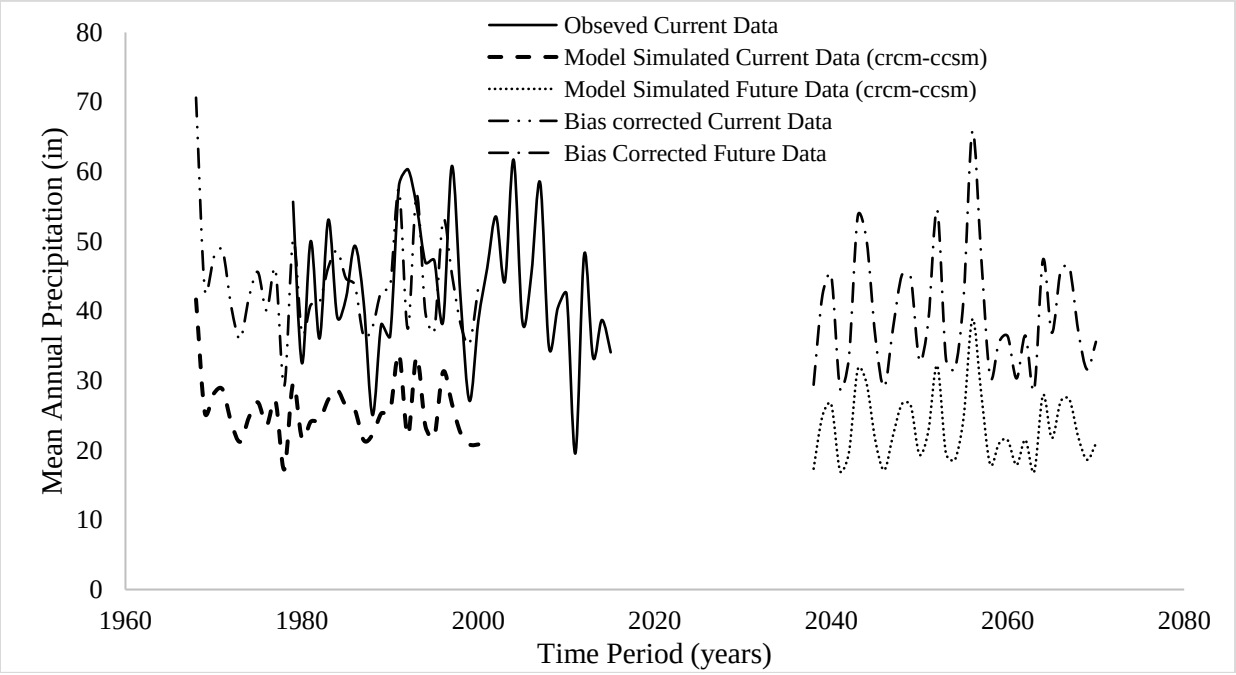

Figure 3-12 Bias Correction for Mean Annual Precipitation, Houston, Texas

The Figure 3-12 clearly shows that model (CRCM-CCSM) simulated current data matches the observed data. After the bias correction, the models predict the precipitation increase for

Huston as high as 10.2%, which has been predicted by MM5I-HADCM3 climate model. All the climate model generated future precipitation data of all the cities of SPTC represented states has been bias-corrected and catalogued in Appendix A.

Chapter 4: Hydraulic Modeling

4.1 Communicating Climate Predictions to Hydraulic Model

The primary factor to evaluate bridge infrastructure to vulnerability is streamflow, which is affected by climate change event like a change of intensity and frequency of precipitation. So precipitation is a main climatic stressor that influences the evaluation of a bridge infrastructure to vulnerability. Linking climate projection data to streamflow simulation models is a novel technology in transportation design analysis (Anderson et al., 2015).Some established and widely used precipitation-runoff models in hydrologic and hydraulic analysis are Hydrologic Engineering Centers Rivers Analysis System (HEC-RAS), which was developed by the U.S Army Corps of Engineers (USACE),Soil and Water Assessment Tool (SWAT), or the U.S. Soil Conservation Service/Natural Resources Conservation Service (NRCS) TR-20 hydrologic model. Given, the goal of the study is to establish a simplified but effective precipitation-streamflow modeling approach to incorporate in estimation of threshold values at which the bridge infrastructure begins to experience impacts such as overtopping or failure due to scour, we used regional regression equations to do the hydrologic analysis and those discharge data used as an input in hydraulic modeling done using HEC-RAS. Both hydrologic and hydraulic modelling for the bridge vulnerability evaluation is discussed in the following sections. Figure 4-1 shows the methodology that has been used in this study to incorporate the predicted precipitation data from climate models to the hydraulic model.

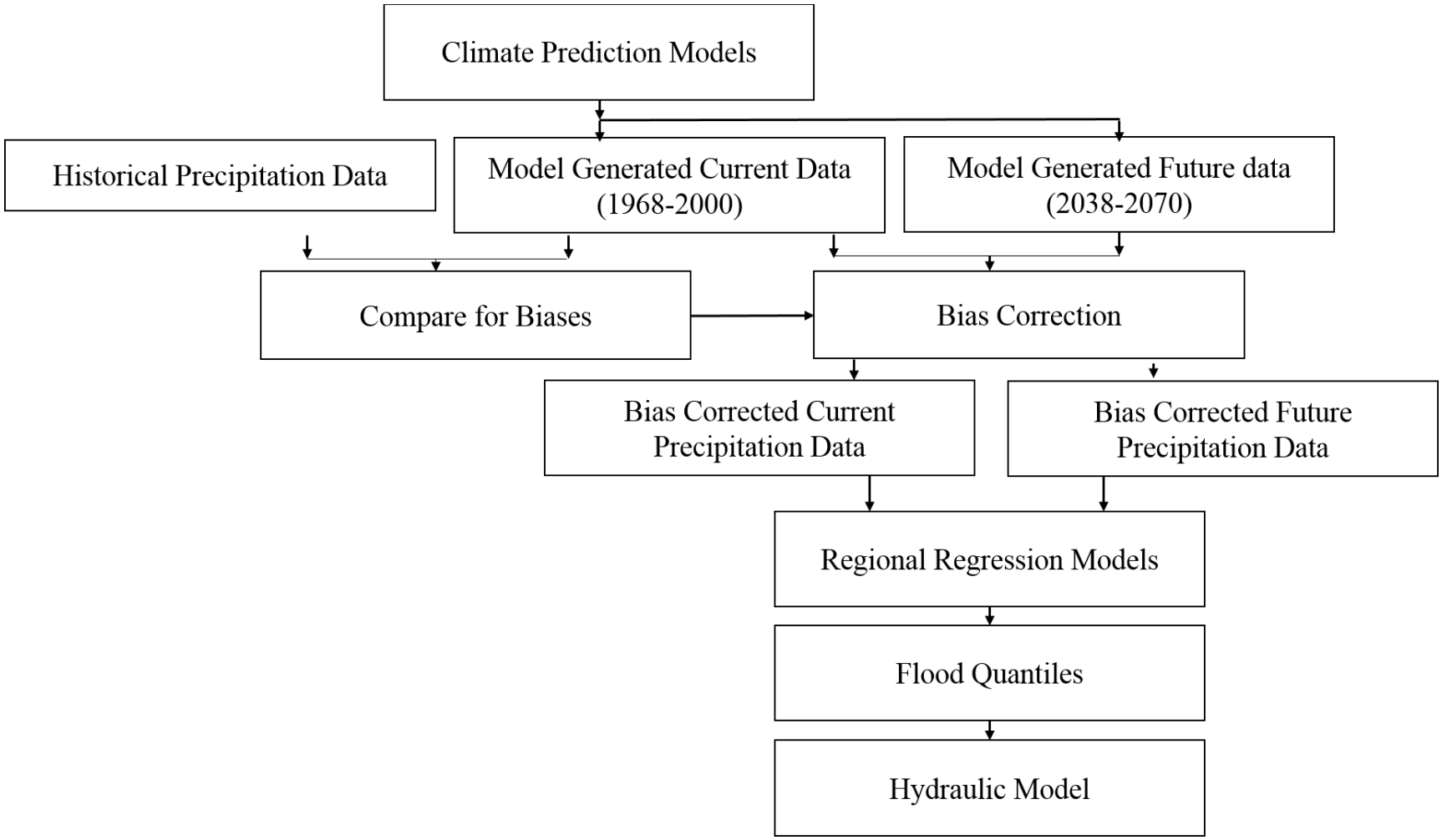

Figure 4-1 Methodology Followed to Communicate Climate Projection Data to Hydraulic Model

4.2 Hydraulic Modeling

This section describes the methodology that has been applied for hydraulic modeling of the bridges. The modeling has been performed using the HEC-RAS model, established by the US Army Corps of Engineers. The modeling can be performed in one or two dimensional for steady and unsteady flow analysis of the river systems. HEC-RAS has been built with the same hydraulic principles that have been followed by most of the transportation agencies for bridge design and which have been inscribed in the HEC-18 manual by FHWA.

The hydraulic modelling using HEC-RAS can be divided into three broad parts. 1) Preprocessing or creating the geometry, 2) Inputting hydrologic data or hydrologic modelling and 3) Hydraulic design computations. A general overview of the method is shown in Figure 4-2.

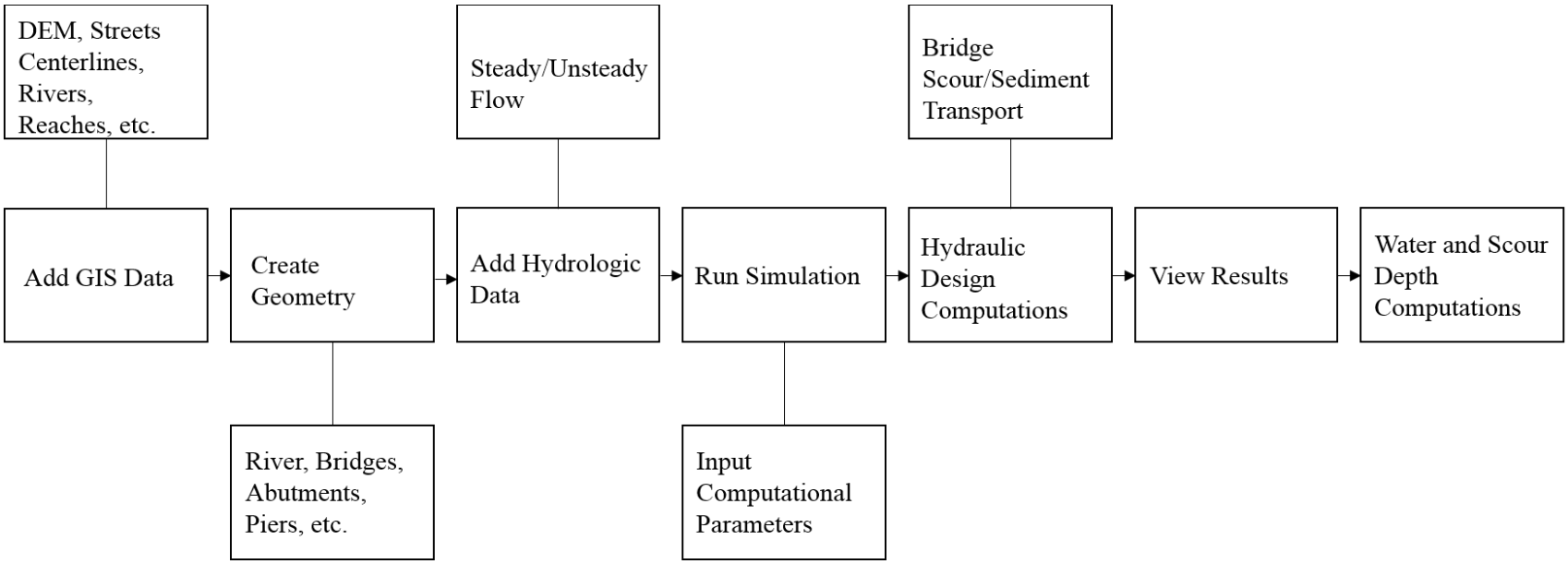

Figure 4-2 General Bridge Hydraulics

4.2.1 Pre-Processing

Preprocessing of the hydraulic model or creating the terrain geometry has been done using ArcGIS. That involves collecting the Digital Elevation Model (DEM) of the study area and creating the raster file of the terrain and shapefiles for the river's reach, cross sections, bridge locations etc. Then the raster file has been converted to the .tiff file to make it usable in RAS-mapper, in HEC-RAS. The following Figure 4-3 shows the terrain file created for the Houston-Galveston area. For this, a 10 m DEM has been collected and processed using ArcGIS.

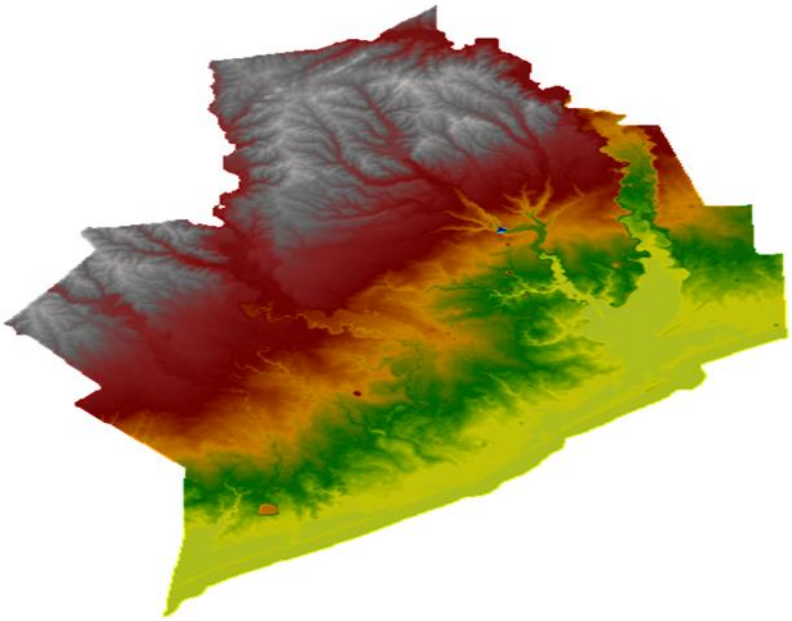

Figure 4-3 Terrain of Houston_Galvaston area

After creating the terrain, next step is to define the river's reach and cross-sections, as well as the creating the bridge with all the required characteristics data like deck width, pier shape and size or abutment properties etc. In order to perform these steps, all the required data have been collected from the TxDOT BRINSAP server. The data also includes the previous routine inspection survey of the bridge condition.

To estimate vulnerability of bridges and predict the risk they may face due to climate change in future two bridges situated in Houston; Texas has been analyzed in this study. The bridges are US 59 crossing over West Fork San Jacinto River and SH 36 Crossing over Big Creek. Among them,

bridge US59 has been identified as scour-critical according to the National Bridge Inventory (NBI) record (FHWA, 2016). Record also shows the bridge SH36 is vulnerable to overtopping, but not to scour. The characteristic parameters of these two bridges have been presented in this section, which has been used as input parameters in performing bridge hydraulic analysis.

Case I: US 59 crossing West Fork San Jacinto River, Houston, Texas

US 59 bridge situated in the Harris County in Houston District of Texas. The characteristics of this bridge are shown in Table 5-1.

Table 4-1 Characteristics of Bridge US 59

Bridge Name	**US 59**
Bridge crossing	West Fork San Jacinto River
TxDOT structural no.	12-102-0177-06-081
Bridge Coordinate	30º1'35.07"N, 95º15'32.29"W
Year built	1961
Bridge Length	1645 feet
No. of piers	25
Pier spacing	60 feet
Pier diameter	16 sq. inches
Foundation	30 feet concrete piles
Bridge Opening	60 feet

Case II: SH 36 crossing Big Creek, Houston, Texas

This bridge situated in the Fort bend county in Houston District of Texas. The characteristics of this bridge are shown in Table 5-2.

Table 4-2 Characteristics of Bridge SH 36

Bridge Name	**SH 36**
Bridge crossing	Big Creek
TxDOT structural no.	0188-02-023
Bridge Coordinate	29°28'35.1"N, 95°48'46.97"W
Year built	1932
Bridge Length	257 feet
No. of piers	10
Pier spacing	25 feet
Pier diameter	14 sq. inches
Foundation	25 ft to 35 ft concrete piles
Bridge Opening	15 feet

4.2.2 Hydrologic Modeling

In order to perform the hydraulic simulation in HEC-RAS, the primary component is the streamflow data. This section describes the precipitation-streamflow modelling approach that has been adopted in this study.

Although several methods are available to perform the precipitation-streamflow simulation, a simple regional regression equation approach is used in this study. While national regression equations are available, Texas has established its own sets of regression equations for the estimation of annual peak streamflow frequency. Annual peak streamflow frequency or flood quantiles represents the peak streamflow with different return periods such as 2, 5, 10, 25, 50, 100, 200, 250 and 500 years.

In 2009 Asquith and Roussel, incorporation with the Texas Department of Transportation (TxDOT) established a set of equations that relate the basin characteristics to the stream flow of the basin. Although, the regional regression equations are developed for ‘natural basins’, where

urban development does not have many effects on rainfall-runoff generation process. So, whenever these equations are used in the human developed area, higher cautions should be taken (Briaud et al., 2009).

Table 4-3 shows the regional regression equations with adjusted R-factor. The flow with a given recurrence interval is related to mean annual precipitation (P [inch]), dimensionless average channel slope (S, [L/L]), Drainage area (A, [mile^2]) and a parameter Ω, that represents the characteristic of the water shade. The Ω can be read from the Figure 4-4 that illustrated the ecoregions in Texas with superimposed values of Ω values.

Table 4-3 the Regional Regression Equations (Asquith and Roussel, 2009)

Return Period	**Equations**	**R-Adjusted**
2	$Q_2 = P^{1.398}S^{0.270}10^{[0.776\Omega+50.98-50.30A^{-0.0058}]}$	0.84
5	$Q_5 = P^{1.308}S^{0.372}10^{[0.885\Omega+16.62-15.32A^{-0.0215}]}$	0.88
10	$Q_{10} = P^{1.203}S^{0.403}10^{[0.918\Omega+13..62-11.97A^{-0.0289}]}$	0.89
25	$Q_{25} = P^{1.140}S^{0.446}10^{[0.945\Omega+11.79-9.819A^{-0.0374}]}$	0.89
50	$Q_{50} = P^{1.105}S^{0.476}10^{[0.961\Omega+11.17-8.997A^{-0.0424}]}$	0.87
100	$Q_{100} = P^{1.071}S^{0.507}10^{[0.969\Omega+10.82-8.448A^{-0.0467}]}$	0.86
200	$Q_{200} = P^{1.034}S^{0.531}10^{[0.975\Omega+10.61-8.058A^{-0.0504}]}$	0.84
250	$Q_{250} = P^{1.021}S^{0.541}10^{[0.977\Omega+10.56-7.943A^{-0.0561}]}$	0.83
500	$Q_{500} = P^{0.988}S^{0.569}10^{[0.976\Omega+10.40-7.605A^{-0.0554}]}$	0.81

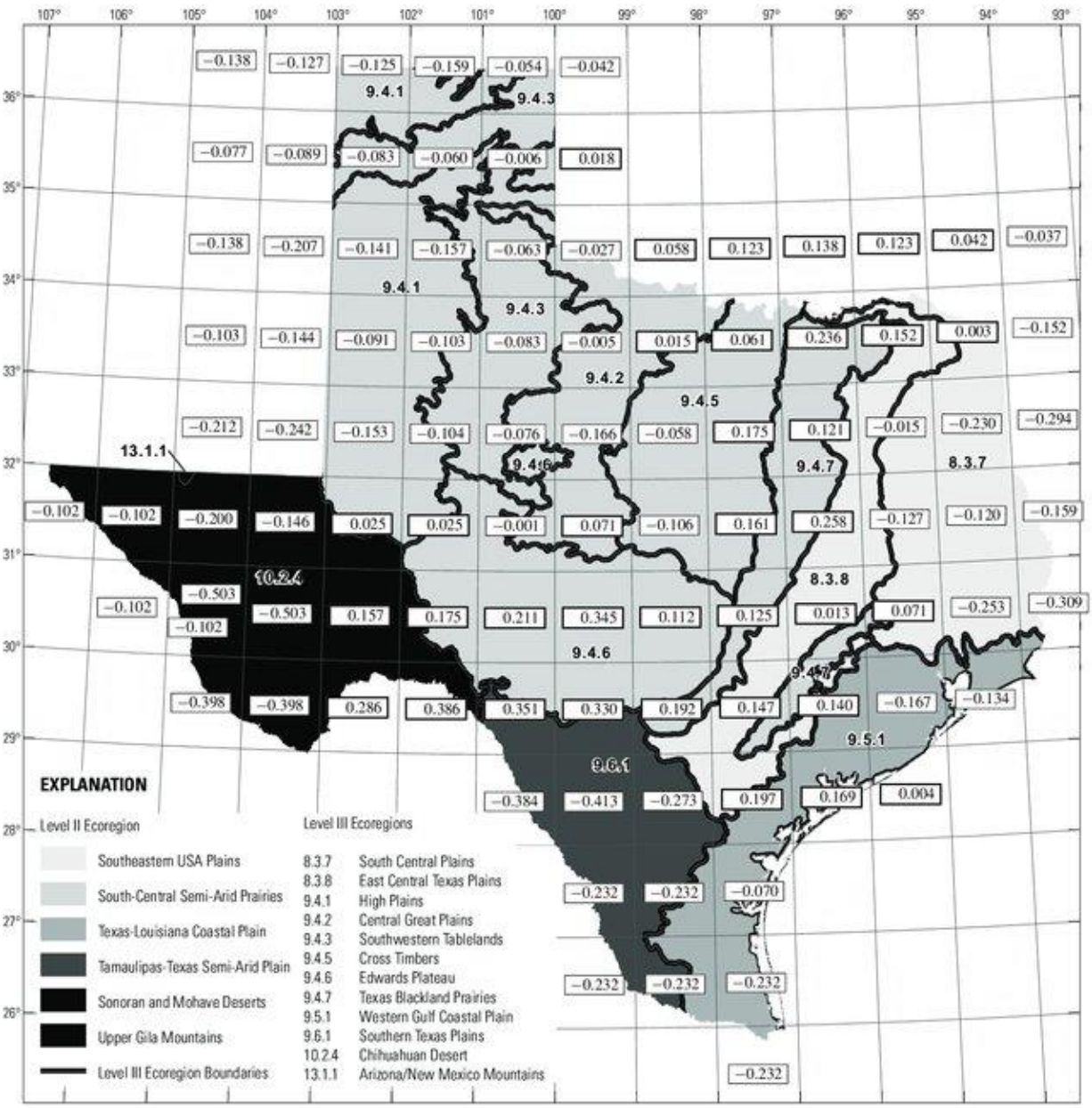

Figure 4-4 Eco-Regional Map of Texas with Superimposed Values of the Omega-Em parameter (Asquith and Roussel, 2009)

The mean annual precipitation data predicted from different climate models are incorporated in these equations, which produce the floods for different recurrence interval.

Example of Flood quantile Estimation:

- River basin: West Fork San Jacinto River

- Area of Drainage Basin, A = 828 mile^2
- Slope, S = 0.003
- Ω = 0.14
- Mean Annual Precipitation, P = Predicted By different models

The resulted floods for different return period has been listed in Table 4-4.

Table 4-4 Flood Quantiles Prediction Using Different Climate Models

	Existing	**CRCM-CCSM**	**CRCM-CGM3**	**ECP2-GFDL**	**ECP2-HADCM3**	**HRM3-GFDL**	**HRM3-HADCM3**	**MM5I-CCSM**	**MM5I-HADCM3**	**RCM3-CGM3**	**RCM3-GFDL**	**WRFG-CCSM**	**WRFG-CGM3**
P	43.2	39.23	40.78	38.24	46.56	39.80	44.90	37.90	48.00	44.48	46.57	43.80	42.71
2	20963.4	18106.8	19114.8	17471.3	23006.3	18475.7	21867.8	17254.5	24007.1	21582.3	23013.2	21122.5	20391.3
5	48983.5	42709.7	44930.2	41305.4	53436.0	43523.2	50957.9	40825.7	55608.0	50335.3	53451.1	49331.2	47731.6
10	70186.3	61873.8	64826.4	60000.3	76033.3	62956.9	72784.1	59359.1	78871.0	71965.8	76052.9	70644.4	68534.8
25	106787.6	94763.9	99043.9	92042.5	115200.0	96335.1	110529.6	91110.1	119270.5	109351.7	115228.3	107448.0	104405.1
50	140682.8	125301.3	130783.0	121811.8	151412.4	127314.5	145458.6	120615.6	156595.3	143955.8	151448.4	141525.9	137639.3
100	181663.8	162379.1	169259.9	157994.4	195077.4	164907.3	187638.0	156490.4	201546.1	185758.8	195122.2	182719.0	177853.4
200	228268.8	204829.2	213202.9	199486.8	244520.9	207907.3	235512.2	197653.1	252344.6	233234.6	244575.2	229548.7	223644.5
250	245254.3	220370.6	229264.1	214694.1	262488.7	223640.3	252937.3	212745.3	270780.1	250521.9	262546.3	246612.2	240347.8
500	301482.5	271832.2	282441.1	265053.6	321960.7	275734.1	310617.2	262725.1	331797.0	307746.3	322029.0	303097.6	295644.1

The flood of different intervals estimated using different predicted climate models is illustrated in Figure 4-5 and 4-. It shows 5 models predict higher flood flows than the existing one in future, while 5 models show flow amount can be less for different return periods. Figure 4-5 shows the flood flow of different return periods for the San Jacinto River. For 100-year flood, MM5I-HADCM3 predicts an increase of around 11% than the existing climatic condition, where MM5I-CCSM, which predicts around 14% less flow intensity than the existing one. The increased in the probability of flow means, in near future 100-year flood event, will be taken place in 78 years interval. This is shown in Figure 4-6.

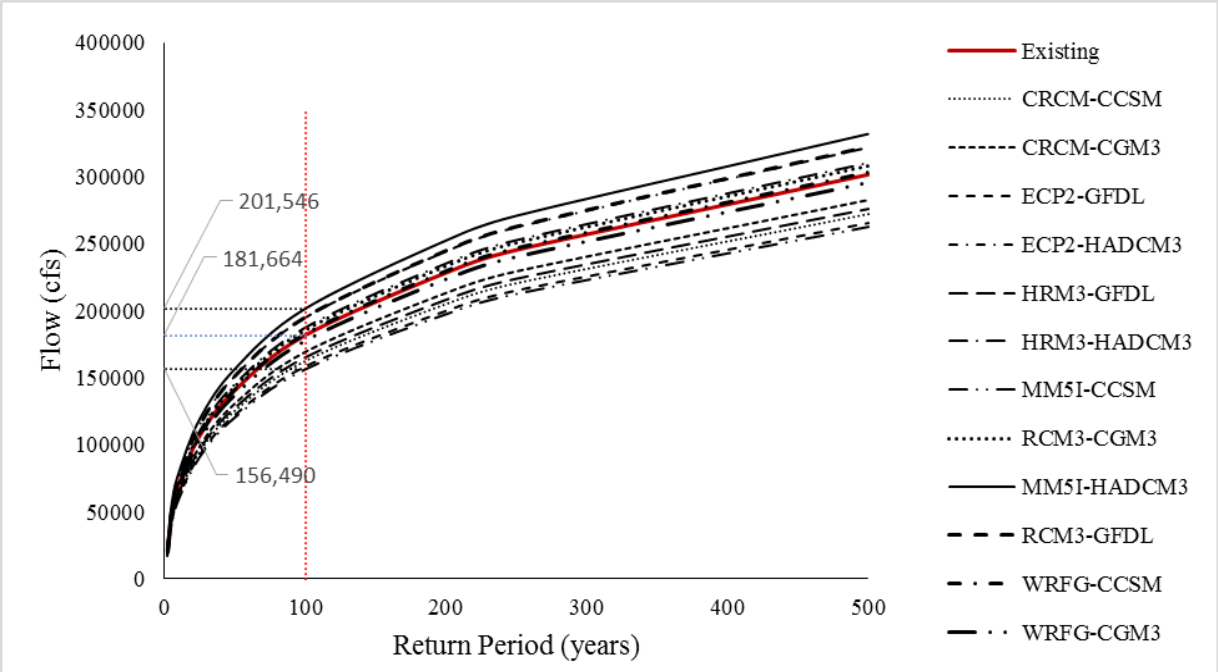

Figure 4-5 Predicted Flood Flows for Future Climate Scenarios, San Jacinto River, Houston, Texas

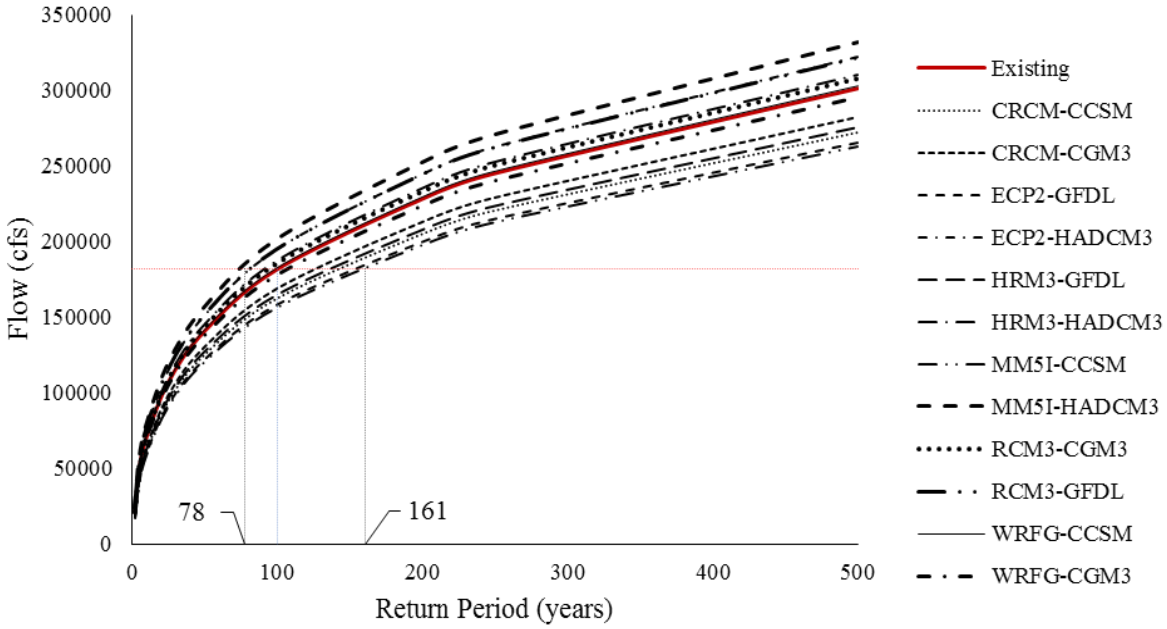

Figure 4-6 Predicted Flood Frequency for Future Climate Scenarios, San Jacinto River, Houston, Texas

Similarly, Figure 4-7 shows the flood events with different return periods for the predicted climate models for the Big Creek river basin. It shows MM5I-HADCM3 predicts almost 11% increase and MM5I-CCSM shows around 16% decrease in future 100-year flood flow. So, as same as the San Jacinto River, in Big Creek 100-year flood events will occur in 78 years interval.

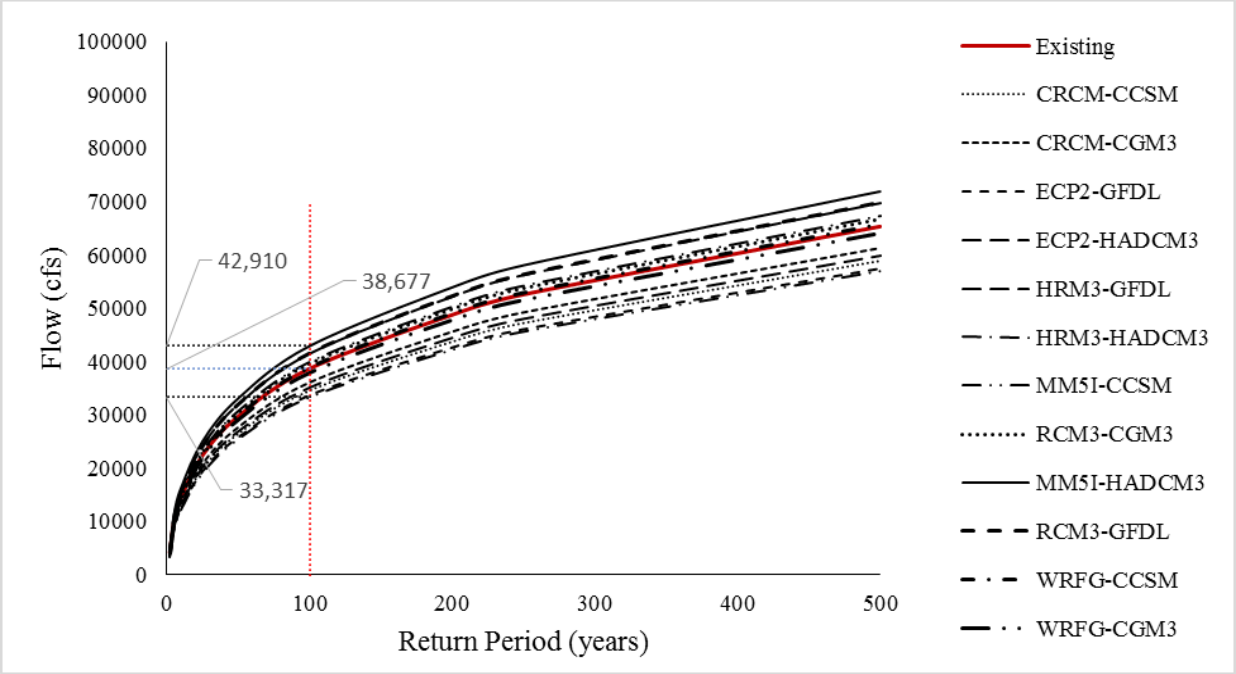

Figure 4-7 Predicted Flood Flows for Future Climate Scenarios, Big Creek, Houston, Texas

4.2.3 Hydraulic Simulations

The very first step in performing the hydraulic modelling in HEC-RAS is to choose the appropriate modelling approach. Several methods are available for bridge hydraulic modelling in HEC-RAS interface, for both low flow and high flow conditions. These methods have been mentioned in chapter 2 section 2.3. The methods are as follows:

For low flow computations the following approaches are available:

- Energy Equation or Standard Step Method
- Momentum Balance Method
- Yarnell Equation:
- FHWA WSPRO Method

And for high flow computations one of the following methods has to be chosen:

- Energy Equation or Standard Step Method
- Pressure Flow Method

For low flow methods, HEC-RAS provides the opportunity to choose all the methods and compute according to the highest energy answer. But for high flow, one has to choose either energy step method or pressure flow method. This study involves the computation of the overtopping potential, so pressure flow method is a proper choice for high flow simulations.

Although HEC-RAS provides an opportunity to perform both steady and unsteady flow analysis, in this study only steady gradually varied flow analysis has been performed. In order to perform a steady analysis, a reach boundary condition has to be set. As from the Digital Elevation Model (DEM), the slope of the reach can be easily evaluated, and boundary conditions have been set using Normal depth of the downstream. Figure 4-8 shows the hydraulic simulations for 100-year flood events for bridge US 59 crossing the West Fork San Jacinto River.

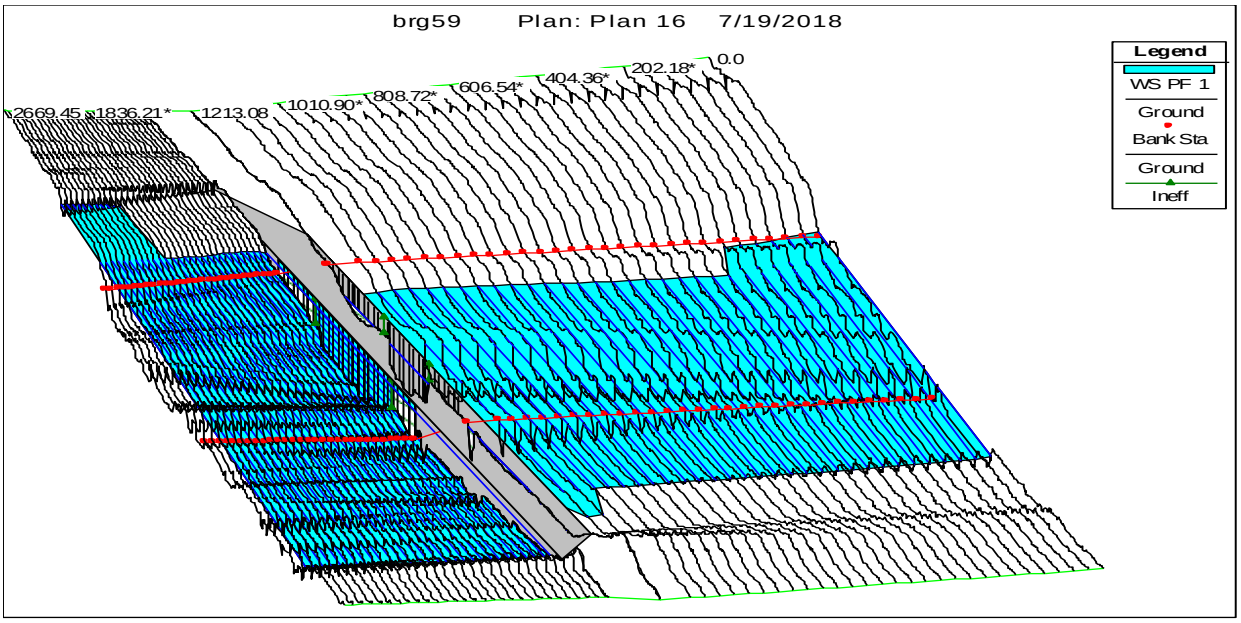

Figure 4-8 Hydraulic Simulation of the Bridge Using HEC-RAS

Calibration of the hydrologic and hydraulic model is an essential part to generate a real-world picture of the flood events. For HEC-RAS calibration parameters are as follows:

- Manning's n value
- Cross-section of the reach

Calibration of the hydraulic model has been done using the data from BRINSAP_TxDOT database and USGS gage station data.

For bridge US 59 crossing over West Fork San Jacinto River, the 50-year and 100-year stream flow data along with the resulted water depth was readily available in the server. Table 4-5 shows the parameters of used USGS gage stations.

Table 4-5 TxDOT_BRINSAP survey record, 2016

Flood Event	Flow (cfs)	Water Depth (ft)
50-year	127,200	62.3
100-year	167,500	63.2

Consequently, calibration of this bridge has been done using these data directly. Table 4-6 shows the model simulated flow and depth for 50-year and 100-year flood events.

Table 4-6 Model Simulated 50-year and 100-year Flood Events, Bridge US-59

Flood Event	Flow (cfs)	Water Depth (ft)
50-year	140,683	57.69
100-year	181,664	61.96

The hydraulic model of SH-36 has been calibrated from the USGS gage station data (HU12070104), which has records of flow data from 1947 to 2017. The model calibrated 50- year and 100-year flow and water depth data have been presented in table 4-7.

Table 4-7 Model Simulated 50-year and 100-year Flood Events, Bridge SH-36

Flood Event	Flow (cfs)	Water Depth (ft)
50-year	29,733	12.85
100-year	38,677	14.4

Chapter 5: Vulnerability and Risk Assessment

5.1 Vulnerability Assessment of Bridge

Bridges are generally vulnerable to failure due to scouring of the foundation materials, overtopping, hydrodynamic forces to bridge superstructures, debris accumulation etc. (Okeil and Cai, 2008, Parola et al., 1998, Bala et al., 2005). Bridge hydraulic design focuses primarily on flows for responsible for overtopping and flows responsible for scouring. So, the evaluation of an existing bridge for the vulnerability is also focused on these two conditions. This section discusses how the future climate change will affect the overtopping and scour condition of the bridge, with respect to the existing climatic condition.

5.1.1 Vulnerability to Overtopping

Overtopping is an important factor of damage to the bridges especially to the approach embankments. Besides the disrupting the commute networks, hydrodynamic forces occur during the submerged condition make the bridge vulnerable to failure. The drag and lift forces pose a serious threat to the stability of the bridge deck (Cigada et al., 2001, Malavasi et al., 2001, Kara et al., 2015).

Bridges are overtopped when the water depth at the peak stream flow is above the bridge high chord elevation. Figure 5-1 shows the water depth resulted from the flow with different return period based on existing climatic condition for the bridge the US 59 over San Jacinto River in Houston, Texas. The elevation of the bridge is 63 feet, which is taken as the threshold value or overtopping depth to analyze the graph. The hydraulic simulation of the model shows that the bridge will be overtopped in the occurrence of a 119-year flood.

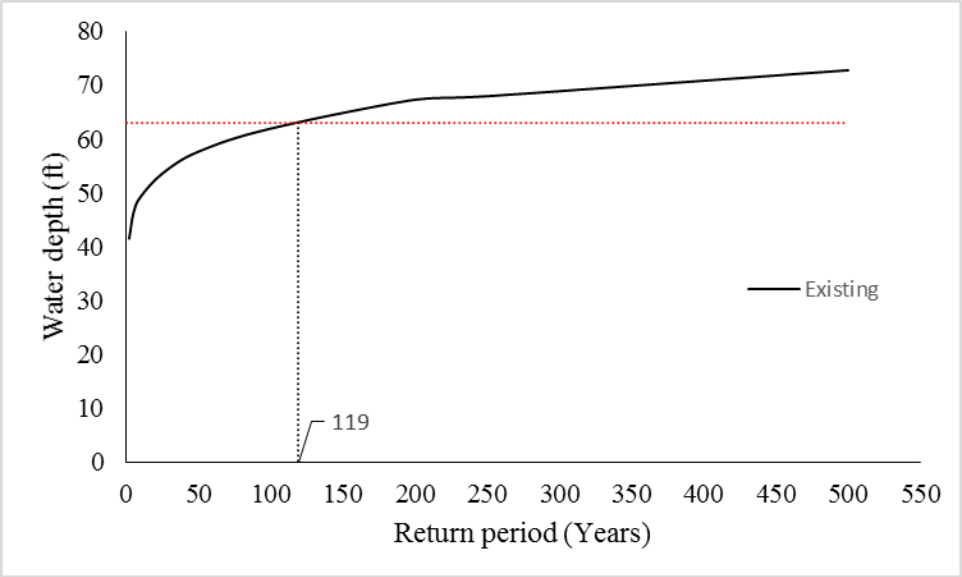

Figure 5-1 Depth of Water for Different Return Periods under Existing Climatic Condition, US59 Bridge, Houston, Texas

Climate models predict change in the flow magnitude for the future emission scenarios. Return periods or flood frequency for the overtopping depth (63') will also change for this future climate predictions. Figure 5-2 shows the predicted water depth for flood with different return period for the San Jacinto River. The simulation suggests the bridge will reach the overtopping depth at 90-years flood flow (predicted by MM5I-HADCM3), which is 29-years less than the existing condition.

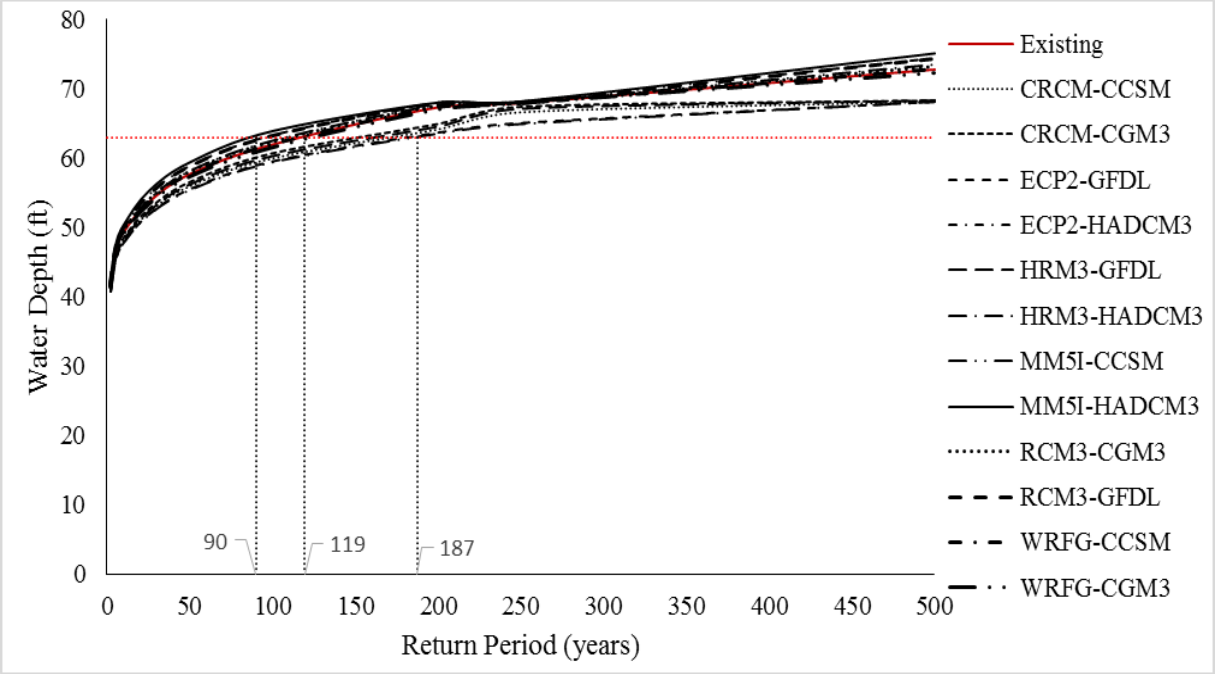

Figure 5-2 Depth of Water for Future Climate Predictions, US59 Bridge, Houston, Texas

Similarly, Figure 5-3 shows the simulated water depth for bridge SH 36 crossing Big Creek watershed for different climate prediction models. According to the hydraulic simulation under existing climatic condition, this bridge will be overtopped for 127-year flood flow. But the future climate prediction shows a possibility of overtopping of the bridge for only 87-years flood flow. So for future predicted models the bridge in risk for failure due to overtopping even before the 100-year flood.

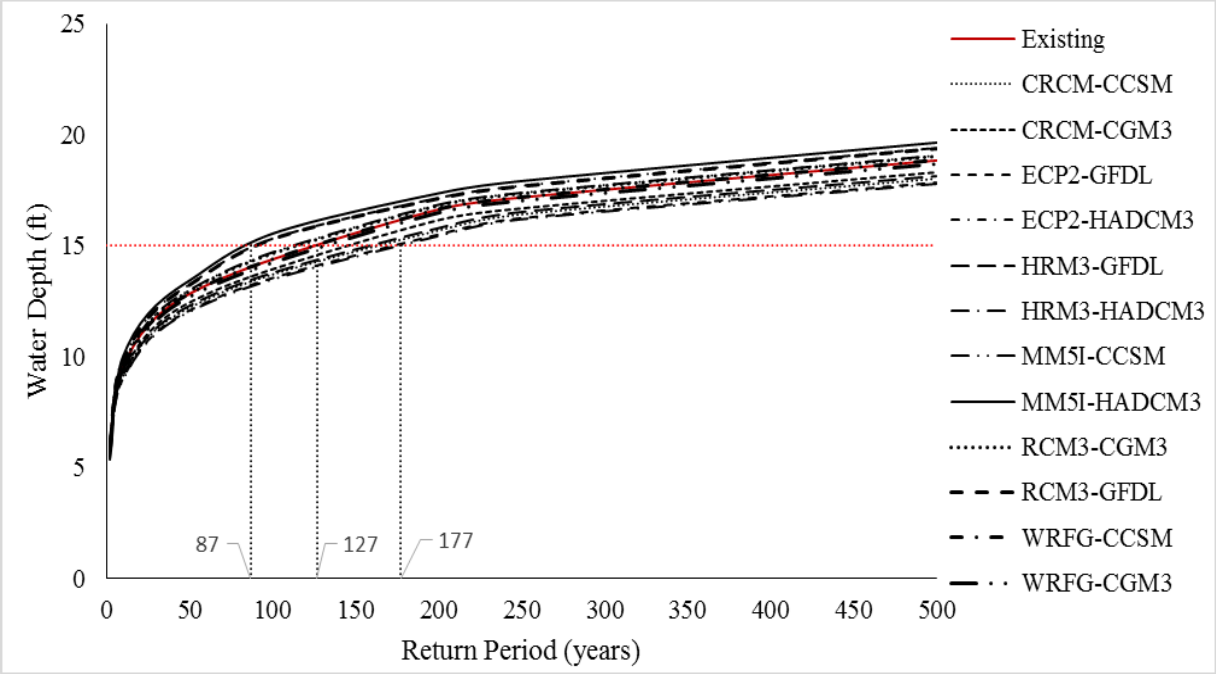

Figure 5-3 Depth of Water for Future Climate Predictions, SH36 Bridge, Houston, Texas

Water depth simulation results from Figure 5-2 and 5-3, also depict that, the smaller water basin (big creek with 84 mile^2) shows similar trends for an increase of water depths for all models, where big basins (West Fork San Jacinto River with 842 mile^2) shows the difference in trends. This may help to conclude, the hydraulic simulation for big basins pose more biases than the smaller basin.

5.1.2 Vulnerability to Scour

The most common reason for bridge failure is the scouring of the bed materials from the foundation of the bridge (Melville and Coleman, 2000). The scour depth is measured in this study using the HEC-18 manual, published by the Federal Highway Administration (FHWA), stated in chapter two. The established equations for the estimation of scour at abutment are not reliable to predict the scour depth (Briaud et al., 2009, TxDOT 2004, AASHTO LRFD 2007). So, the total scour depth comprises the scour occurred due to contraction and underneath of the pier foundation.

The study compares the scour vulnerability of an individual bridge for different climate models as well as existing condition, with respect to the allowable scour depth. Allowable scour depth is the function of depth of foundation. The common practices estimate allowable scour depth as,

Allowable Scour Depth = ½ x Foundation Depth

Table 5-1 shows the scour depth estimated for the existing climatic condition for the flood of different return interval for the bridge the US 59 over San Jacinto River in Houston, Texas. The sour depth for the 100-year flood is 21.96 ft., where the allowable scour depth of this bridge is 16 feet. So, this bridge is a scour critical bridge. Figure 5-4 illustrates the resulting scour depths for different floods. As per as the illustration the bridge will reach the threshold value, or allowable scour depth (16') only for a 55-year flood flow.

Table 5-1 Scour Depths for Different Flood Events, US59 Bridge, Houston, Texas

Return Period	**Scour Depth (ft.)**
2	3.47
5	4.59
10	6.6
25	9.89
50	15.09
100	21.96
200	15.59
250	15.63
500	14.34

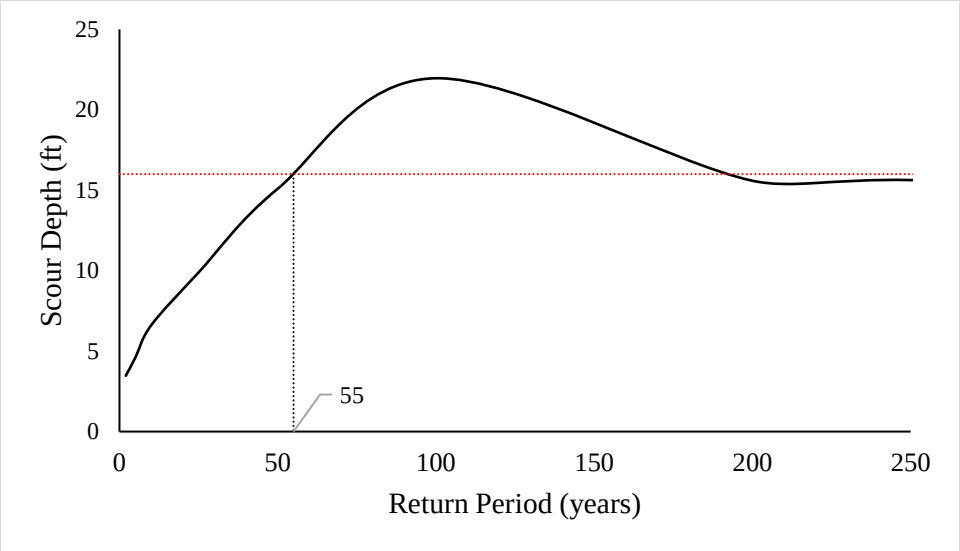

Figure 5-4 Scour Depth for Different Return Periods under Existing Climatic Condition, US59 Bridge, Houston, Texas

Figure 5-5 illustrates the scour depth resulted for different future climate models. The MM5I-HADCM3 model predicts the bridge will reach to the allowable scour depth for a 43-year flood event. Although, the highest scour depth (which is 27.33 feet) results from the flow predicted by MM5i-CCSM climate model. So, MM5I-HADCM3 shows the scour depth will exceed the allowable scour depth earliest, but MM5I-CCSM predicts the highest amount of scour depth (for 250-year Flood), which is 6 feet higher than the highest scour depth predicted for existing climatic condition.

.

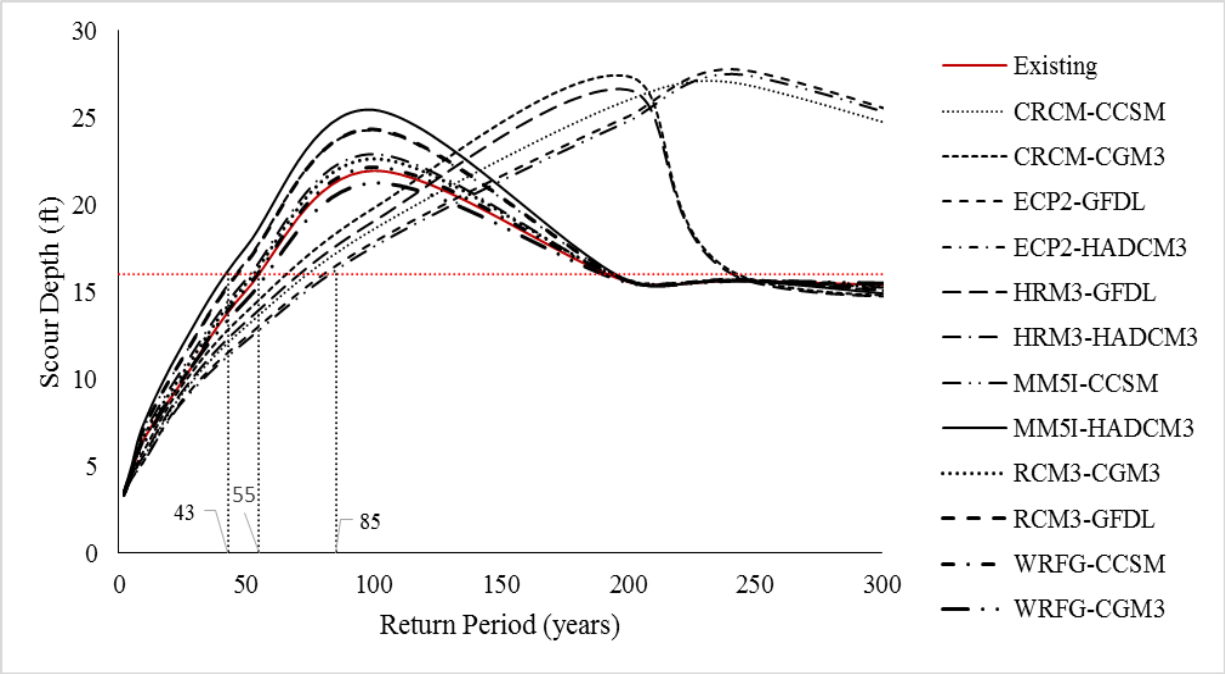

Figure 5-5 Scour Depth for Future Climate Predictions, US59 Bridge, Houston, Texas

Similarly, bridge SH 36 is also assessed for scouring. According to NBI (National Bridge Inventory) record, this bridge is stable for scours. And also, as our model prediction. The bridge does not cross the allowable scour depth which is 12.5 feet, under existing or future climatic condition.

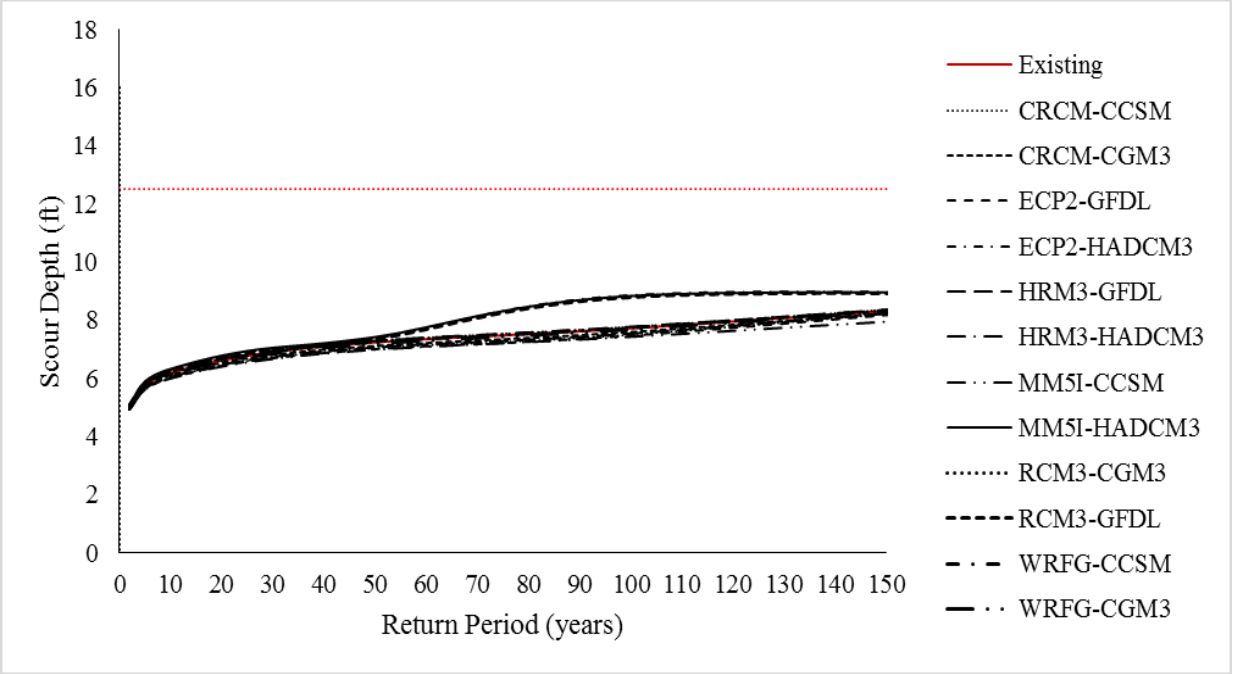

Figure 5-6 Scour Depth for Future Climate Predictions, SH36, Houston, Texas

5.2 Risk Analysis

Risk can be delineated as the probability that a particular climate change event occurs during a stated period of time causing damage to assets times the cost of the damage, including injury and loss of life. In this study to perform risk analysis for bridges, the 'HYRISK' a tool developed for FHWA has been used. This tool performs a risk analysis of the bridge based on the 'probability of failure', which accounts for the overtopping frequency and scour criticality of the bridge. HYRISK used the NBI database and evaluated the risk of failure with the expected annual loss. According to researchers (Stein and Sedmera, 2006, Khelifa et al., 2013, Pearson et al., 2000), HYRISK is the most complete method available to perform a risk analysis of the bridges.

The HYRISK model is a combination of Response model, Damage model and Loss model (Khelifa et al., 2013). Response model estimates the probability of overtopping based on the bridge's functional class and water adequacy. Damage models estimate the probability of damage

based on substructure condition, channel protection, overtopping probability and age of the bridge. And finally based on the damage the loss model estimates the total economic costs.

The economic loss model has been presented below:

$$\text{Cost} = \underbrace{(C_0 + C_1)eWL}_{\text{Rebuilding cost}} + \underbrace{[C_2\,(1\text{-}T/100) + C_3\,T/100]Dad}_{\text{Vehicle running cost}}$$

$$+ \underbrace{[C_4 O\,(1\text{-}T/100) + C_5\,T/100]Dad/S}_{\text{Time loss cost}}$$

Where, Cost = total cost of bridge failure ($), C1 = unit rebuilding cost ($/ft2), e = cost multiplier for early replacement based on average daily traffic ,W = bridge width, L = bridge length, C2 = cost of running automobile (i.e. $0.45/mi), C3 = cost of running truck ($1.30 /mi), D = detour length, A = average daily traffic (ADT), d = duration of detour, C4 = value of time per adult in passenger car ($/hr), O = average occupancy rate(typically 1.63 adults), T = average daily truck traffic (ADTT) form NBI item 109 (% of ADT), C5 = value of time for truck ($22.01/hr), S = average detour speed (typically 40 mph).

The final model calculated the annual risk based on the results of all these models.

$$\text{Expected annual loss} = KP \times \text{Cost}$$

Where,

K = Risk adjustment factor

P = Probability of bridge failure

Data required from the NBI database to calculate the risk has been presented in Table 5-2. These data are for bridge US59 crossing West Fork San Jacinto River.

Table 5-2 NBI Data for Risk Analysis (FHWA, 2016)

Bridge Data		
Bridge Length	501.4	km
Bridge Width	25.2	m
Year built	1961	
Construction Type	Steel Construction	
Detour Length	2	km
Service under bridge	Waterway	
Substructure	Satisfactory Condition	
Waterway Adequacy	Bridge deck and approaches above flood elevations; remote chance of overtopping	
Scour Criticality	The bridge is scoured critically; bridge foundations determined to be unstable for calculated scour	
Average Daily Traffic	43220	
Truck Traffic (%of ADT)	10	
Route Functional Class	Urban freeway	

The cost analysis for the bridge is done using the costs embedded in the software. The basic assumptions of the calculation of the cost and the risk are listed in Table 5-3.

Table 5-3 Basic Assumptions for Risk Analysis

Detour speed (km/h)	64
Occupancy rate	1.57
Person Time Cost ($/h)	8
Vehicle Running Cost ($/km)	0.25
Truck Time Cost ($/h)	30
Rebuild Cost ($/sq.m)	645.83

For the existing condition, the model shows the annual failure probability of the bridge is 0.03959, which results in the expected annual loss of $631600.92. The results are shown in Table 5-4.

Table 5-4 Annual Loss for Existing Climate Condition, Bridge US59, Houston, Texas

Annual Fail Probability	0.03959
Rebuilding Cost ($)	$16,320,485.76
Running Cost ($)	$3,954,630.00
Time Cost ($)	$3,535,439.22
Total Cost ($)	$23,810,554.98
Risk ($/yr)	$631,600.92

After considering the climate prediction by the climate models, which implied a 10% increase in the annual average precipitation, the annual failure probability is also increased. To account for this increased precipitation scenario the annual failure probability of the bridge has been calculated based on the following equation (Khelifa et al., 2013).

$$P_v^a = min\{P_v x C_a\} \quad (5\text{-}1)$$

Where, C_a is the percent increase in precipitation and P_v is the probability of bridge failure for an existing condition.

After the estimation for the predicted increased precipitation, the annual risk of economic loss becomes $694740.00 which is $63,139 more than for the existing climate condition..

5.3 Possible Adaptation to Vulnerability

Assessment of bridges for risk and vulnerability should follow with evaluation of possible adaptation and protection measures to counteract the problems. Agencies (State DOTs, FHWA etc.) have their set of guidelines for possible mitigation and protection measures to vulnerabilities. AASHTO LRFD bridge design specification guide (2005) has suggested certain sets of bridge modification that has been adopted and practised by several agencies like the Oklahoma DOT. The modifications suggested by AAHTO LRFD bridge design specifications (2005) are as follows:

- Relocating or changing the shapes of piers or abutments to avoid areas with deep scour or overtopping scour holes from adjacent foundation elements
- Constructing river training works such as guide banks, dykes etc. for regulating the flow transitions

- Enlargement of the water passing area
- Relocating the crossing of the bridge over waterbody, to avoid an undesirable location

5.3.1 Grade Increase

One possible solution to overtopping is raising the grade of the bridges to create more waterways to pass the excess stream flow that may occur due to the future predicted climate extremes. Then the bridges can accommodate larger flood events, e.g. in Figure 5-7 and 5-8. These graphs show, a mere increase of 1 foot height, can allow the bridges to survive for a greater flood flow. US 59, which have overtopping potential of 90-years (under MM5I-HADCM3 model), can survive 100-year flood flow after raising of 1 foot.

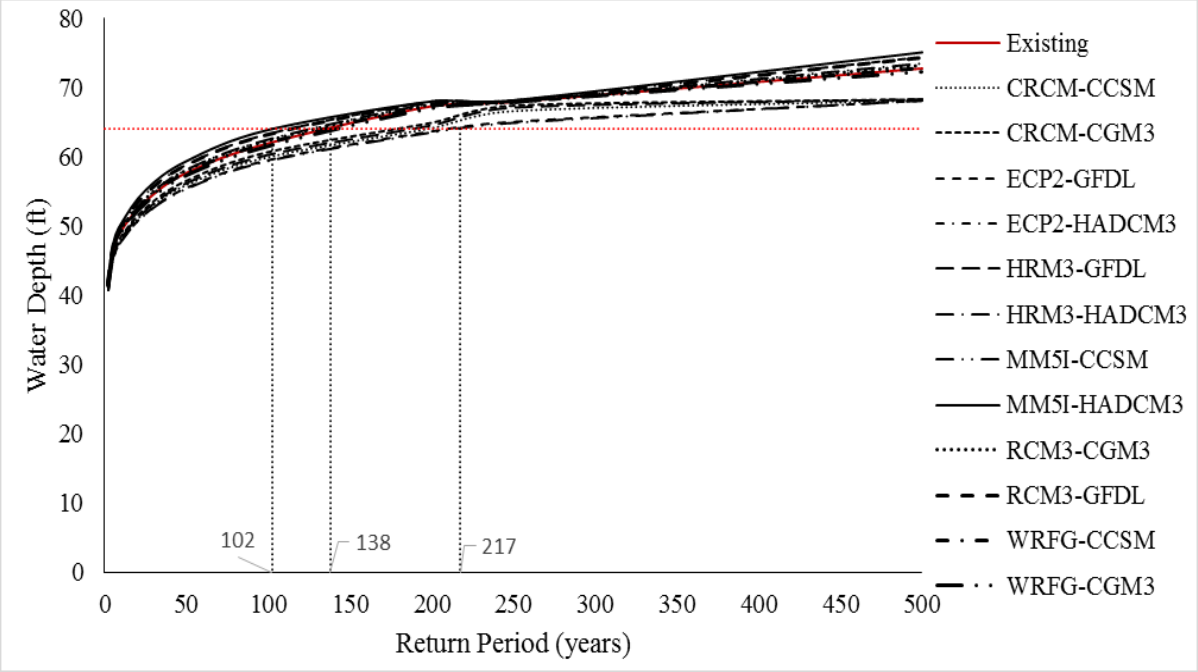

Figure 5-7 Grade Increment of the Bridge US59, Houston, Texas

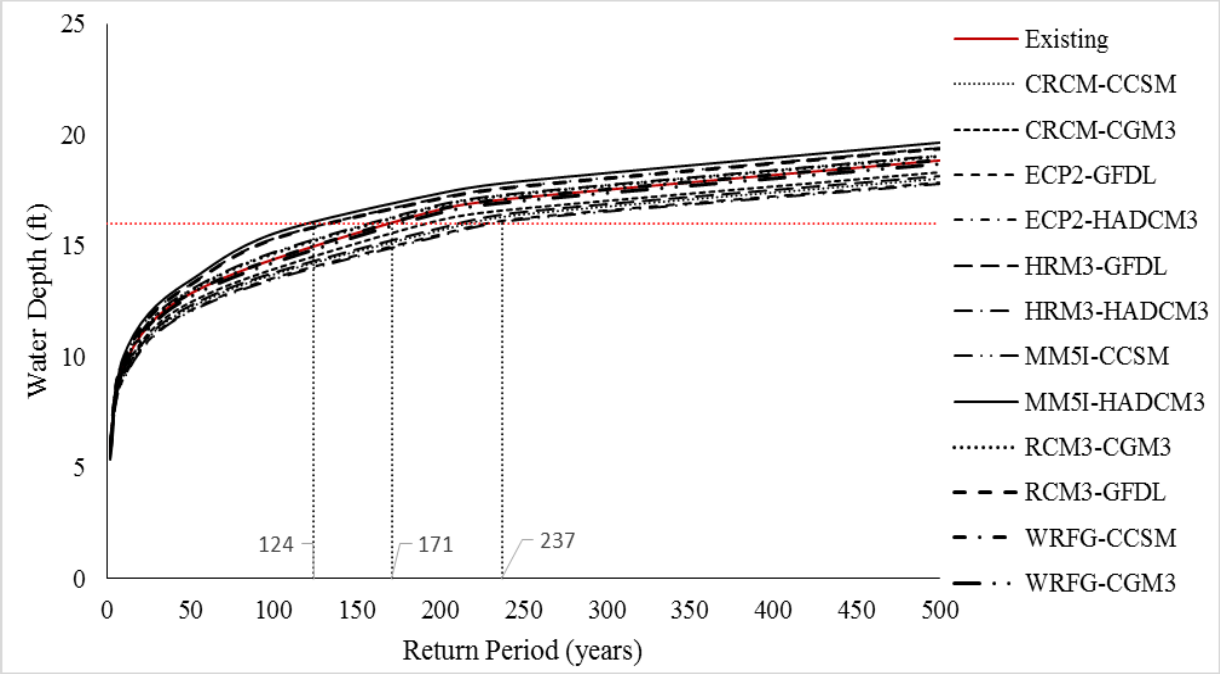

Figure 5-8 Grade Increment of the Bridge SH36, Houston, Texas

Besides, huge cost implication, the raising of the grade may make the bridge more vulnerable to scouring. Because more water will pass through the bridge opening with higher pressure. So, the elevation increase should be associated with proper countermeasures for scouring.

5.3.2 Scour Countermeasures

Scour countermeasures can be delineated as the measures, techniques or practices that are applied to bridge sites to forfeit or minimize the effect of scouring of foundation materials (Wang et al., 2017; Deng et al., 2010 and Lagasse et al., 2007). Based on the functionality of the countermeasures, they have been divided into two categories armouring countermeasures and flow altering countermeasures (Deng and Cai, 2010):

Riprap, blocks, grout filled bags, mattresses etc. are example of armouring countermeasures, whose basic purpose is to act as a resistant layer to the erodible material underneath and protect form scouring due to the shear pressure of the streamflow. Armouring countermeasures are works well in most of the situations and easy to install on the bridge sites,

make them most used countermeasures for pier and abutments. Among them, the most common countermeasure is riprap (Lauchlan and Melville, 2001). The example of riprap placing has been captured in Figure 5.10, which shows three placement conditions of riprap, (a) on the surface, (b) placement on excavated or scoured surface and in (c) riprap has been placed in depth in the bed.

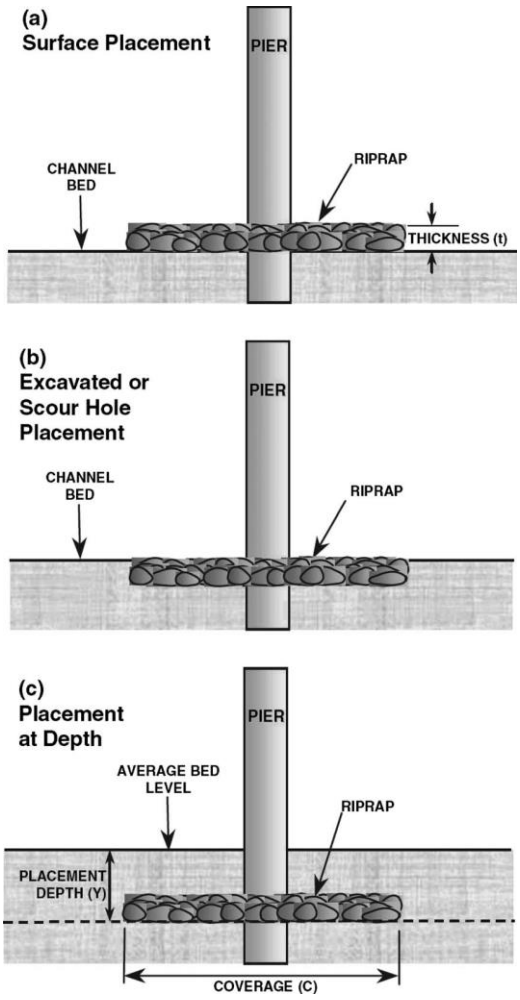

Figure 5-9 Pier Protection against Scouring Using Riprap [Reprinted from Lagasse et al., (2007)]

On the other hand, flow altering countermeasures change the hydraulic flow properties such as alter the flow alignments or break up the vortices and thereby reduces the scouring effect of the bed materials of pier and abutments. Some common practices of flow altering countermeasures are spur dikes, guide banks, collars etc.

Researchers have been studied different techniques over the years for the proper protection of the bridge piers and abutments from scouring. Some of the researches are listed in Table 5.8.

Table 5-8 Common Techniques used as Scour Countermeasures

Technique	Reference	Key Points
Riprap	Lunchen and Melville, 2011	Although riprap is an effective countermeasure technique for clear-water scours conditions in piers, this study investigated their effectiveness in live-bed condition. The study shows the effectiveness of riprap for a wide range of flow conditions and also evaluate the proper placing level of riprap.
	Lagasse et al.,2007	Placement of riprap around piers prevents the strong vortex flow at the front of the pier from entraining bed sediment and forming a scour hole. This study also analyzes the ability of the riprap to protect against scour as a function of stone size.
Slots and Collars	Kumar et al., 1999	Rectangular slots and circular collars extended to bed are effective in reducing the local scour at piers of the bridge. But the slot is ineffective if the approach flow has a high obliquity with respect to the slot.
Parallel Walls	Li, et al.,2006	Parallel walls are effective to measure for the abutment scour mitigation both live-bed and clear-water condition. If the wall anchored below the scour depth, this technique would likely be feasible for situations where the rock is expensive.
Bed Sill	Grimaldi et al., 2009	Bed sills are generally placed downstream at a short distance of the piers to reduce the scour depth, area and volume. The smaller the distance between the pier and the bed sill, the larger the effectiveness of this countermeasure, which reaches about 26% in scour depth reduction in front of the pier and is greater than 80% in scour area and volume reduction in the best configurations.
	Chiew and Lim, 2003	They proposed the use of a sacrificial sill, set upstream to the pier, as a countermeasure acting by protecting the pier from the approach flow.
Submerged Vane	Ghorbani and Kells, 2008	Submerged vanes are an effective countermeasure for scour at piers, especially cylindrical pier. The study has found that, if two vanes are being attached to the Pier, a reduction of 87.7% in scour depth of the pier for constant flow depth, a constant angle and at 0 distance upstream from the pier for a vane height of 0 cm.

The selection of a proper countermeasure for a particular scour condition needs many considerations based on scour mechanism, stream characteristics, construction or maintenance

requirements, the potential for vandalism and costs (Lagasse et al., 2009). Johnson and Niezgada (2004), have proposed a risk-based approach for ranking, comparing and choosing the most appropriate scour countermeasures using failure modes and effect analysis and risk priority numbers.

Lagasse et al. (2007) proposed a selection matrix for appropriate countermeasures for the protection of piers, based on characteristics of bed materials, constructability, inspection and maintenance requirements and life cycle costs of the technique. This matrix can be employed for the primary selection of countermeasures (as suggested by HEC-23). It does not require any site investigation or elaborate testing for effectiveness of the countermeasure. The selection matrix is presented in Figure 5-10. The selection index (SI) consists of five factors to consider, and the technique with the highest SI value is selected as an appropriate solution for the bridge. SI is calculated as follows:

SI = (S1 x S2 x S3 x S4)/LCC

Where,

S1: Bed Materials size and transport

S2: Severity of debris or ice loading

S3: Constructability constraints

S4: Inspection and maintenance requirements

LCC: Life-cycle costs

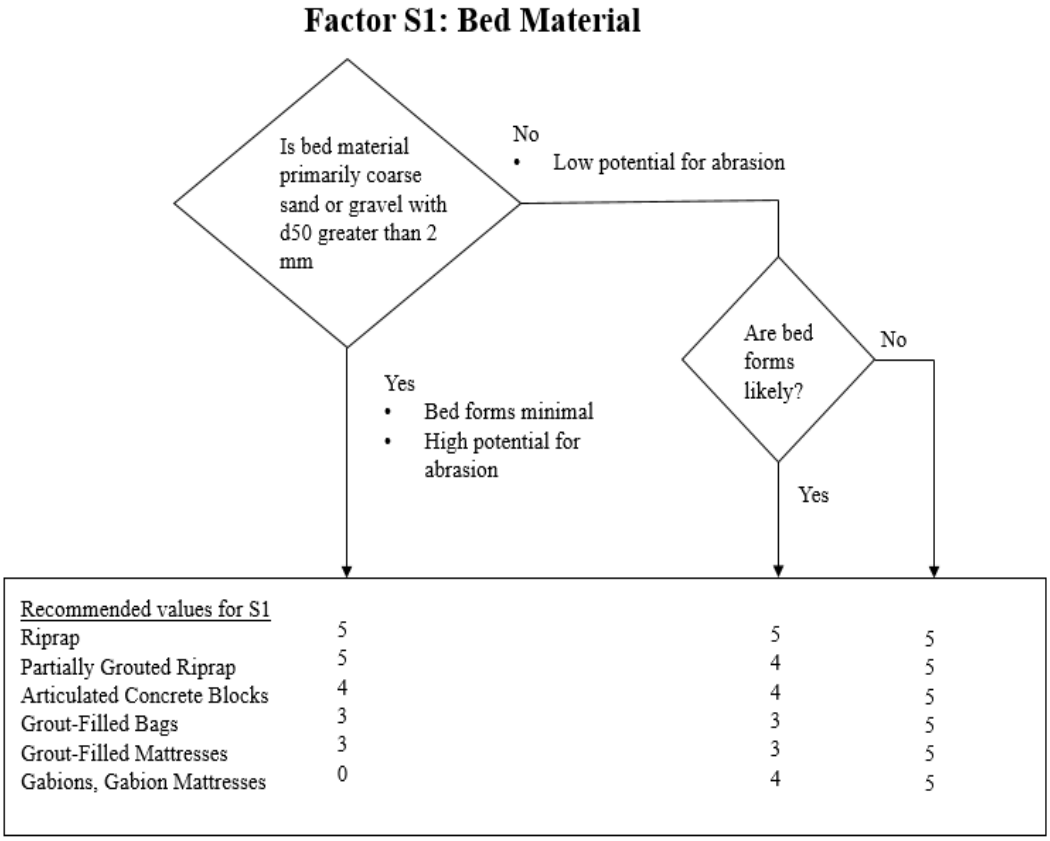

Figure 5-10A Flow Chart Illustrating Selection Factor for Scour Countermeasures based on Bed Material Characteristics [Reprinted from Lagasse et al., (2007)]

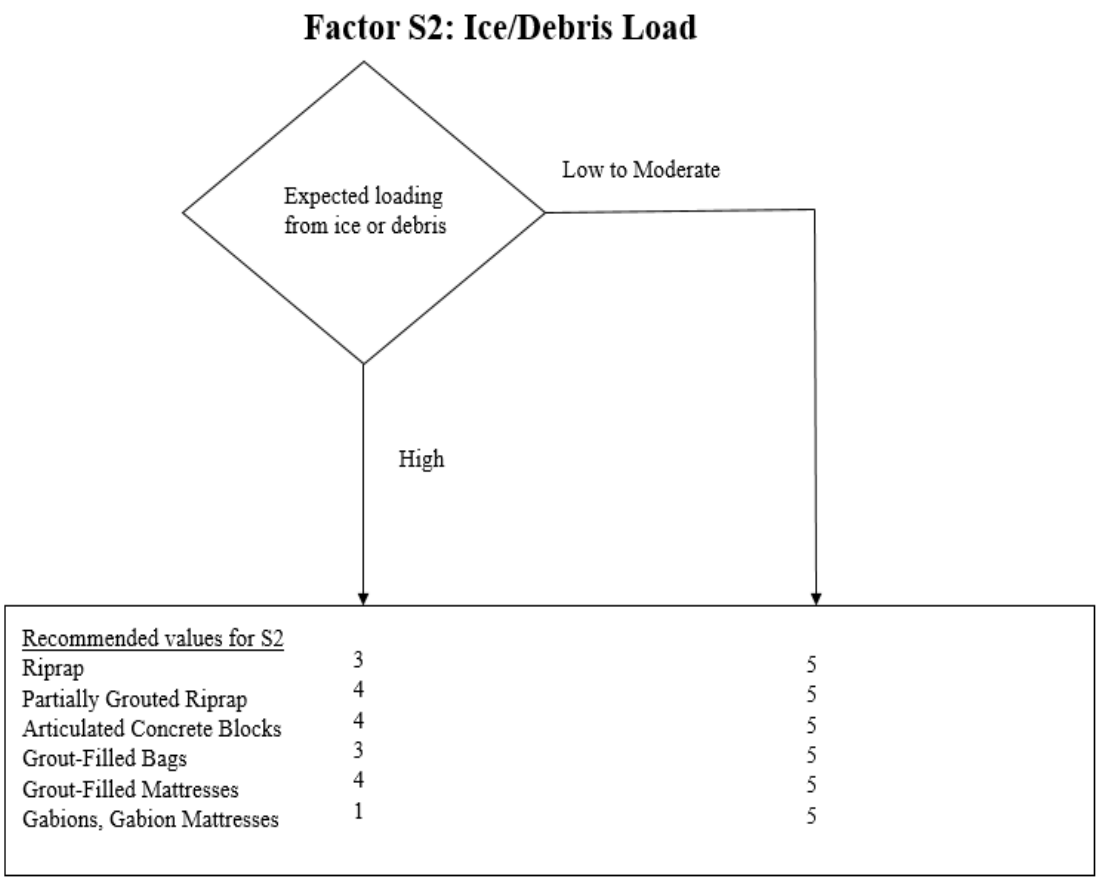

Figure 5-10B Flow Chart Illustrating Selection Factor for Scour Countermeasures based on Impact of Ice or Debris Load [Reprinted from Lagasse et al., (2007)]

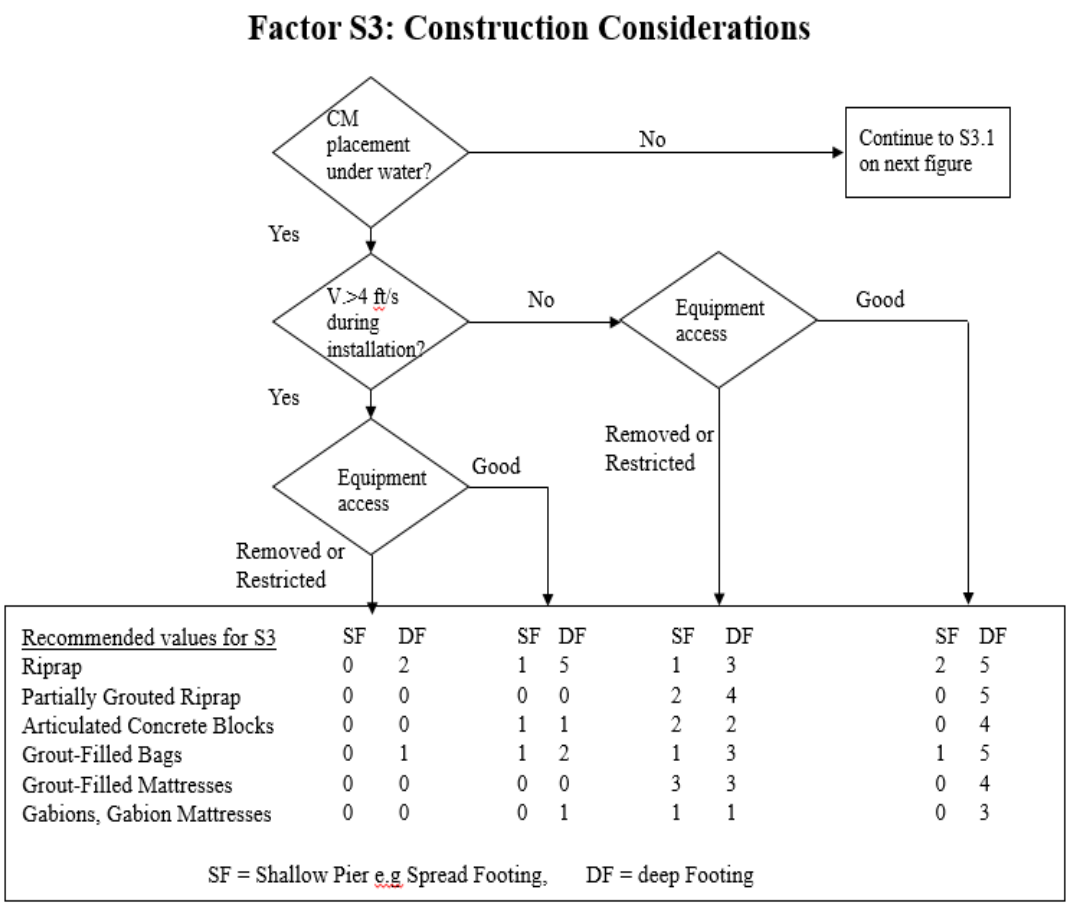

Figure 5-10C Flow Chart Illustrating Selection Factor for Scour Countermeasures based on Considerations During Construction Underwater [Reprinted from Lagasse et al., (2007)]

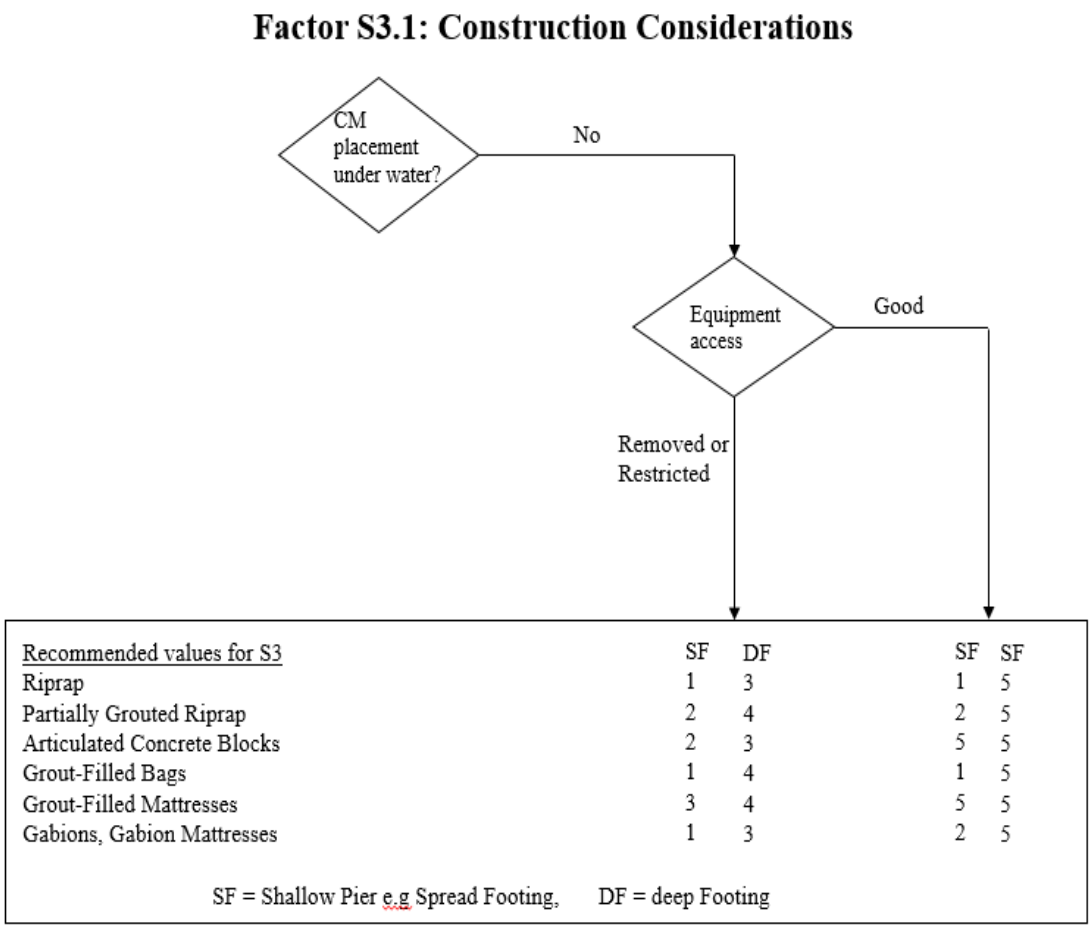

Figure 5-10D Flow Chart Illustrating Selection Factor for Scour Countermeasures based on Considerations During Construction Above Water [Reprinted from Lagasse et al., (2007)]

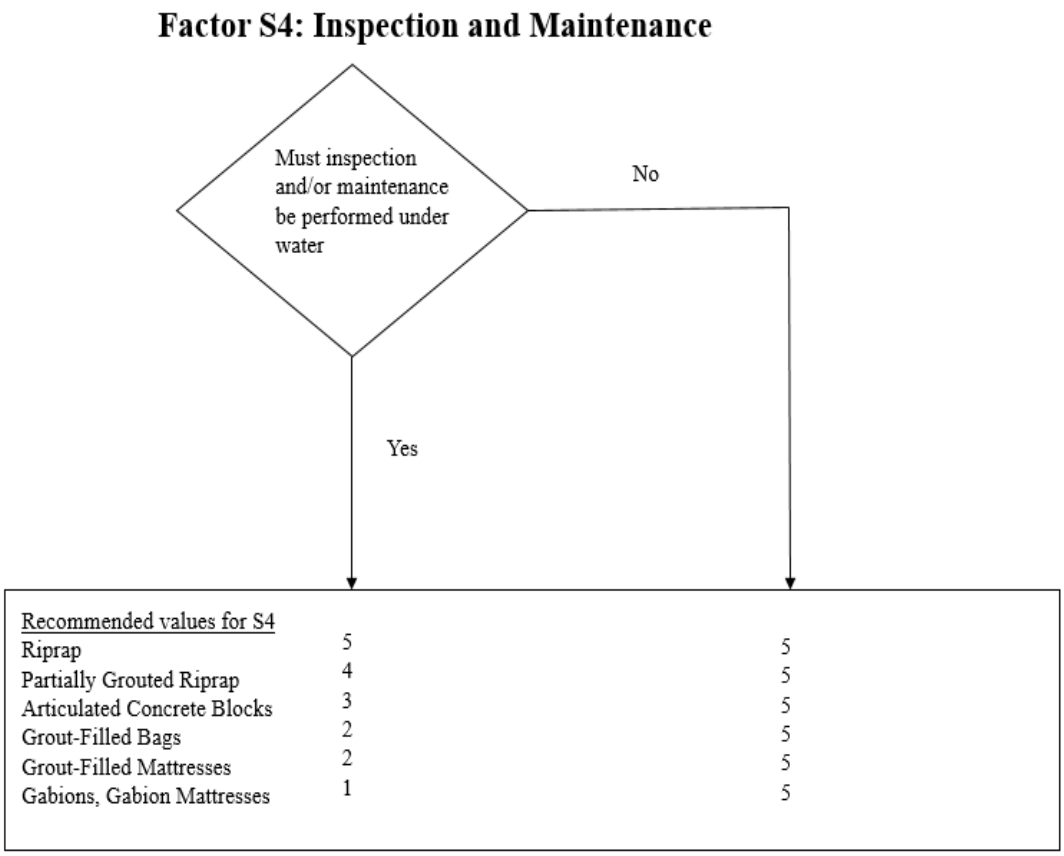

Figure 5-10E Flow Chart Illustrating Selection Factor for Scour Countermeasures based on Inspection and Maintenance [Reprinted from Lagasse et al., (2007)]

Bridge US 59 crossing over San Jacinto River has been analyzed using this matrix. The input parameters are listed in Table 5-9.

Table 5-9 Input Parameters to Countermeasure Selection Matrix

Size of Bed Material	0.03	mm
Ice/Debris Loading	Low to Moderate	
The velocity of the river reach	3 to 20	ft/sec
Foundation Type	Deep footing	

The basic assumptions to perform the selection of countermeasure for bridge US 59 are listed below:

- Underwater placement of the instruments
- Equipment access is good
- Inspection and maintenance operation has to be performed underwater
- Same Life-cycle costs for all techniques

Considering all the factors mentioned in the matrix, the value of SI for different techniques are as follows:

Table 5-10 Selection Index for bridge US59, Houston, Texas

Countermeasure	S1	S2	S3	S4	SI
Riprap	5	5	5	4	19
Partially Grouted Riprap	5	5	0	4	14
Articulating Concrete Blocks	5	5	1	3	14
Grout-filled Bags	5	5	2	2	14
Grout-filled Mattresses	5	5	0	2	12
Gabions, Gabion Mattresses	5	5	1	1	12

So, based on SI value, for bridge US59, Riprap is the preferable countermeasure technique.

Chapter 6: Closure

6.1 Summary

Global climates are significantly changing over the years and causing an increased number of extreme weather events. These changes of climate have a significant effect on the highway infrastructures, such as bridges. Hydraulic design of bridges is primarily focused on the flood frequency for plausible vulnerability such as overtopping and scouring. Climate change causes the change in the frequency of these flood events. This study was done to find out the future climate change predicted from climate models extracted from NARCCAP database and using them to quantify the vulnerability of bridges in the Houston-Galveston area of Texas. For this, a hydraulic model has been developed using HEC-RAS. This study also evaluates the annual economic loss for bridge failure and suggest possible adaptation measures.

6.2 Conclusions

The primary findings of this study are stated as follows:

- Most of the climate models predict increased precipitation in future for cities of Texas and New Mexico. But no significant changes are predicted for cities of Louisiana, Arkansas and Oklahoma.
- Climate prediction by the climate models varies with location. For instance, in Texas MM5I-HADCM3 predicts more precipitation than the existing one, but in Oklahoma, the same model predicts less than the existing precipitation.
- For Houston, Texas, climate models predict the highest increase of precipitation of 10.2%, which results in 11% more streamflow in West Fork San Jacinto River.
- The increased amount of flow in future will increase the overtopping potential for bridges. Bridges will be overtopped for earlier flood events. For example, US59 Bridge will be overtopped for 90-years flood event instead of 119-years flood event and SH36 Bridge will be overtopped at 87-year flood event instead of a 127-year flood event.

- Scour condition will also worsen under the increased precipitation scenario. Bridge US 59 is a scour critical bridge as per as the NBI record and the allowable scour depth for this bridge will reach for 55-year flood events under existing climatic condition. However, for future climate data, the bridge will undergo the exceeding of allowable scour depth for 43-year flood events, which is 12-years earlier than the existing climatic condition.
- The model predicted increased precipitation poses a risk of $63,139 more annual loss for the bridge US59.
- Raising the grade of the bridge can solve the overtopping problem. Increasing the grade of the bridge by only one-foot for bridge US59 will allow 12-years more intense flood events through the bridge without overtopping.
- Proper choice of scour countermeasures can be made by a site visit and a clear understanding of the field condition of the bridge and the channel.

6.3 Limitations and Future Work

This study has been performed using different models, such as climate models, hydrologic models, and hydraulic model, scour model, etc. All of these models have some limitations due to inherent uncertainties. The uncertainties associated with the models have been stated below:

- The uncertainties in climate models primarily come from three main sources, such as the unpredicted nature of the climatic systems (natural variability), the inability to model the earth's many complex processes (model uncertainty) and the inability to project future societal choices such as energy use (scenario uncertainty). Climate data sources such as NARCCAP uses ensembles to reduce the amount of uncertainty in climate prediction. Besides proper bias correction method has to be applied to reduce the anomaly in predicted climate data. Although climate uncertainty cannot be eliminated completely, and it remains as a barrier to effective adaptation (Green et al., 2014 and Reeder et al. 2011).

- Estimation of flood frequency using hydrologic models such as regional regression models possesses their source of uncertainty. Like in this study, USGS regional regression equations have been used, which have been generated based on 683-gauge station data and the characteristic of the catchment area has been defined with a single parameter 'omega.'
- In bridge scour assessment most, common practice is using the empirical models. 22 empirical models have been found for scouring estimation by Sheppard et al. (2014). Uncertainty arises using these models, as scour depends on the non-linear interaction between water flow and sediment transport, which can be evaluated with high-resolution geomorphological simulation models (Dikanski et al.,2018). Lagasee et al. (2013), has evaluated HEC-18 models' uncertainty by comparing model simulated results to observational field data. Results show that uncertainties of models may vary based on the flow conditions. The study also found that local scour is less sensitive to the flow conditions than the contraction scour, which lead to the conclusion by Dikanski et al. (2018), contraction scour is more sensitive to climate change compared to local scour.

Recommendation for future research are stated below:

- Comparative analysis between climate prediction data sources should be performed, to find out more suitable climate prediction models to incorporate in bridge hydraulics study.
- For installation or adaptation of countermeasures for scour, details field survey should be performed to analyze the suitability of a technique.

References

Almodovar-Rosario, N., Dorney, C., Flood, M., Lennon, J., & Lockman, J. T. (2014). MnDOT Flash Flood Vulnerability and Adaptation Assessment Pilot Project.

American Association of State Highway and Transportation Officials (AASHTO).2007. AASHTO LRFD Bridge Design Specifications. 4th Ed., AASHTO, Washington, DC.

Anderson, C.J., Claman, D., and Mantilla, R.2015. Iowa's Bridge and Highway Climate Change and Extreme Weather Vulnerability Assessment Pilot, Institute for Transportation Iowa State University.

Arneson, L. A., L. W. Zevenbergen, P. F. Lagasse, and P. E. Clopper. (2012). "Evaluating Scour at Bridges, Hydraulic Engineering Circular No. 18 (HEC-18)." Publication No. FHWA-HIF-12-003.

Arkansas State Highway and Transportation Department (ASHTD).1982. Drainage manual, Hydraulics Section, ASHTD, Arkansas.

Asquith, William H., and Meghan C. Roussel.2009. Regression equations for estimation of annual peak-streamflow frequency for undeveloped watersheds in Texas using an L-moment-based, PRESS-Minimized, residual-adjusted approach. No. FHWA/TX-09/0-5521-1. US Geological Survey.

Bala, Sujit Kumar, M. Mozammel Hoque, and S. M. U. Ahmed. (2005). "Failure of a Bridge Due to Flood in Bangladesh-A Case Study." UAP Journal of Civil and Environmental Engineering 1, no. 1: 38-44.

Brekke, L., B. L. Thrasher, E. P. Maurer, and T. Pruitt. (2013). Downscaled CMIP3 and CMIP5 climate and hydrology projections: Release of downscaled CMIP5 climate projections, comparison with preceding information, and summary of user needs. US Army Corps of Engineers, US Geological Survey.

Briaud, Jean-Louis, Anand V. Govindasamy, Dongkyun Kim, Paolo Gardoni, Francisco Olivera, Hamn-Ching Chen, Christopher Mathewson, and Kenneth Elsbury.(2009). A simplified method for estimating scour at bridges. No. FHWA/TX-09/0-5505-1.

Brunner, G.W. 2008.HEC-RAS River Analysis System User's Manual Version 4.0. Report CPD-68 (Davis, CA: US Army Corps of Engineers, Hydrologic Engineering Center).

Karl, Thomas R., Gerald A. Meehl, Christopher D. Miller, Susan Joy Hassol, Anne M. Waple, and William L. Murray.2008. Weather and climate extremes in a changing climate. US Climate Change Science Program.

Cigada, Alfredo, Stefano Malavasi, and M. Vanalil.2001. "Direct force measurements on a submerged bridge model." WIT Transactions on the Built Environment 56.

CMIP5 Coupled Model Intercomparison Project, Program for Climate Model Diagnosis and Intercomparison, World Climate Research Programme

http://cmip-pcmdi.llnl.gov/cmip5/forcing.html

Deng, Lu, and C. S. Cai.2009. "Bridge scour: Prediction, modeling, monitoring, and countermeasures." Practice periodical on structural design and construction 15, no. 2: 125-134.

FHWA,2012 "Climate Change and Extreme Weather Vulnerability Assessment Framework,"FHWA-:HEP-13-005 http://www.fhwa.dot.gov/environment/climate_change/adaptation/resources_and_publications/v ulnerability_assessment_framework/index.cfm

Filosa, Gina, and Alexandra Oster. (2015). International practices on climate adaptation in transportation: findings from a virtual review. No. DOT-VNTSC-FHWA-15-01; FHWA-HEP-15-012. John A. Volpe National Transportation Systems Center (US).

Filosa, G., Plovnick, A., Stahl, L., Miller, R., & Pickrell, D. H. (2017). Vulnerability Assessment and Adaptation Framework (No. DOT-VNTSC-FHWA-18-04). The United States. Federal Highway Administration. Office of Planning, Environment, and Realty.

Gutowski Jr, William J., Raymond W. Arritt, Sho Kawazoe, David M. Flory, Eugene S. Takle, Sébastien Biner, Daniel Caya et al.(2010)."Regional extreme monthly precipitation simulated by NARCCAP RCMs." Journal of Hydrometeorology 11, no. 6: 1373-1379.

Hayhoe, K., and A. Stoner. (2012). "Gulf Coast Study, Phase 2 Temperature and Precipitation Projections for the Mobile Bay Region." US DOT Center for Climate Change and Environmental Forecasting Final Rep.

Hempel, S., K. Frieler, L. Warszawski, J. Schewe, and F. Piontek. (2013). A trend-preserving bias correction–the ISI-MIP approach. Earth System Dynamics, 4(2), 219-236.

Hogan, Michael, David Elder, and Stephanie Molden. (2014)."Connecticut Department of Transportation Climate Change and Extreme Weather Vulnerability Pilot Project Final Report."

IPCC - Intergovernmental Panel on Climate Change. http://www.ipcc.ch/ . Accessed June 16, 2018.

Intergovernmental Panel on Climate Change. (2000). Working Group III. Emissions Scenarios: Summary for Policymakers. A Special Report of IPCC Working Group III. Intergovernmental Panel on Climate Change.

Stocker, T. (Ed.). (2014). *Climate change 2013: the physical science basis: Working Group I contribution to the Fifth assessment report of the Intergovernmental Panel on Climate Change*. Cambridge University Press.

http://www.climatechange2013.org/images/report/WG1AR5_SPM_FINAL.pdf

Johnson, P. A., and Niezgoda, S. L. (2004). “Risk-based method for selecting bridge scour countermeasures.” J. Hydraul. Eng., 130(2), 121–128.

Kara, Sibel, Thorsten Stoesser, Terry W. Sturm, and Saad Mulahasan.2015. "Flow dynamics through a submerged bridge opening with overtopping." Journal of Hydraulic Research 53, no. 2: 186-195.

Khelifa, A., Garrow, L. A., Higgins, M. J., & Meyer, M. D.2013. Impacts of climate change on scour-vulnerable bridges: Assessment based on HYRISK. Journal of Infrastructure Systems, :19(2), 138-146.

Kilgore, Roger T., George Rudy Herrmann, Wilbert O. Thomas Jr, and David B. Thompson.2016. Highways in the river environment—Floodplains, extreme events, risk, and resilience. No. FHWA-HIF-16-018.

Kumar, V., Ranga Raju, K. G., and Vittal, N.1999 "Reduction of local scour around bridge piers using slots and collars." J. Hydraul. Eng.,125(12), 1302–1305.

Lagasse, Peter Frederick.2007.Countermeasures to protect bridge piers from scour. Vol. 593. Transportation Research Board.

Lagasse, P. F., P. E. Clopper, J. E. Pagán-Ortiz, L. W. Zevenbergen, L. A. Arneson, J. D. Schall, and L. G. Girard.2009. Bridge scour and stream instability countermeasures: experience, selection, and design guidance: Volume 1. No. FHWA-NHI-09-111. National Highway Institute (US).

Lauchlan, C. S., and Melville, B. W.2001. "Riprap protection at bridge piers." J. Hydraul. Eng., 127(5), 412–418.

Laursen, Emmett M.1963. "An analysis of relief bridge scour." Journal of the Hydraulics Division 89, no. 3 : 93-118.

Li, H., Barkdoll, B. D., Kuhnle, R., and Alonso, C.2006. "Parallel walls as an abutment scour countermeasure." J. Hydraul. Eng., 132(5), 510–520.

MACA Statistically Downscaled Climate Data from CMIP5, University of Idaho. http://maca.northwestknowledge.net/index.php

Malavasi, Stefano, Monica Riva, Marcello Vanali, and Enrico Larcan.2001. "Hydrodynamic forces on a submerged bridge." WIT Transactions on The Built Environment 56.

Markus, Momcilo, James Angel, Gregory Byard, Sally McConkey, Chen Zhang, Ximing Cai, Michael Notaro, and Moetasim Ashfaq.2018. "Communicating the impacts of projected climate change on heavy rainfall using a weighted ensemble approach." Journal of Hydrologic Engineering 23, no. 4: 04018004.

Mearns, L. O., W. J. Gutowski, R. Jones, L.-Y. Leung, S. McGinnis, A. M. B. Nunes, and Y. Qian.2009. A regional climate change assessment program for North America. EOS, Vol. 90, No. 36, pp. 311-312.

Mearns, L. O., W. J. Gutowski, R. Jones, L.-Y. Leung, S. McGinnis, A. M. B. Nunes, and Y. Qian. The North American Regional Climate Change Assessment Program dataset. National Center for Atmospheric Research Earth System Grid data portal, Boulder, CO. 2007, updated 2014, Data downloaded 2015-10-23.

Mearns, L. O., W. J. Gutowski, R. Jones, L.-Y. Leung, S. McGinnis, A. M. B. Nunes, and Y. Qian. The North American Regional Climate Change Assessment Program dataset. National Center for Atmospheric Research Earth System Grid data portal, Boulder, CO. 2007, updated 2014, Data downloaded 2015-10-23.

Melville, Bruce W., and Stephen E. Coleman.2000. Bridge Scour. Water Resources Publication.

National Oceanic and Atmospheric Administration (NOAA) (2016). Earth System Research Laboratory, Global Monitoring Division, retrieved on 17 February 2016 from http://www.esrl.noaa.gov/gmd/ccgg/trends/global.html#global.

National Climate Change Viewer (NCCV), Climate Research and Development Program, USGS, https://www2.usgs.gov/climate_landuse/clu_rd/nccv.asp

Nakicenovic, Nebojsa, and Rob Swart.2000. "Emissions Scenarios. Special report of the Intergovernmental panel on climate change."

New Mexico Department of Transportation (NMDOT).1998. Drainage Manual, Volume II-Hydraulics, Sedimentation and Erosion, Drainage Section, NMDOT, Albuquerque, NM.

NORTH AMERICAN REGIONAL REANALYSIS: A long-term, consistent, high-resolution climate dataset for the North American domain, as a major improvement upon the earlier global reanalysis datasets in both resolution and accuracy, Fedor Mesinger et al., submitted to BAMS 2004.

Odgaard, A. J., and Wang, Y.1987. “Scour prevention at bridge piers.” Proc., 1987 National Conf. on Hydraulic Engineering, New York, 523–527.

Okeil, Ayman M., and C. S. Cai.2008. "Survey of short-and medium-span bridge damage induced by Hurricane Katrina." Journal of Bridge Engineering 13, no. 4: 377-387.

Parker, G., Toro-Escobar, C., and Voight, R. L., Jr. 1998.“Countermeasures to protect bridge piers from scour.” Users’ Guide (revised 1999) and Final Report, NCHRP Project No. 24-7, Prepared for National Cooperative Highway Research Program, Transportation Research Board by St. Anthony Falls Hydraulic Laboratory, Univ. of Minnesota, Minn.

Parola, Arthur C., and Arthur C. Parola.1998. Highway infrastructure damage caused by the 1993 upper Mississippi River basin flooding. No. 417. Transportation Research Board.

Pearson, David, J. Jones, and Stuart Stein.2000. "Risk-based design of bridge scour countermeasures." Transportation Research Record: Journal of the Transportation Research Board 1696 : 229-235.

Räty, Olle, Jouni Räisänen, and Jussi S. Ylhäisi.2014. "Evaluation of delta change and bias correction methods for future daily precipitation: intermodel cross-validation using ENSEMBLES simulations." Climate Dynamics 42, no. 9-10: 2287-2303.

Roads, J., S-C. Chen, and M. Kanamitsu.2003. "US regional climate simulations and seasonal forecasts." Journal of Geophysical Research: Atmospheres 108, no. D16.

Savonis, M. J., V. Burkett, and J. R. Potter.2008. Impacts of climate change and variability on transportation systems and infrastructure: Gulf coast study, Phase I. U.S. Climate Change Science Program and Global Change Research.

Schuring, John R., Robert Dresnack, and Eugene Golub.2017. Design and Evaluation of Scour for Bridges Using HEC-18. No. FHWA-NJ-2017-011. New Jersey Department of Transportation.

State of Louisiana Department of Transportation and Development (LDOT).2011. Hydraulics manual, Baton Rouge, Louisiana.

Stein, Stuart, and Karsten Sedmera.2006. Risk-based management guidelines for scour at bridges with unknown foundations. Transportation Research Board of the National Academies.

Stocker, T. F., D. Qin, G.K. Plattner, M. Tignor, S. K. Allen, J. Boschung, A. Nauels, Y. Xia, V. Bex, and P. M. Midgley.2014. Climate change 2013: The physical science basis. Cambridge University Press, New York.

Texas Department of Transportation (TxDOT).2004. Hydraulic design manual, Design Division, TxDOT, Austin, Tex.

Wang, Chen, Xiong Yu, and Fayun Liang.2017. "A review of bridge scour: mechanism, estimation, monitoring and countermeasures." Natural Hazards 87, no. 3: 1881-1906.

Warren, F. J, R. Schwartz, J., Andrey, B. Mills, and D. Riedel.2004. Climate Change Impacts and Adaptation: A Canadian Perspective. In Climate Change Impacts and Adaptation Directorate, Natural Resources Canada, Ottawa, Ontario, ISBN: 0-662-33123-0.

Wardhana, Kumalasari, and Fabian C. Hadipriono.2003. "Analysis of recent bridge failures in the United States." Journal of performance of constructed facilities 17, no. 3 (2003): 144-150.

Zarrati, A. R., Nazahira, M., and Mashahir, M. B.2006. “Reduction of local scour in the vicinity of bridge pier groups using collars and riprap.” J. Hydraul. Eng., 132(2), 154–162.

Zevenbergen, L. W., L. A. Arneson, J. H. Hunt, and Arthur Carl Miller.2012. Hydraulic design of safe bridges. No. FHWA-HIF-12-018.

Appendix A: Climate Data

Bias Correction for Amarillo, Texas:

Table A-1 Bias Corrected Precipitation Data, Amarillo, Texas

Climate Models	Future Simulation (in)	Current Simulation (in)	Bias Corrected (in)
CRCM-CCSM	17.9	18.2	18.1
CRCM-CGCM3	19.7	18.9	19.2
ECP2-GFDL	21.4	24.5	16.1
ECP2-HADCM3	15.3	17.6	15.9
HRM3-GFDL	27.0	29.7	16.7
HRM3-HADCM3	21.5	23.1	17.1
MM5I-CCSM	17.1	17.9	17.6
MM5I-HADCM3	21.3	21.7	18.0
RCM3-CGCM3	20.0	21.7	16.9
RCM3-GFDL	29.0	29.7	18.0
WRFG-CCSM	14.5	14.5	18.4
WRFG-CGCM3	15.1	13.6	20.4

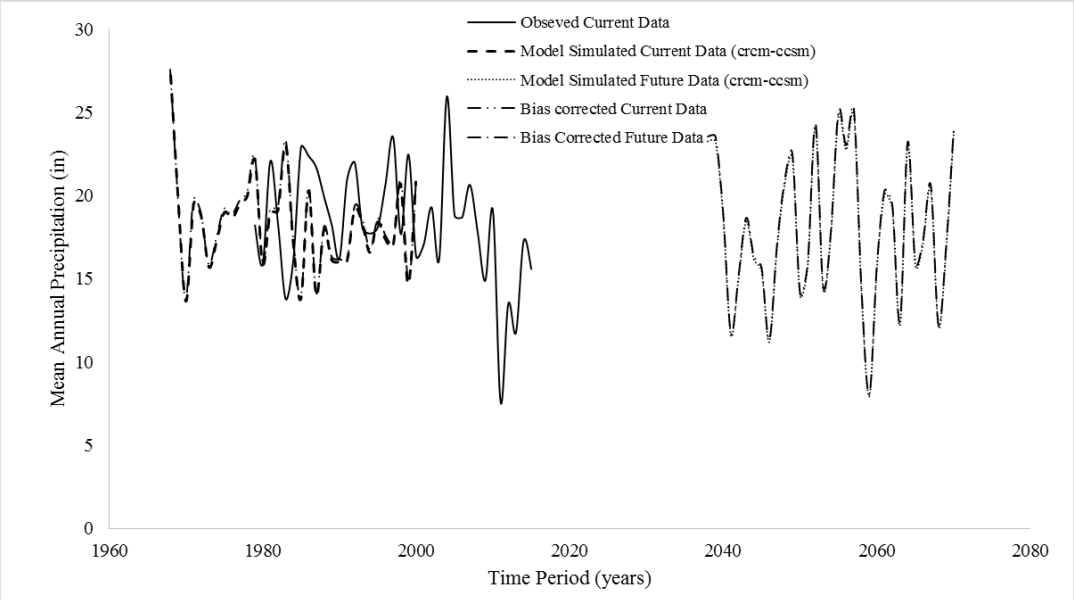

Figure A-1 Bias Correction for Mean Annual Precipitation, Amarillo, Texas

Bias Correction for Austin, Texas:

Table A-2 Bias Corrected Precipitation Data, Austin, Texas

Climate Models	Future Simulation (in)	Current Simulation (in)	Bias Corrected (in)
CRCM-CCSM	18.6	20.7	28.4
CRCM-CGCM3	27.7	27.7	31.7
ECP2-GFDL	33.4	36.7	28.7
ECP2-HADCM3	41.0	37.5	34.6
HRM3-GFDL	34.7	37.6	29.2
HRM3-HADCM3	42.4	38.6	34.7
MM5I-CCSM	17.2	19.2	28.2
MM5I-HADCM3	37.5	32.9	36.1
RCM3-CGCM3	35.3	34.5	32.3
RCM3-GFDL	43.2	43.4	31.5
WRFG-CCSM	24.3	24.4	31.5
WRFG-CGCM3	28.2	27.0	33.0

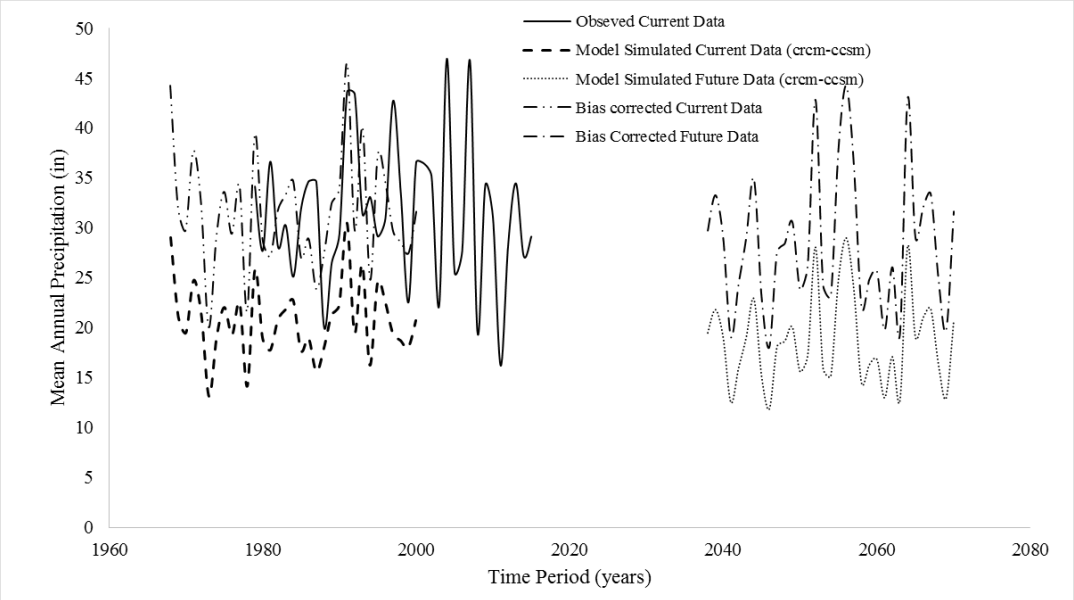

Figure A-2 Bias Correction for Mean Annual Precipitation, Austin, Texas

Bias Correction for Dallas, Texas:

Table A-3 Bias Corrected Precipitation Data, Dallas, Texas

Climate Models	Future Simulation (in)	Current Simulation (in)	Bias Corrected (in)
CRCM-CCSM	21.0	22.0	33.2
CRCM-CGCM3	27.6	26.8	35.8
ECP2-GFDL	32.2	37.1	30.2
ECP2-HADCM3	33.3	33.2	34.9
HRM3-GFDL	36.8	37.1	34.5
HRM3-HADCM3	36.3	34.7	36.4
MM5I-CCSM	21.9	23.2	32.9
MM5I-HADCM3	31.0	29.5	36.5
RCM3-CGCM3	30.9	31.8	33.9
RCM3-GFDL	37.8	37.2	35.3
WRFG-CCSM	25.0	22.7	38.4
WRFG-CGCM3	25.3	25.3	34.8

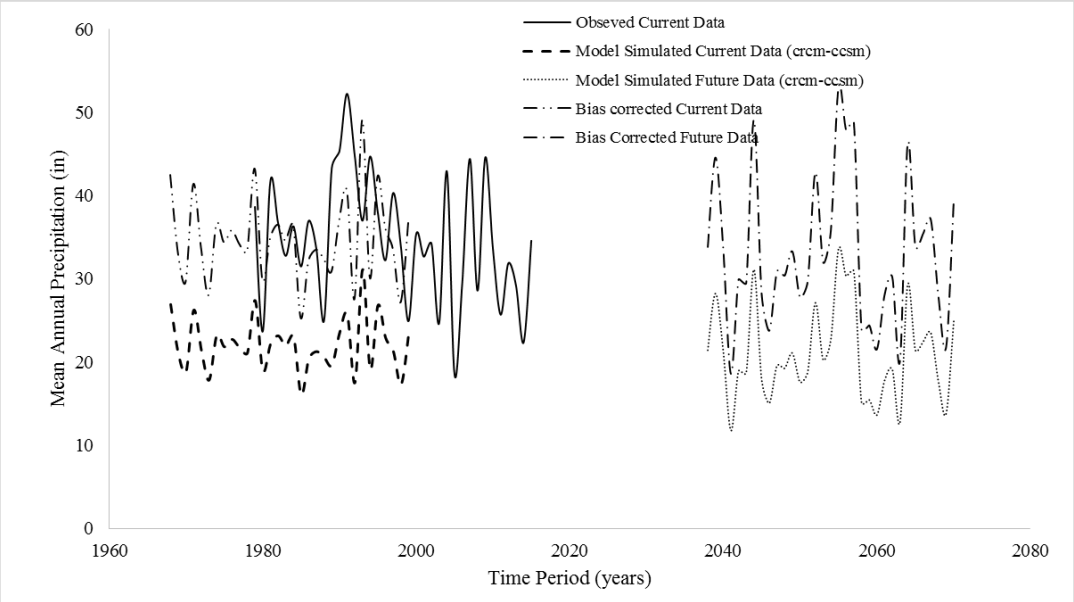

Figure A-3 Bias Correction for Mean Annual Precipitation, Dallas, Texas

Bias Correction for El Paso, Texas:

Table A-4 Bias Corrected Precipitation Data, El Paso, Texas

Climate Models	Future Simulation (in)	Current Simulation (in)	Bias Corrected (in)
CRCM-CCSM	13.2	15.6	8.1
CRCM-CGCM3	11.6	12.5	8.8
ECP2-GFDL	16.7	16.8	9.4
ECP2-HADCM3	8.4	9.0	8.9
HRM3-GFDL	21.9	23.8	8.7
HRM3-HADCM3	12.2	15.1	7.7
MM5I-CCSM	9.3	11.7	7.5
MM5I-HADCM3	12.7	11.1	10.9
RCM3-CGCM3	34.3	35.3	9.2
RCM3-GFDL	41.6	42.3	9.3
WRFG-CCSM	9.8	10.9	8.5
WRFG-CGCM3	7.1	7.1	9.5

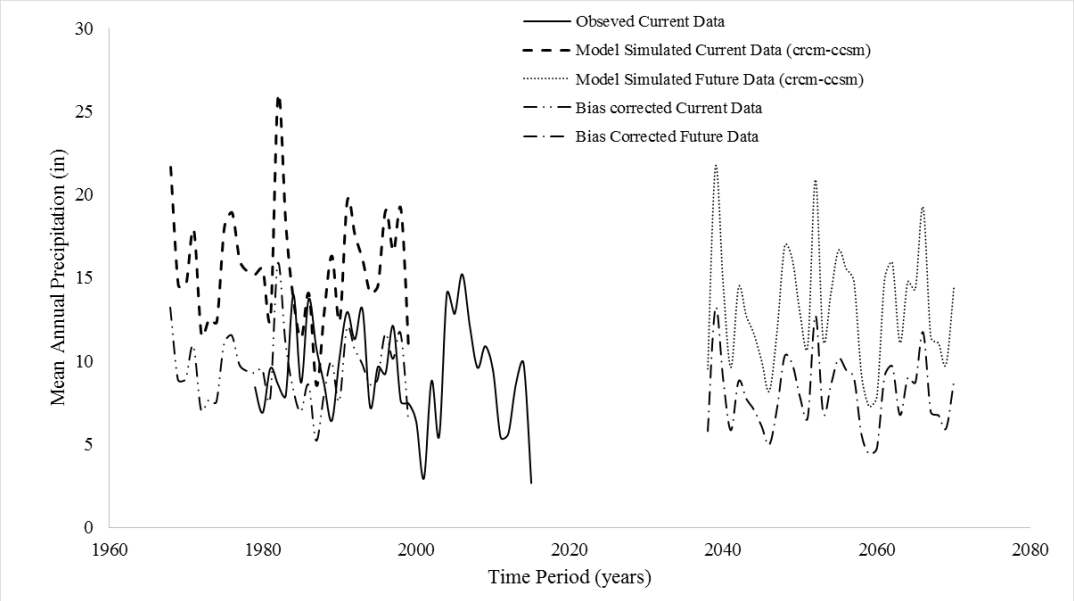

Figure A-4 Bias Correction for Mean Annual Precipitation, El Paso, Texas

Bias Correction for Fort Worth, Texas:

Table A-5 Bias Corrected Precipitation Data, Fort Worth, Texas

Climate Models	Future Simulation (in)	Current Simulation (in)	Bias-Corrected (in)
CRCM-CCSM	19.8	20.6	32.8
CRCM-CGCM3	22.0	24.4	30.8
ECP2-GFDL	31.0	36.1	29.2
ECP2-HADCM3	32.0	31.6	34.5
HRM3-GFDL	36.4	37.9	32.7
HRM3-HADCM3	35.2	33.7	35.7
MM5I-CCSM	21.0	21.9	32.8
MM5I-HADCM3	28.2	27.1	35.5
RCM3-CGCM3	21.5	30.1	24.3
RCM3-GFDL	36.0	36.1	34.0
WRFG-CCSM	22.6	20.6	37.3
WRFG-CGCM3	22.0	21.6	34.7

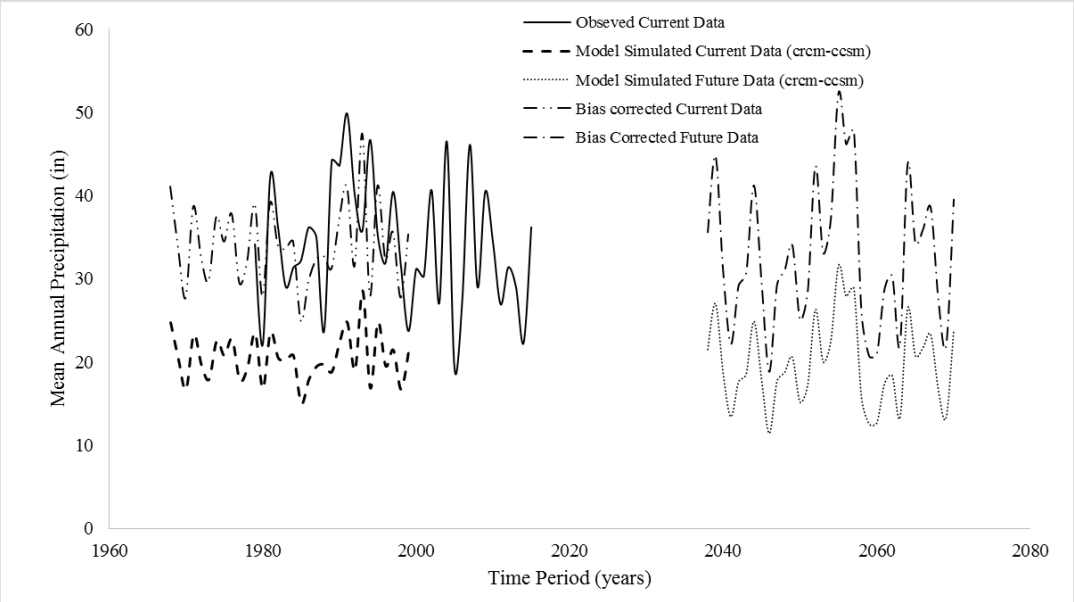

Figure A-5 Bias Correction for Mean Annual Precipitation, Fort Worth, Texas

Bias Correction for McAllen, Texas:

Table A-6 Bias Corrected Precipitation Data, McAllen, Texas

Climate Models	Future Simulation (in)	Current Simulation (in)	Bias-Corrected (in)
CRCM-CCSM	24.0	29.2	14.9
CRCM-CGCM3	42.5	44.1	17.5
ECP2-GFDL	33.0	38.5	15.5
ECP2-HADCM3	46.1	35.4	23.6
HRM3-GFDL	24.2	27.4	16.0
HRM3-HADCM3	39.6	34.7	20.7
MM5I-CCSM	10.7	15.6	12.4
MM5I-HADCM3	44.5	46.3	17.5
RCM3-CGCM3	51.1	49.7	18.6
RCM3-GFDL	69.7	69.4	18.2
WRFG-CCSM	21.4	25.0	15.5
WRFG-CGCM3	32.0	34.7	16.8

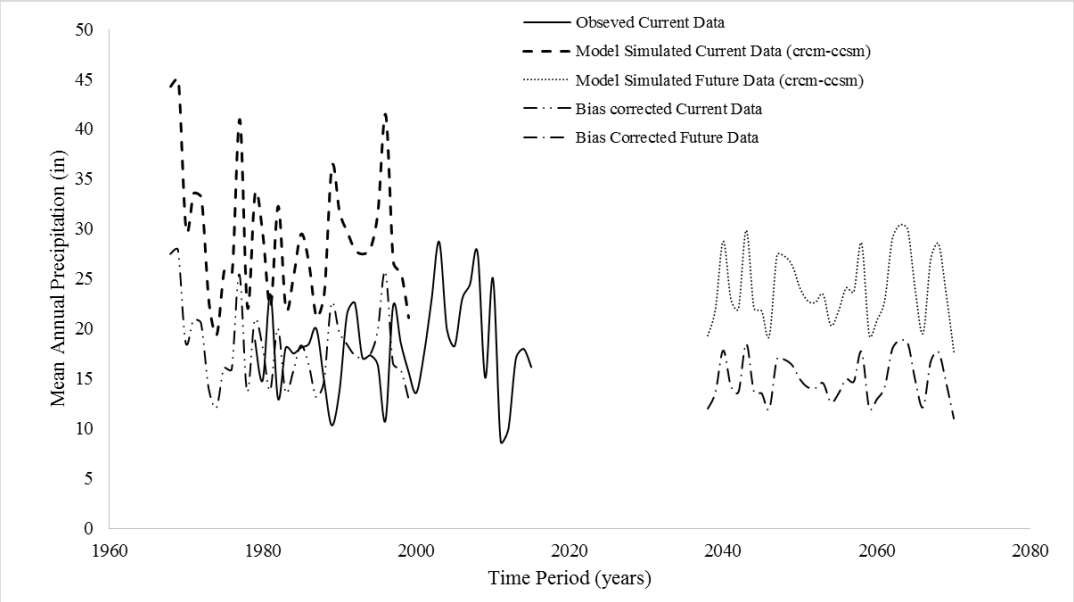

Figure A-6 Bias Correction for Mean Annual Precipitation, McAllen, Texas

Bias Correction for San Antonio, Texas:

Table A-7 Bias Corrected Precipitation Data, San Antonio, Texas

Climate Models	Future Simulation (in)	Current Simulation (in)	Bias-Corrected (in)
CRCM-CCSM	17.1	19.5	26.5
CRCM-CGCM3	27.0	27.0	30.2
ECP2-GFDL	29.4	34.6	25.7
ECP2-HADCM3	39.1	34.3	34.5
HRM3-GFDL	30.3	32.6	28.1
HRM3-HADCM3	39.1	32.9	35.9
MM5I-CCSM	14.7	16.1	27.5
MM5I-HADCM3	34.4	30.2	34.5
RCM3-CGCM3	33.3	32.5	31.0
RCM3-GFDL	41.7	42.0	30.0
WRFG-CCSM	24.0	24.4	29.8
WRFG-CGCM3	25.4	24.8	30.9

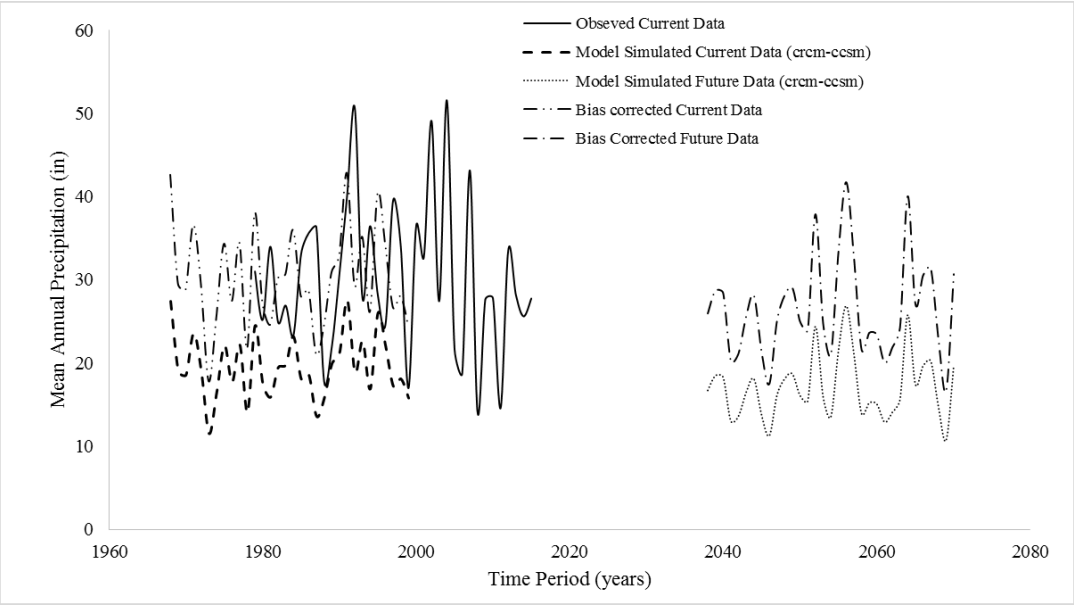

Figure A-7 Bias Correction for Mean Annual Precipitation, San Antonio, Texas

Bias Correction for Albuquerque, New Mexico:

Table A-8 Bias Corrected Precipitation Data, Albuquerque, New Mexico

Climate Models	Future Simulation (in)	Current Simulation (in)	Bias Corrected (in)
CRCM-CCSM	13.1	14.6	9.2
CRCM-CGCM3	11.3	11.5	10.1
ECP2-GFDL	22.8	19.8	11.8
ECP2-HADCM3	9.4	10.1	9.4
HRM3-GFDL	22.9	24.4	9.6
HRM3-HADCM3	15.4	17.7	8.9
MM5I-CCSM	9.4	11.1	8.7
MM5I-HADCM3	15.8	15.7	10.3
RCM3-CGCM3	12.0	14.3	8.6
RCM3-GFDL	25.4	26.2	9.9
WRFG-CCSM	14.5	14.6	10.2
WRFG-CGCM3	12.6	13.3	9.7

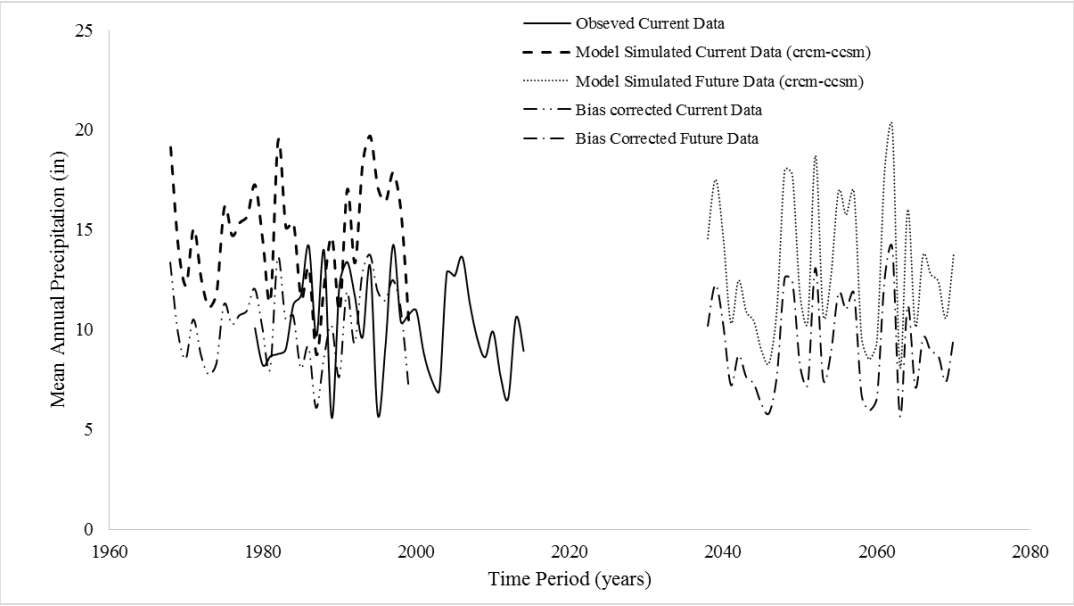

Figure A-8 Bias Correction for Mean Annual Precipitation, Albuquerque, New Mexico

Bias Correction for Las Cruces, New Mexico:

Table A-9 Bias Corrected Precipitation Data, Las Cruces, New Mexico

Climate Models	Future Simulation (in)	Current Simulation (in)	Bias Corrected (in)
CRCM-CCSM	16.1	18.4	9.0
CRCM-CGCM3	14.3	15.3	9.7
ECP2-GFDL	16.7	15.9	10.8
ECP2-HADCM3	7.2	8.2	9.2
HRM3-GFDL	25.6	28.9	9.2
HRM3-HADCM3	15.4	19.3	8.2
MM5I-CCSM	9.7	11.9	8.4
MM5I-HADCM3	12.9	11.5	11.6
RCM3-CGCM3	8.6	9.1	9.8
RCM3-GFDL	19.2	20.7	9.6
WRFG-CCSM	11.0	11.8	9.6
WRFG-CGCM3	8.9	8.7	10.6

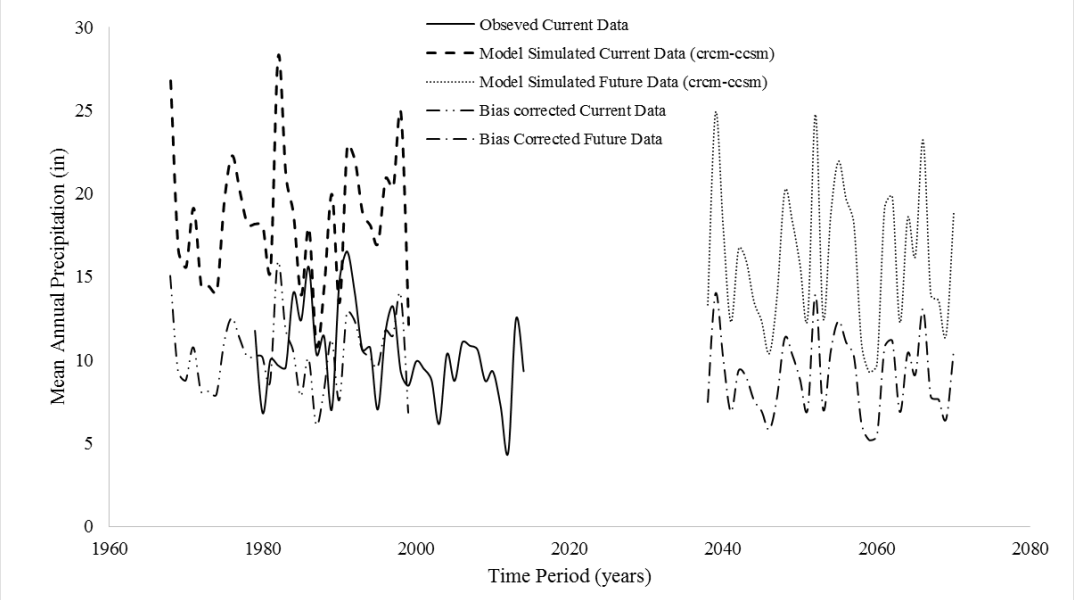

Figure A-9 Bias Correction for Mean Annual Precipitation, Las Cruces, New Mexico

Bias Correction for Taos, New Mexico:

Table A-10 Bias Corrected Precipitation Data, Taos, New Mexico

Climate Models	Future Simulation (in)	Current Simulation (in)	Bias-Corrected (in)
CRCM-CCSM	17.2	18.3	14.6
CRCM-CGCM3	15.6	16.1	15.0
ECP2-GFDL	35.3	42.0	13.0
ECP2-HADCM3	26.3	29.7	13.7
HRM3-GFDL	33.6	36.1	14.4
HRM3-HADCM3	26.0	28.9	14.0
MM5I-CCSM	17.2	21.8	12.2
MM5I-HADCM3	34.1	32.6	16.2
RCM3-CGCM3	31.3	31.8	15.3
RCM3-GFDL	41.4	40.6	15.8
WRFG-CCSM	17.5	17.9	15.2
WRFG-CGCM3	16.9	18.4	14.3

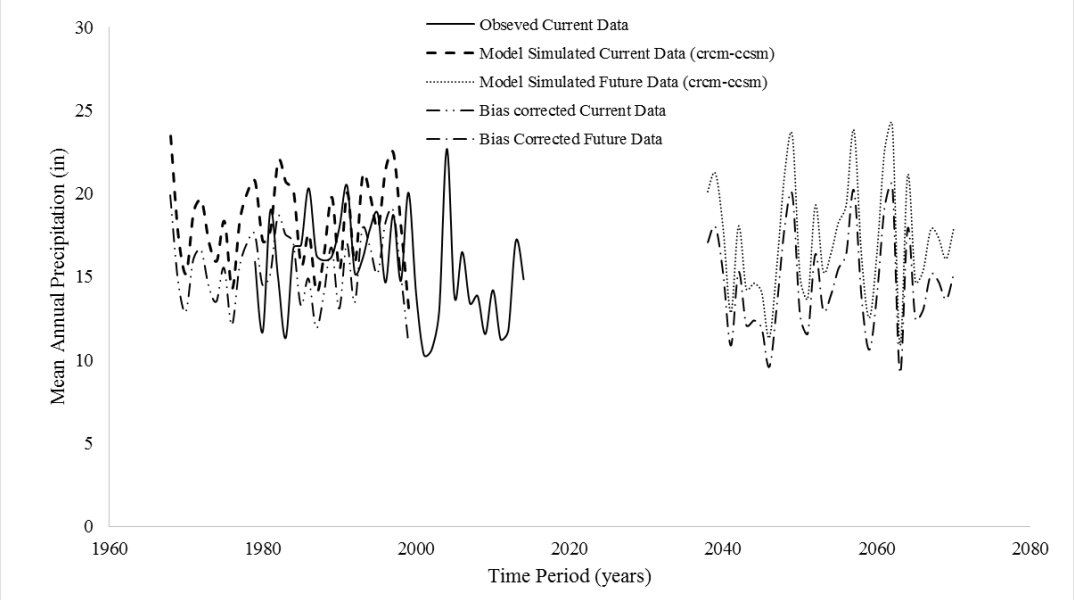

Figure A-10 Bias Correction for Mean Annual Precipitation, Taos, New Mexico

Bias Correction for Santa Fe, New Mexico:

Table A-11 Bias Corrected Precipitation Data, Santa Fe, New Mexico

Climate Models	Future Simulation (in)	Current Simulation (in)	Bias-Corrected (in)
CRCM-CCSM	18.5	20.0	12.2
CRCM-CGCM3	16.6	17.1	12.8
ECP2-GFDL	32.2	32.7	13.0
ECP2-HADCM3	19.6	21.6	12.0
HRM3-GFDL	21.9	23.6	12.3
HRM3-HADCM3	15.5	17.6	11.6
MM5I-CCSM	13.3	16.1	10.9
MM5I-HADCM3	25.2	24.0	13.8
RCM3-CGCM3	15.3	18.1	11.1
RCM3-GFDL	30.9	30.9	13.2
WRFG-CCSM	16.2	16.8	12.7
WRFG-CGCM3	15.0	15.7	12.6

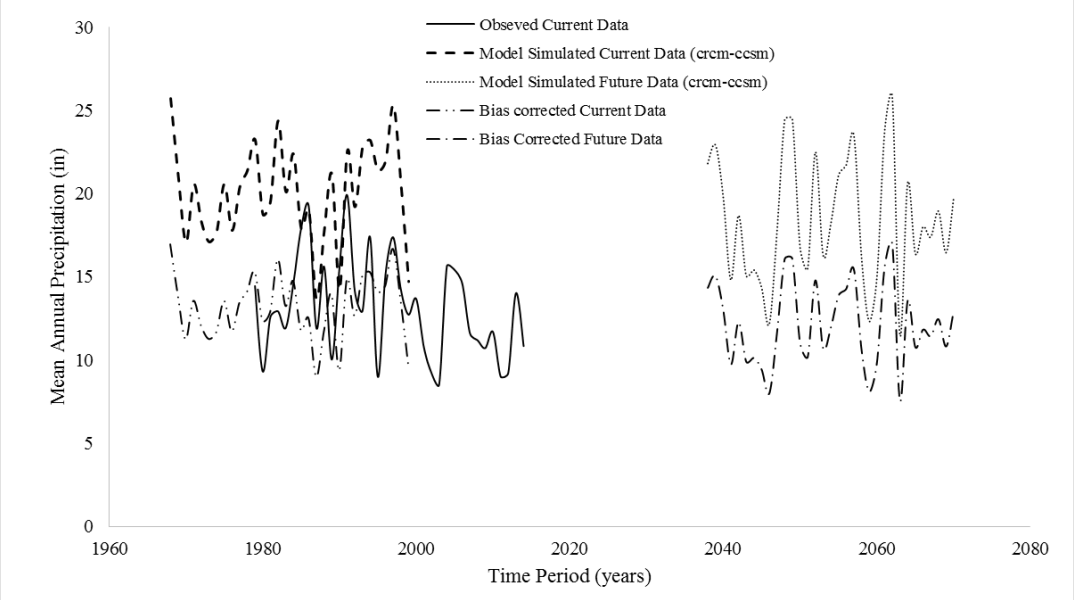

Figure A-11 Bias Correction for Mean Annual Precipitation, Santa Fe, New Mexico

Bias Correction for Roswell, New Mexico:

Table A-12 Bias Corrected Precipitation Data, Roswell, New Mexico

Climate Models	Future Simulation (in)	Current Simulation (in)	Bias-Corrected (in)
CRCM-CCSM	14.9	15.4	11.4
CRCM-CGCM3	13.8	14.5	11.2
ECP2-GFDL	17.3	16.8	12.2
ECP2-HADCM3	7.7	8.7	10.4
HRM3-GFDL	20.4	23.8	10.1
HRM3-HADCM3	13.1	15.8	9.8
MM5I-CCSM	10.6	10.7	11.6
MM5I-HADCM3	13.0	11.4	13.4
RCM3-CGCM3	14.7	16.0	10.8
RCM3-GFDL	25.8	27.3	11.1
WRFG-CCSM	13.9	14.1	11.6
WRFG-CGCM3	13.9	12.3	13.4

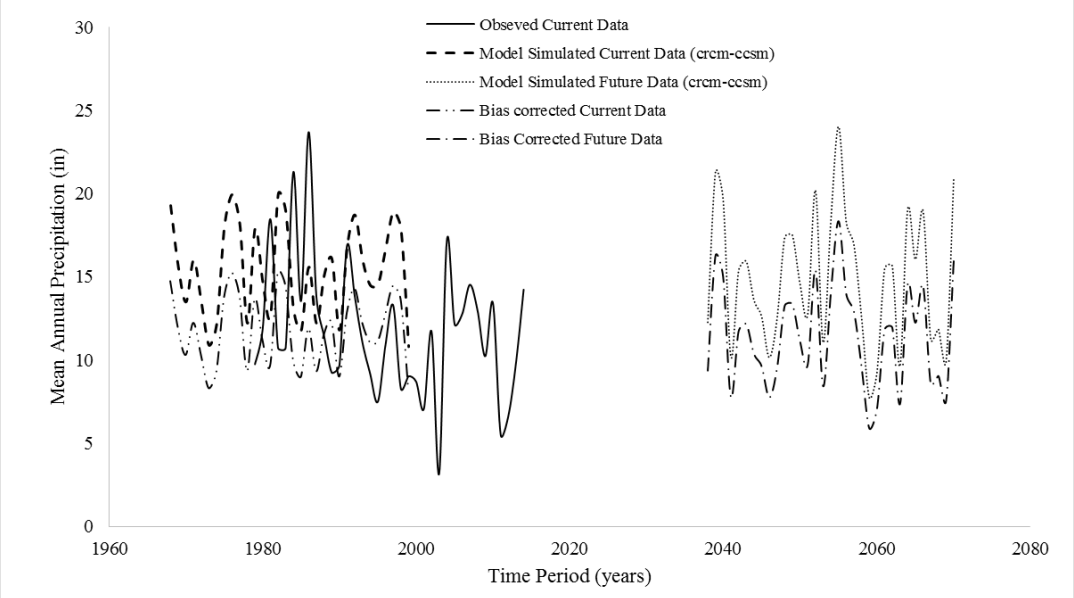

Figure A-12 Bias Correction for Mean Annual Precipitation, Roswell, New Mexico

Bias Correction for Farmington, New Mexico:

Table A-13 Bias Corrected Precipitation Data, Farmington, New Mexico

Climate Models	Future Simulation (in)	Current Simulation (in)	Bias-Corrected (in)
CRCM-CCSM	17.4	19.7	8.2
CRCM-CGCM3	14.2	14.6	9.0
ECP2-GFDL	29.9	27.0	10.3
ECP2-HADCM3	15.3	15.8	9.0
HRM3-GFDL	15.6	16.5	8.8
HRM3-HADCM3	10.2	12.0	7.9
MM5I-CCSM	10.5	12.4	7.9
MM5I-HADCM3	17.3	17.5	9.2
RCM3-CGCM3	16.9	19.0	8.2
RCM3-GFDL	34.0	34.1	9.3
WRFG-CCSM	12.5	13.1	8.9
WRFG-CGCM3	11.3	11.7	9.0

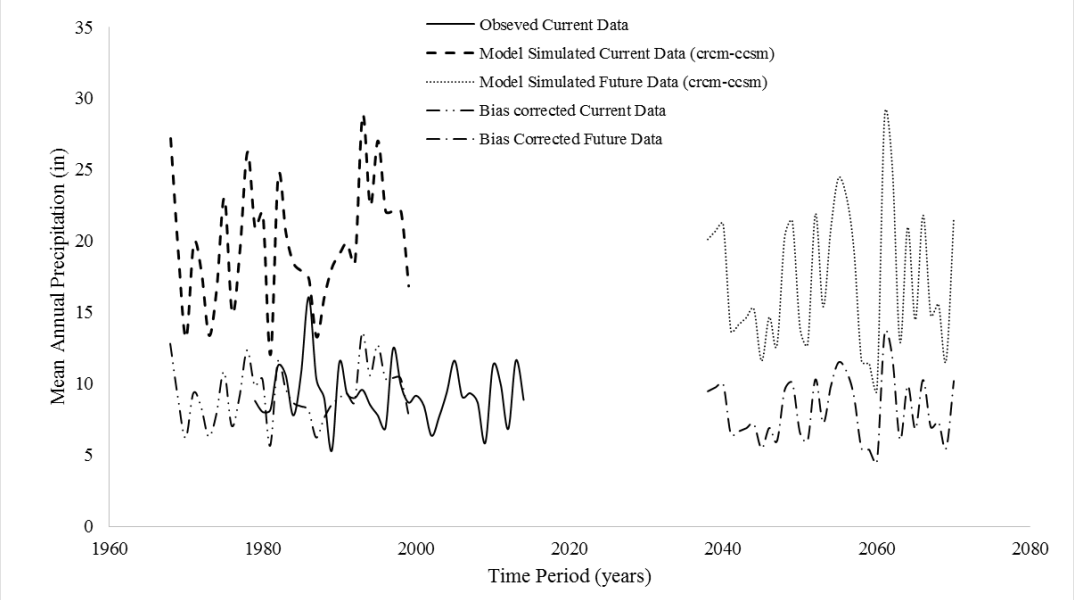

Figure A-13 Bias Correction for Mean Annual Precipitation, Farmington, New Mexico

Bias Correction for Lordsburg, New Mexico:

Table A-14 Bias Corrected Precipitation Data, Lordsburg, New Mexico

Climate Models	Future Simulation (in)	Current Simulation (in)	Bias-Corrected (in)
CRCM-CCSM	12.6	16.1	9.8
CRCM-CGCM3	10.7	11.0	12.2
ECP2-GFDL	22.8	20.5	13.9
ECP2-HADCM3	11.1	11.3	12.3
HRM3-GFDL	25.5	28.2	11.3
HRM3-HADCM3	12.8	15.1	10.6
MM5I-CCSM	9.4	13.3	8.9
MM5I-HADCM3	14.7	13.2	13.9
RCM3-CGCM3	9.5	10.1	11.8
RCM3-GFDL	22.6	24.6	11.5
WRFG-CCSM	10.4	13.3	9.8
WRFG-CGCM3	8.9	8.6	13.0

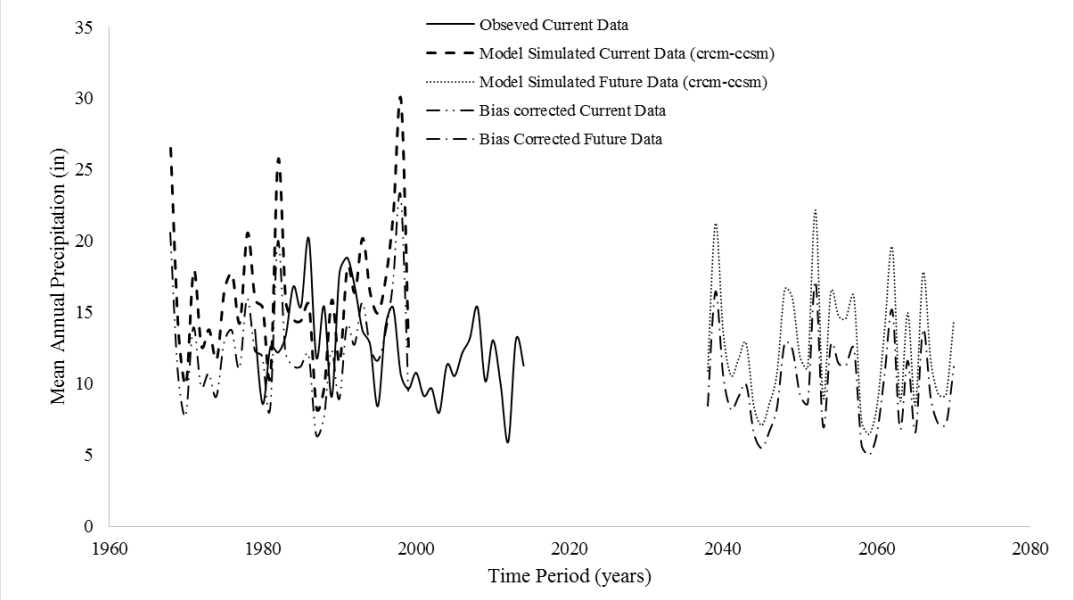

Figure A-14 Bias Correction for Mean Annual Precipitation, Lordsburg, New Mexico

Bias Correction for Lafayette, Louisiana:

Table A-15 Bias Corrected Precipitation Data, Lafayette, Louisiana

Climate Models	Future Simulation (in)	Current Simulation (in)	Bias Corrected (in)
CRCM-CCSM	24.1	26.4	54.0
CRCM-CGCM3	41.8	41.5	59.8
ECP2-GFDL	37.8	40.5	55.3
ECP2-HADCM3	48.0	45.9	62.1
HRM3-GFDL	36.2	40.3	53.2
HRM3-HADCM3	48.8	48.1	60.1
MM5I-CCSM	30.6	32.7	55.5
MM5I-HADCM3	60.1	55.1	64.6
RCM3-CGCM3	58.7	57.5	60.6
RCM3-GFDL	56.2	55.5	60.1
WRFG-CCSM	28.5	31.1	54.3
WRFG-CGCM3	53.3	51.3	61.7

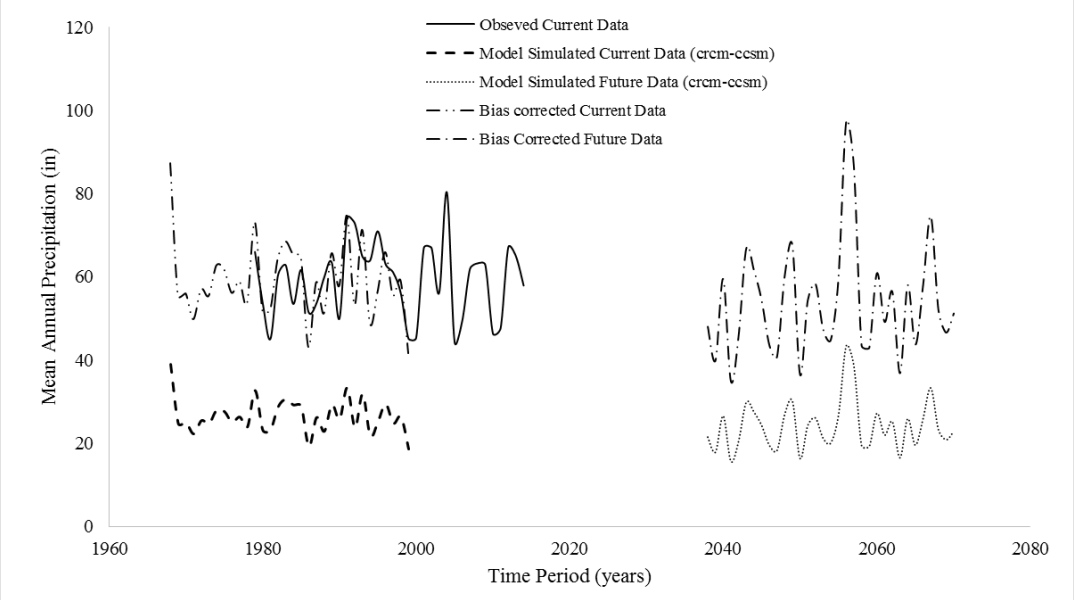

Figure A-15 Bias Correction for Mean Annual Precipitation, Lafayette, Louisiana

Bias Correction for Baton Rouge, Louisiana:

Table A-16 Bias Corrected Precipitation Data, Baton Rouge, Louisiana

Climate Models	Future Simulation (in)	Current Simulation (in)	Bias Corrected (in)
CRCM-CCSM	23.7	26.1	55.0
CRCM-CGCM3	40.1	38.2	63.5
ECP2-GFDL	51.5	58.1	53.6
ECP2-HADCM3	65.2	64.4	61.3
HRM3-GFDL	38.6	43.0	54.3
HRM3-HADCM3	49.8	49.2	61.3
MM5I-CCSM	32.9	34.8	57.2
MM5I-HADCM3	61.5	56.1	66.4
RCM3-CGCM3	60.8	59.0	62.4
RCM3-GFDL	58.0	56.2	62.5
WRFG-CCSM	29.5	32.8	54.4
WRFG-CGCM3	58.1	54.5	64.6

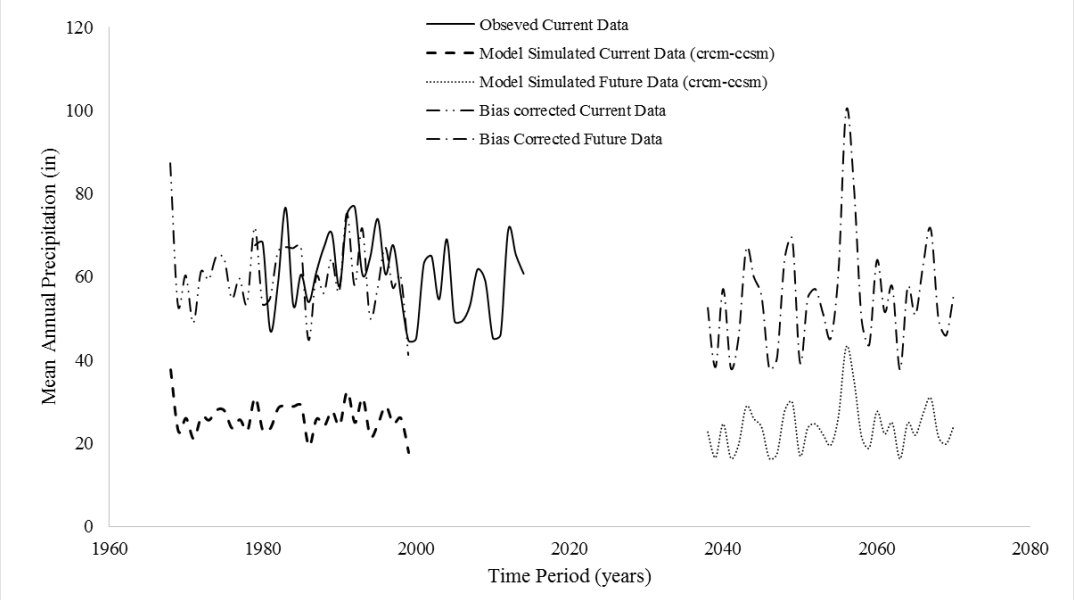

Figure A-16 Bias Correction for Mean Annual Precipitation, Lafayette, Louisiana

Bias Correction for New Orleans, Louisiana:

Table A-17 Bias Corrected Precipitation Data, New Orleans, Louisiana

Climate Models	Future Simulation (in)	Current Simulation (in)	Bias-Corrected (in)
CRCM-CCSM	24.1	26.7	49.7
CRCM-CGCM3	42.3	41.4	56.1
ECP2-GFDL	58.1	60.2	53.0
ECP2-HADCM3	76.9	64.6	65.3
HRM3-GFDL	38.6	42.4	50.0
HRM3-HADCM3	49.8	50.0	54.7
MM5I-CCSM	24.7	27.1	50.1
MM5I-HADCM3	106.2	71.4	81.7
RCM3-CGCM3	70.6	66.7	58.1
RCM3-GFDL	64.2	64.5	54.7
WRFG-CCSM	32.8	36.1	49.9
WRFG-CGCM3	66.7	66.7	54.9

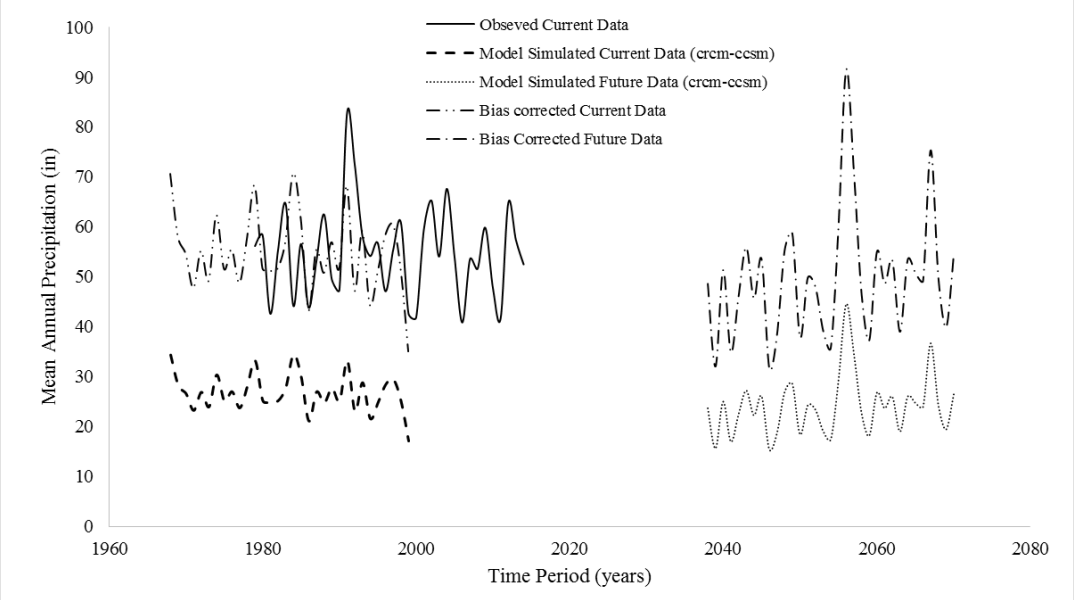

Figure A-17 Bias Correction for Mean Annual Precipitation, New Orleans, Louisiana

Bias Correction for Shreveport, Louisiana:

Table A-18 Bias Corrected Precipitation Data, Shreveport, Louisiana

Climate Models	Future Simulation (in)	Current Simulation (in)	Bias-Corrected (in)
CRCM-CCSM	26.1	27.7	44.9
CRCM-CGCM3	36.6	34.9	49.9
ECP2-GFDL	45.9	48.2	45.3
ECP2-HADCM3	45.1	46.3	46.4
HRM3-GFDL	41.6	44.8	44.1
HRM3-HADCM3	43.5	44.1	46.9
MM5I-CCSM	28.4	30.6	44.1
MM5I-HADCM3	43.8	41.6	50.1
RCM3-CGCM3	38.4	40.6	45.0
RCM3-GFDL	45.0	45.4	47.2
WRFG-CCSM	26.3	27.3	45.8
WRFG-CGCM3	36.3	35.4	48.8

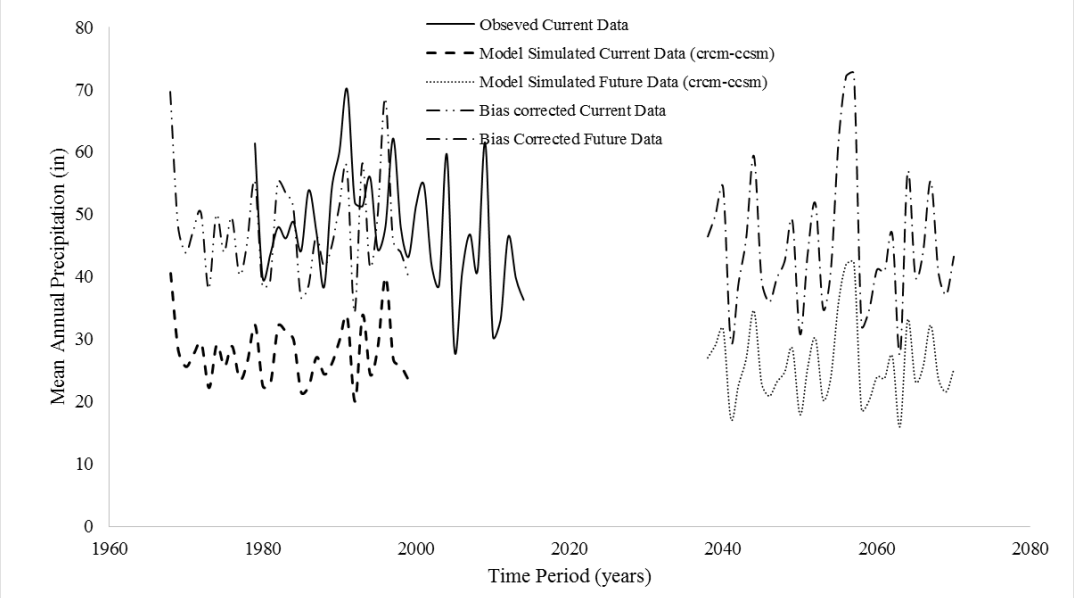

Figure A-18 Bias Correction for Mean Annual Precipitation, Shreveport, Louisiana

Bias Correction for Oklahoma City, Oklahoma:

Table A-19 Bias Corrected Precipitation Data, Oklahoma City, Oklahoma

Climate Models	Future Simulation (in)	Current Simulation (in)	Bias-Corrected (in)
CRCM-CCSM	21.2	21.0	35.7
CRCM-CGCM3	26.2	24.7	37.5
ECP2-GFDL	28.9	32.5	31.5
ECP2-HADCM3	23.1	25.9	31.5
HRM3-GFDL	34.8	37.7	32.6
HRM3-HADCM3	32.3	31.7	36.0
MM5I-CCSM	23.7	23.0	36.4
MM5I-HADCM3	26.4	24.9	37.5
RCM3-CGCM3	27.8	30.2	32.5
RCM3-GFDL	35.1	34.7	35.8
WRFG-CCSM	19.9	18.6	37.9
WRFG-CGCM3	19.7	18.7	37.1

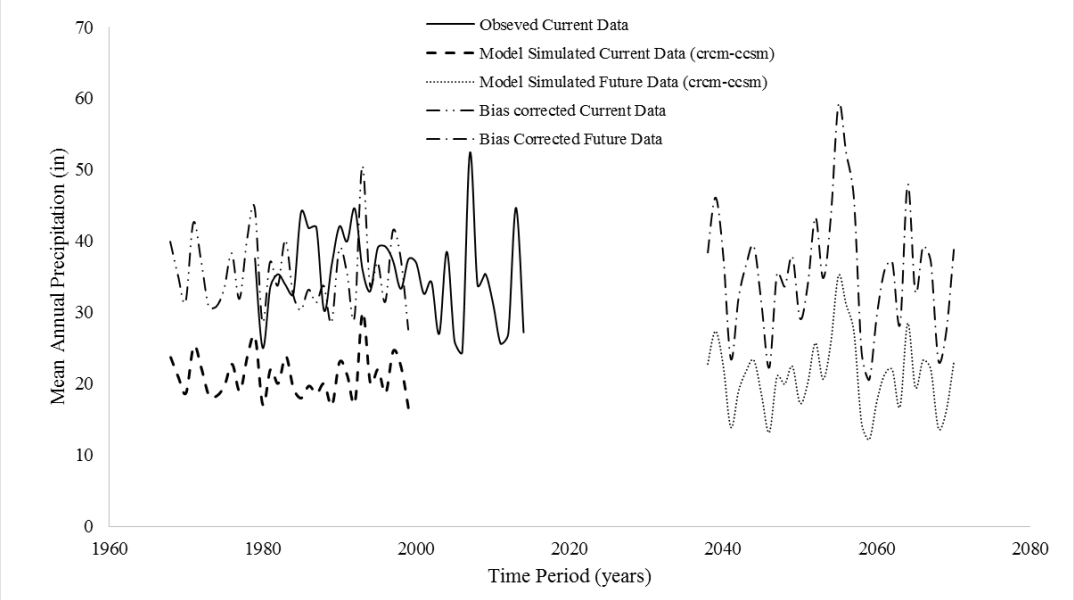

Figure A-19 Bias Correction for Mean Annual Precipitation, Oklahoma City, Oklahoma

Bias Correction for Tulsa, Oklahoma:

Table A-20 Bias Corrected Precipitation Data, Tulsa, Oklahoma

Climate Models	Future Simulation (in)	Current Simulation (in)	Bias Corrected (in)
CRCM-CCSM	27.2	27.6	38.5
CRCM-CGCM3	33.9	31.5	42.2
ECP2-GFDL	32.1	36.2	34.7
ECP2-HADCM3	26.8	29.7	35.3
HRM3-GFDL	41.2	43.3	37.2
HRM3-HADCM3	38.0	37.8	39.2
MM5I-CCSM	28.3	27.9	39.6
MM5I-HADCM3	31.5	29.1	42.3
RCM3-CGCM3	32.7	34.6	36.9
RCM3-GFDL	39.8	40.4	38.5
WRFG-CCSM	21.0	20.3	40.5
WRFG-CGCM3	25.3	21.8	45.3

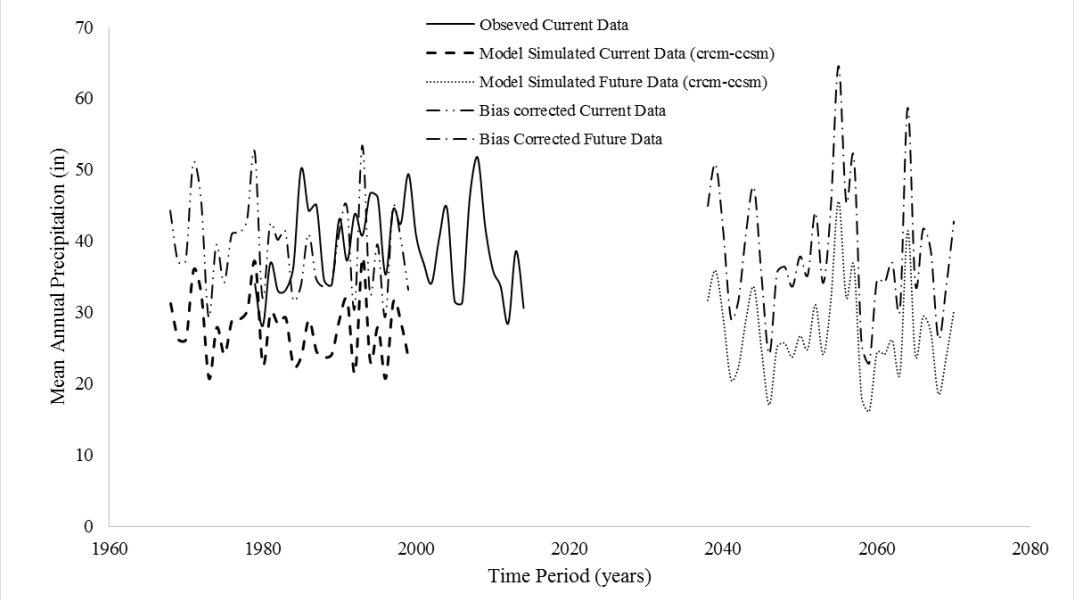

Figure A-20 Bias Correction for Mean Annual Precipitation, Tulsa, Oklahoma

Bias Correction for Stillwater, Oklahoma:

Table A-21 Bias Corrected Precipitation Data, Stillwater, Oklahoma

Climate Models	Future Simulation (in)	Current Simulation (in)	Bias-Corrected (in)
CRCM-CCSM	23.7	23.3	36.7
CRCM-CGCM3	28.9	26.9	38.6
ECP2-GFDL	29.8	32.8	32.6
ECP2-HADCM3	23.4	26.4	31.8
HRM3-GFDL	36.9	39.2	33.8
HRM3-HADCM3	33.7	33.8	35.9
MM5I-CCSM	23.9	24.1	35.7
MM5I-HADCM3	27.6	25.7	38.5
RCM3-CGCM3	29.5	32.0	33.2
RCM3-GFDL	37.3	37.1	36.2
WRFG-CCSM	17.9	17.9	36.0
WRFG-CGCM3	21.2	18.4	41.4

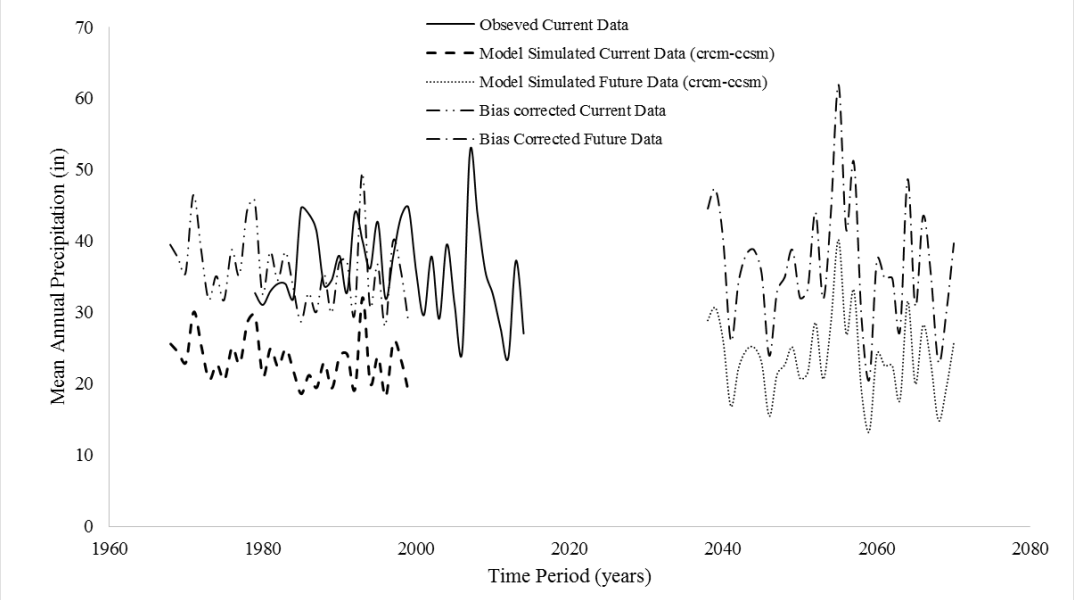

Figure A-21 Bias Correction for Mean Annual Precipitation, Stillwater, Oklahoma

Bias Correction for Lawton, Oklahoma:

Table A-22 Bias Corrected Precipitation Data, Lawton, Oklahoma

Climate Models	Future Simulation (in)	Current Simulation (in)	Bias-Corrected (in)
CRCM-CCSM	20.0	20.2	30.1
CRCM-CGCM3	24.7	23.3	32.3
ECP2-GFDL	25.1	29.2	26.1
ECP2-HADCM3	20.2	22.4	27.4
HRM3-GFDL	18.2	20.1	27.6
HRM3-HADCM3	15.1	14.8	31.0
MM5I-CCSM	20.9	20.2	31.5
MM5I-HADCM3	24.4	23.0	32.3
RCM3-CGCM3	23.7	23.8	30.3
RCM3-GFDL	29.3	30.4	29.3
WRFG-CCSM	17.7	16.5	32.8
WRFG-CGCM3	17.3	16.4	32.2

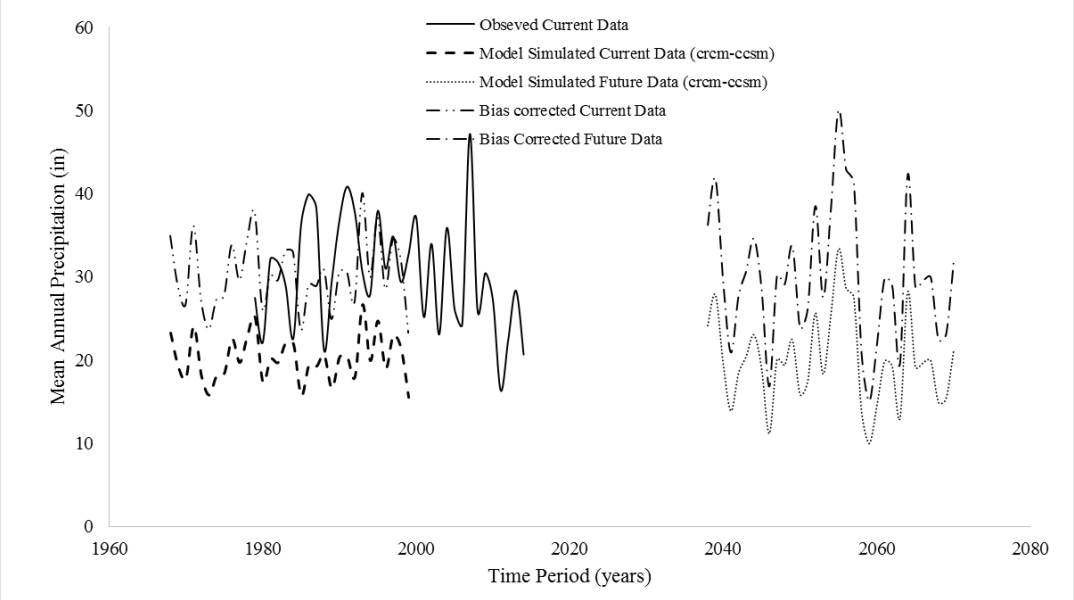

Figure A-22 Bias Correction for Mean Annual Precipitation, Lawton, Oklahoma

Bias Correction for Ardmore, Oklahoma:

Table A-23 Bias Corrected Precipitation Data, Ardmore, Oklahoma

Climate Models	Future Simulation (in)	Current Simulation (in)	Bias-Corrected (in)
CRCM-CCSM	22.2	22.6	29.8
CRCM-CGCM3	27.9	26.9	31.4
ECP2-GFDL	28.5	33.5	25.8
ECP2-HADCM3	25.9	27.7	28.4
HRM3-GFDL	37.6	42.4	26.9
HRM3-HADCM3	36.4	35.9	30.8
MM5I-CCSM	25.1	23.6	32.3
MM5I-HADCM3	28.5	27.3	31.7
RCM3-CGCM3	28.5	29.9	29.0
RCM3-GFDL	35.6	35.2	30.7
WRFG-CCSM	20.5	19.9	31.3
WRFG-CGCM3	21.5	20.6	31.7

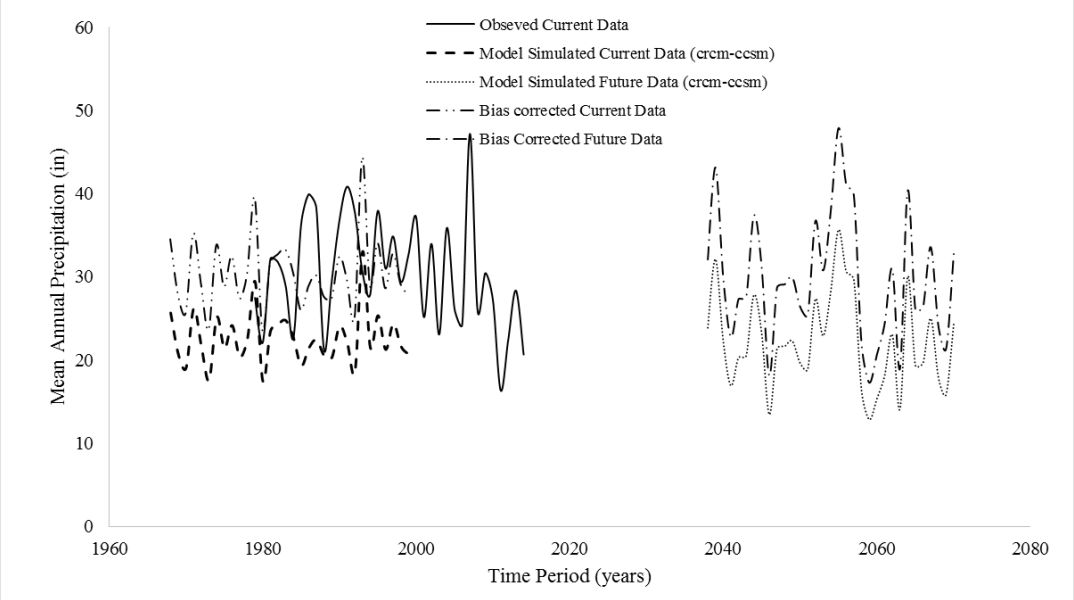

Figure A-23 Bias Correction for Mean Annual Precipitation, Ardmore, Oklahoma

Bias Correction for Fayetteville, Arkansas:

Table A-24 Bias Corrected Precipitation Data, Fayetteville, Arkansas

Climate Models	Future Simulation (in)	Current Simulation (in)	Bias-Corrected (in)
CRCM-CCSM	31.8	32.0	44.6
CRCM-CGCM3	38.6	36.7	47.2
ECP2-GFDL	39.8	45.1	39.6
ECP2-HADCM3	36.0	37.1	43.6
HRM3-GFDL	46.7	47.7	43.9
HRM3-HADCM3	43.8	42.2	46.6
MM5I-CCSM	32.5	32.0	45.5
MM5I-HADCM3	35.1	33.0	47.7
RCM3-CGCM3	37.9	39.3	43.3
RCM3-GFDL	43.0	41.8	46.1
WRFG-CCSM	25.6	24.9	46.1
WRFG-CGCM3	31.3	27.9	50.2

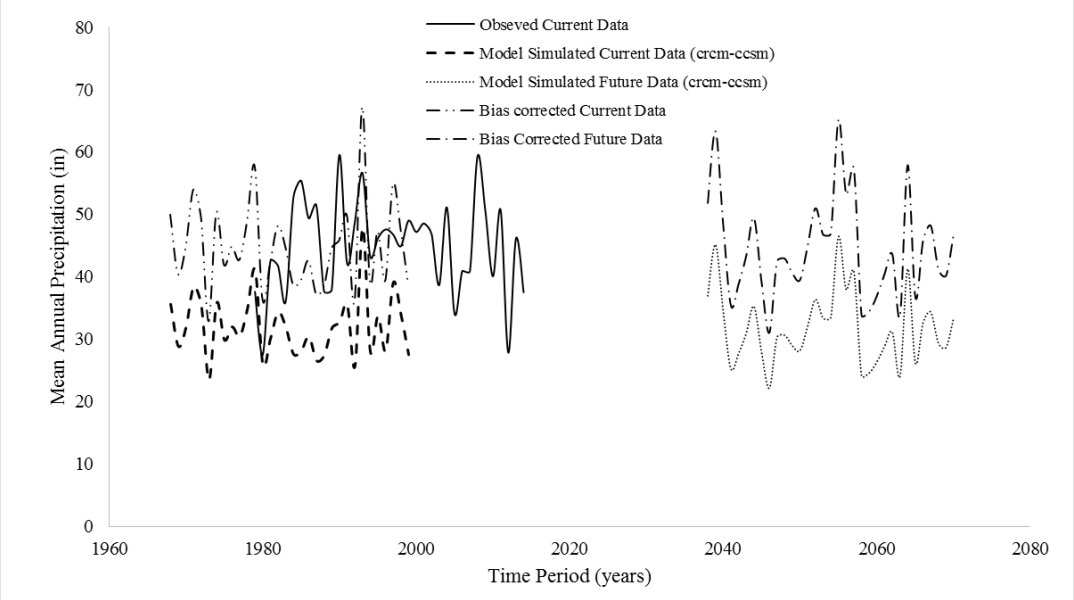

Figure A-24 Bias Correction for Mean Annual Precipitation, Fayetteville, Arkansas

Bias Correction for Fort Smith, Arkansas:

Table A-25 Bias Corrected Precipitation Data, Fort Smith, Arkansas

Climate Models	Future Simulation (in)	Current Simulation (in)	Bias-Corrected (in)
CRCM-CCSM	29.0	29.7	44.4
CRCM-CGCM3	36.5	35.6	46.7
ECP2-GFDL	38.2	42.8	40.6
ECP2-HADCM3	34.5	35.6	44.1
HRM3-GFDL	38.6	38.4	45.7
HRM3-HADCM3	34.7	33.3	47.4
MM5I-CCSM	29.7	30.2	44.7
MM5I-HADCM3	33.5	31.5	48.5
RCM3-CGCM3	36.8	39.6	42.3
RCM3-GFDL	41.4	41.0	45.9
WRFG-CCSM	27.5	26.1	47.9
WRFG-CGCM3	30.8	29.6	47.4

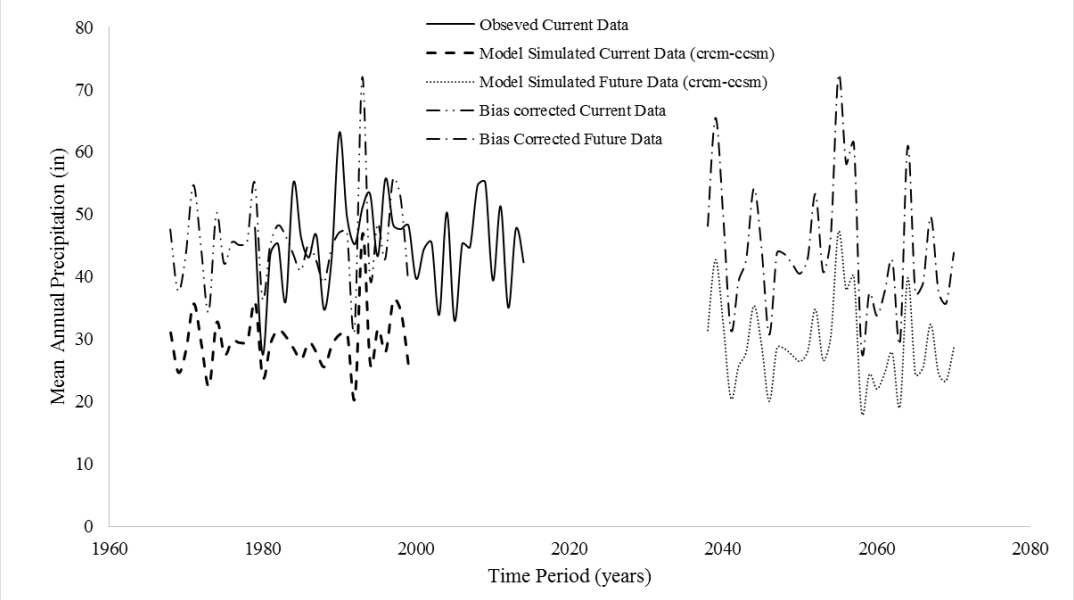

Figure A-25 Bias Correction for Mean Annual Precipitation, Fort Smith, Arkansas

Bias Correction for Conway, Arkansas:

Table A-26 Bias Corrected Precipitation Data, Conway, Arkansas

Climate Models	Future Simulation (in)	Current Simulation (in)	Bias-Corrected (in)
CRCM-CCSM	30.0	30.3	45.3
CRCM-CGCM3	38.4	37.2	47.2
ECP2-GFDL	43.0	47.2	41.8
ECP2-HADCM3	41.0	40.2	46.7
HRM3-GFDL	29.9	33.4	41.1
HRM3-HADCM3	39.3	34.9	51.7
MM5I-CCSM	34.0	34.6	45.1
MM5I-HADCM3	42.7	38.0	51.4
RCM3-CGCM3	42.0	42.0	45.8
RCM3-GFDL	43.7	43.6	46.0
WRFG-CCSM	32.0	31.7	46.4
WRFG-CGCM3	39.4	37.0	48.8

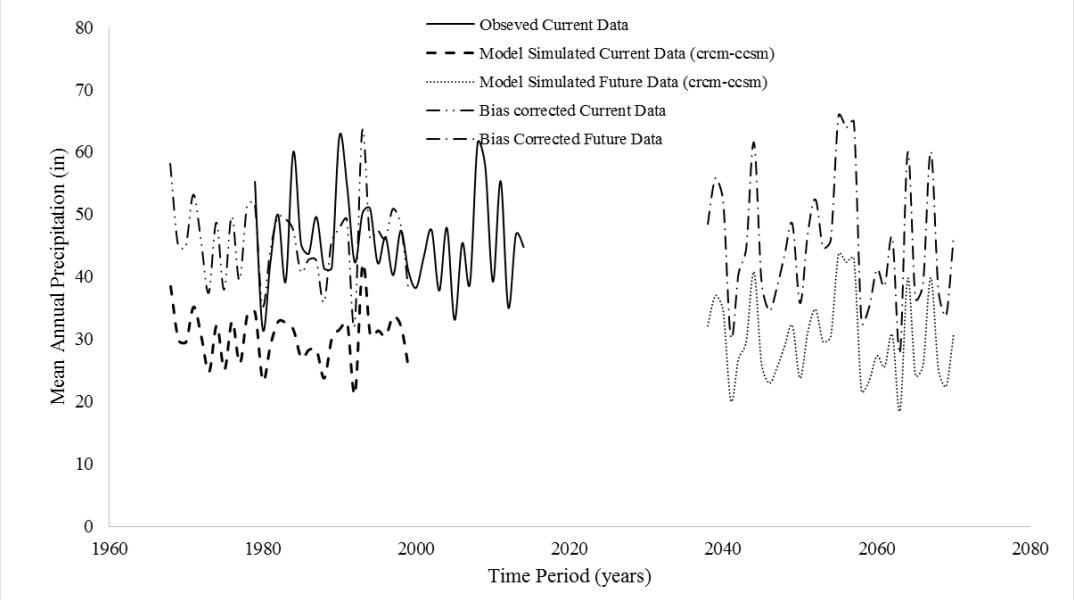

Figure A-26 Bias Correction for Mean Annual Precipitation, Conway, Arkansas

Bias Correction for Hot Springs, Arkansas:

Table A-27 Bias Corrected Precipitation Data, Hot Springs, Arkansas

Climate Models	Future Simulation (in)	Current Simulation (in)	Bias-Corrected (in)
CRCM-CCSM	28.1	29.2	50.7
CRCM-CGCM3	37.0	36.6	53.2
ECP2-GFDL	44.3	48.7	47.8
ECP2-HADCM3	41.6	42.4	51.7
HRM3-GFDL	26.3	29.1	47.5
HRM3-HADCM3	34.9	30.8	59.7
MM5I-CCSM	34.9	36.0	51.1
MM5I-HADCM3	44.2	39.9	58.3
RCM3-CGCM3	41.4	42.0	51.8
RCM3-GFDL	45.4	45.2	52.8
WRFG-CCSM	30.4	30.2	53.0
WRFG-CGCM3	38.6	36.3	56.0

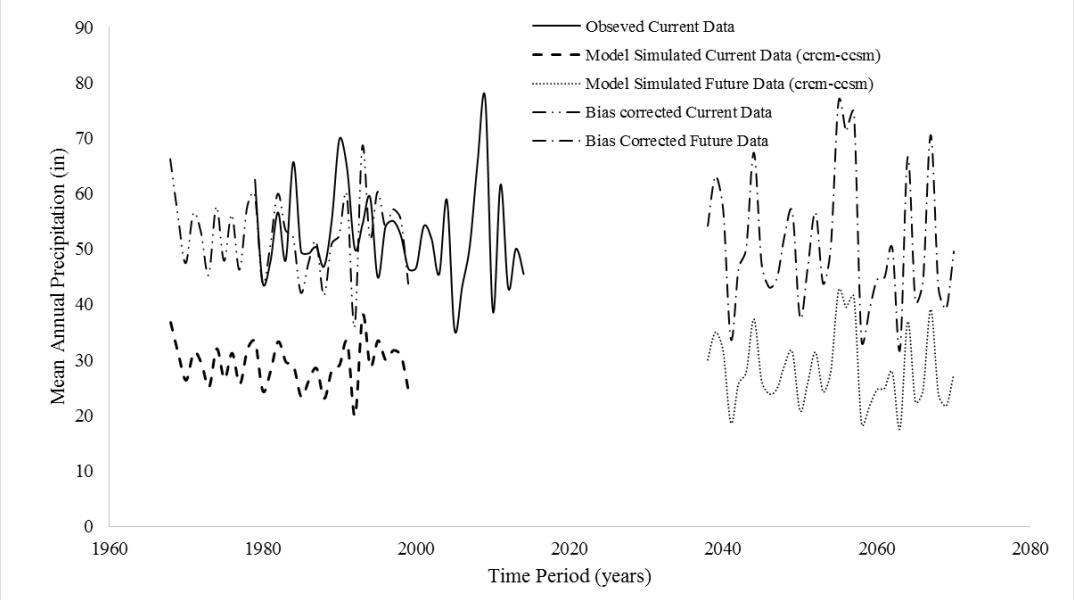

Figure A-27 Bias Correction for Mean Annual Precipitation, Hot Springs, Arkansas

Bias Correction for Pine Bluff, Arkansas:

Table A-28 Bias Corrected Precipitation Data, Pine Bluff, Arkansas

Climate Models	Future Simulation (in)	Current Simulation (in)	Bias-Corrected (in)
CRCM-CCSM	30.4	31.2	45.3
CRCM-CGCM3	39.1	37.6	48.5
ECP2-GFDL	44.6	49.0	42.5
ECP2-HADCM3	44.0	44.6	46.1
HRM3-GFDL	45.1	48.0	43.8
HRM3-HADCM3	45.0	44.2	47.5
MM5I-CCSM	34.2	34.9	45.7
MM5I-HADCM3	45.1	39.5	53.2
RCM3-CGCM3	43.5	43.6	46.5
RCM3-GFDL	45.6	45.5	46.7
WRFG-CCSM	30.0	30.2	46.3
WRFG-CGCM3	38.7	36.9	48.9

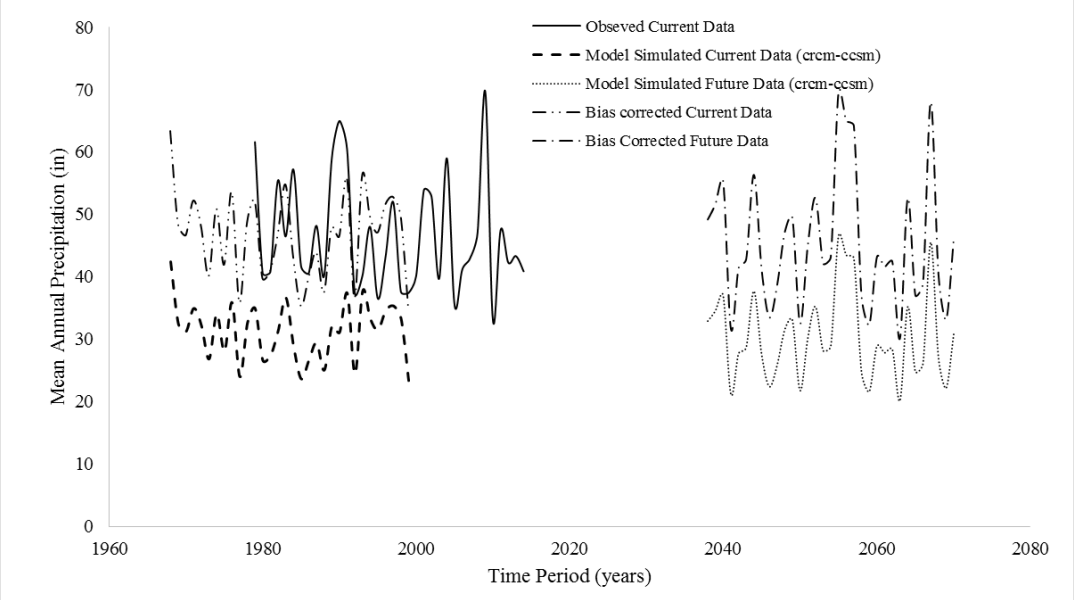

Figure A-28 Bias Correction for Mean Annual Precipitation, Pine Bluff, Arkansas

Vita

Anjuman Ara Akhter has received her B.Sc in Civil Engineering from Bangladesh University of Engineering and Technology, Bangladesh in 2014. In January 2017, she has started her M.Sc in Civil Engineering at the University of Texas, El Paso (UTEP).

After B.Sc, Anjuman has worked for two years in the construction industry in Bangladesh. Currently, she is working in UTEP as Graduate Research and Teaching Assistant for the Department of Civil Engineering. She was involved in projects funded by U.S Government agencies during her study period in UTEP. Anjuman has been the first author in Final Report of Project named 'Understanding Climate Change Impact on the Hydraulic Design of Highway infrastructures' funded by SPTC (Southern Plains Transportation Center). She has been awarded Graduate Scholarship from 'Women in Transportation_San Antonio Region' in 2018.

Anjuman's thesis titled, 'Assessment of Climate Change Impact on Hydraulic Design of Bridge Infrastructures' has been supervised by Dr. Vivek Tandon. Anjuman has been accepted a PhD Position in Civil Engineering in the University of Maryland, College Park from Spring 2019.

Contact Information: aakhter@miners.utep.edu